

Healing water

using pure water jets to perform bone debridement treatments in orthopedic surgery

den Dunnen, Steven

DOI

[10.4233/uuid:ce13d0b5-e00d-4d91-81f8-c7bd7d273345](https://doi.org/10.4233/uuid:ce13d0b5-e00d-4d91-81f8-c7bd7d273345)

Publication date

2018

Document Version

Final published version

Citation (APA)

den Dunnen, S. (2018). *Healing water: using pure water jets to perform bone debridement treatments in orthopedic surgery*. [Dissertation (TU Delft), Delft University of Technology].
<https://doi.org/10.4233/uuid:ce13d0b5-e00d-4d91-81f8-c7bd7d273345>

Important note

To cite this publication, please use the final published version (if applicable).
Please check the document version above.

Copyright

Other than for strictly personal use, it is not permitted to download, forward or distribute the text or part of it, without the consent of the author(s) and/or copyright holder(s), unless the work is under an open content license such as Creative Commons.

Takedown policy

Please contact us and provide details if you believe this document breaches copyrights.
We will remove access to the work immediately and investigate your claim.

A close-up photograph of a surgical procedure. A high-pressure water jet, emerging from a dark, metallic nozzle, is directed at a realistic, light-colored bone model. The bone is held in place by a yellow surgical vise. The background is a vibrant, saturated red, and the scene is filled with fine mist and water droplets, emphasizing the precision and power of the water jet technology.

Healing water

using pure water jets to perform
bone debridement treatments
in orthopedic surgery

Steven den Dunnen

Healing water:

using pure water jets to perform
bone debridement treatments
in orthopedic surgery

Proefschrift

ter verkrijging van de graad van doctor
aan de Technische Universiteit Delft,
op gezag van de Rector Magnificus prof. dr. ir. T.H.J.J. van der Hagen,
voorzitter van het College voor Promoties,
in het openbaar te verdedigen op
woensdag 12 december 2018 om 10:00 uur
door

Steven DEN DUNNEN

Ingenieur, Technische Universiteit Delft, Nederland

geboren te Papendrecht, Nederland

Dit proefschrift is goedgekeurd door de promotoren.

Samenstelling promotiecommissie bestaat uit:

Rector Magnificus	voorzitter
Prof. dr. J. Dankelman	Technische Universiteit Delft, promotor
Prof. dr. G.M.M.J. Kerkhoffs	Universiteit van Amsterdam, promotor
Dr. ir. G.J.M. Tuijthof	U Maastricht, Universiteit van Amsterdam, copromotor

Onafhankelijke leden:

Prof. dr. D. Eygendaal	Universiteit van Amsterdam
Dr. ir. B. van Rietbergen	Technische Universiteit Eindhoven
Prof. dr. ir. H.H. Weinans	Technische Universiteit Delft, UMC Utrecht
Prof. dr. ir. J. L. Herder	Technische Universiteit Delft
Prof. dr. ir. P. Breedveld	Technische Universiteit Delft, reservelid

This research was funded by the Dutch Technology Foundation STW (Grant number 10851), which is part of the Netherlands Organisation for Scientific Research (NWO), and which is partly funded by Ministry of Economic Affairs. Additional support was granted by the Marti-Keuning Eckhart Stichting.

Copyright:	S. den Dunnen 2018
Cover photo by:	Sam Rentmeester

Table of contents

SUMMARY	5
----------------	----------

SAMENVATTING	9
---------------------	----------

CHAPTER 1	13
------------------	-----------

Introduction

CHAPTER 2	25
------------------	-----------

Feasibility of using pure water jets for bone drilling

<i>Pure waterjet drilling of articular bone: an in vitro feasibility study</i>	27
--	----

CHAPTER 3	39
------------------	-----------

Bone debridement treatments: optimal hole dimensions to improve cartilage regeneration

<i>Is technique performance a prognostic factor in bone marrow stimulation of the talus?</i>	41
--	----

<i>No effect of hole geometry in microfracture for talar osteochondral defects</i>	55
--	----

CHAPTER 4	71
------------------	-----------

Water jet drilling in bone: the influence of the primary machine settings and the bone architecture on the hole dimensions

<i>Waterjet drilling in porcine bone: the effect of the nozzle diameter and bone architecture on the hole dimensions</i>	73
--	----

<i>How do jet time, pressure and bone volume fraction influence the drilling depth when water jet drilling in porcine bone?</i>	91
---	----

<i>The influence of water jet diameter and bone structural properties on the efficiency of pure water jet drilling in porcine bone</i>	107
--	-----

CHAPTER 5	117
Depth control for water jet drilling in bone tissue	
<i>Colliding jets provide depth control for water jetting in bone tissue</i>	<i>119</i>
CHAPTER 6	141
Discussion	
ACKNOWLEDGEMENTS	159
CURRICULUM VITAE	163
LIST OF PUBLICATIONS	165

Summary

Orthopedic surgery is a surgical discipline that is concerned with the treatment of the musculoskeletal system. Many orthopedic treatments involve cutting or drilling in bones by using rigid drills or oscillating saws. Using waterjets instead of conventional instruments can be beneficial due to the absence of thermal damage and a consistent sharp cut. Additionally, waterjet technology allows the development of flexible instruments that facilitate maneuvering through complex or narrow joint spaces. Therefore, the aim of this thesis is to develop a compliant or flexible arthroscopic surgical instrument, based on water jet technology, that is able to drill in bone tissue.

The intended target surgical procedure of the water jet instrument is bone debridement and marrow stimulation. Bone debridement treatments are performed to treat damaged cartilage in joints that are generally caused by trauma. The treatment involves the removal of the damaged cartilage, followed by making 2-4 mm deep holes in the underlying bone to induce bleeding. This introduces stem cells that regenerate the bone and the cartilage, resulting in pain relief and improved mobility for the patient.

For the development of a compliant arthroscopic surgical water jet instrument, the following systematic approach was followed:

1. Determining whether water jets are able to drill in bone tissue.
2. Determining what hole dimensions result in optimal healing for the patient.
3. Controlling the drilling depth of a water jet.
4. Developing a prototype instrument by applying the results of 1-3.

Each consecutive step is discussed in the following paragraphs, indicating the contents of each chapter. Step 3, controlling the drilling depth, is the primary challenge of this research since it is a prerequisite to ensure clinical safety. The challenge in depth control when water jet drilling lies in the inhomogeneous structure of the bone, which interacts with the water jet beam and causes the drilling depth to vary.

In **Chapter 2**, the feasibility of using pure water jets to machine bone is investigated (step 1) by using an industrial water jet machine to drill holes in pig, sheep, goat and human bone tissue. The results show that machining of bone tissue is possible without adding abrasives, which are potentially harmful to a patient. The minimum pressure required to drill in bone differs for each animal and bone specimen. This means that the mechanical or structural properties of the bone tissue affect the drilling depth. Water jet machined holes are conically shaped which offers

potential use for bone debridement treatments and for drilling guidance holes for screw fixations.

The dimensions of the holes that are to be drilled with the water jet to achieve optimal regeneration of the bone and cartilage are considered in **Chapter 3** (step 2). A systematic review of available literature was inconclusive on the possible influence of variation within the surgical technique on the outcome of bone marrow stimulation. Key elements of a successful treatment are the removal of unstable cartilage, a hole depth between 2 and 4 mm until bleeding or fat droplets appear, and a distance between the holes of 3 to 4 mm. A caprine animal study was performed to determine whether deeper holes or holes with a smaller diameter would improve the quality of the regenerated tissue. The results indicate that the regeneration of tissue does not appear to be improved by changing the depth or diameter of the holes. Hence, controlling the drilling depth within the range of 2 to 4 mm suffices with regards to water jet machining for the caprine talus.

In **Chapter 4** the cause of the variation in hole depth is presented that can occur whilst water jet drilling in bone. Also, the first two methods are presented for controlling the drilling depth a (step 3). The volume of mineralized bone per unit volume (BV/TV) is the bone structural property that correlates best with the drilling depth. We have shown experimentally that when the BV/TV is known, the drilling depth can be predicted. To compensate for the varying local BV/TV of bone tissue, the machine settings of the water jet can be adjusted. The primary machine settings that affect the drilling depth are the pressure, jet time and nozzle diameter. A mathematical model was constructed that allows accurate prediction of the drilling depth and diameter for a given machine setting and BV/TV. Hence, control over the drilling depth is achieved when the local BV/TV of the bone tissue is known. A challenge in this control method is the determination of the local BV/TV of the bone tissue, which requires a medical imaging instrument that is not commonly available in hospitals.

A second method to control the drilling depth is to use low impact machine settings that allow gradual machining of bone tissue. An orthopedic surgeon can intermittently apply a burst of water to gradually increase the drilling depth, using an arthroscope for visual feedback on the drilling progress. In this case the surgeon is the controller, which has the disadvantage that the execution is slower and a lower depth-accuracy can be achieved than the first control method. The advantage is that the surgeon is in full control, and the intended water jet instrument can be built compact and simple which keeps the dimensions as small as possible.

The third method for controlling the drilling depth is presented in **Chapter 5**.

To achieve depth control, two water jets are set to collide at a specific point. Above the collision point the individual water jets are capable to machine bone tissue. At the collision point, the coherency of individual water jets will collapse. The resulting incoherent spray of water is not powerful enough to machine bone tissue. As a result, the collision point determines the drilling depth. Hence, control over the drilling depth is achieved. Experiments on bone tissue determined that the accuracy of the depth control is within the limits set for bone marrow stimulation treatments. A challenge of implementing two water jets in an arthroscopic instrument is the increased construction volume, which can impair the maneuverability in human joints.

The fourth method for controlling the drilling depth is presented in **Chapter 6**. A sensor located at the nozzle can interrupt the water supply when a predetermined depth is achieved. The shutdown mechanism can be located at the nozzle or the pump. Experiments with an on-scale prototype and simulations determined that the accuracy of this control system is within the limits for bone marrow stimulation treatments. A challenge is that the sensor that measures the drilling depth increases the size of the nozzle, which can impair the ability to maneuver in human joints.

To allow a developer of a medical water jet instrument design freedom (step 4), a study was performed to determine whether the total volume of water that exits the nozzle correlates with the volume of bone tissue that is removed. The total volume of water that exits the nozzle combined with the known BV/TV determine the volume of bone material that is removed. This provides design freedom in the sense that the nozzle diameter, pressure and jet time can be chosen in accordance to the maximum operating time requirements or dimensional limitations of the intended water jet instrument. For example, to minimize the dimensions of a water jet instrument, a smaller nozzle diameter and a lower pressure can be used, at the cost of an increased operating time (jet time).

There are five primary challenges that need to be addressed for further development of the arthroscopic water jet instrument (step 4). First, an in vivo animal experiment with an industrial sized water jet instrument is required to determine if water jetting in bone is clinically safe. Secondly, for the development of an actual on-scale prototype, the nozzle should be fully stabilized when water jet drilling to guarantee accurate drilling and prevent unwanted damage to surrounding tissue. Third, additional testing of the connections between the nozzle and the tubing are required to further reduce the length of the rigid nozzle, which will allow optimal instrument compliance. Fourth, experiments with on-scale prototypes in cadaver knees and ankles are required to quantify the loss in machining capacity of the water jet when scaling down from an industrial size water jet set-up to a minimally invasive

sized set-up. Lastly, the ergonomics of the instrument should be addressed to provide optimal instrument control to the orthopedic surgeon. All five primary challenges have been investigated briefly and are considered non-insurmountable.

This thesis has shown that using pure water jet technology for bone debridement treatments is feasible. The applicability of this research can be extended to other orthopedic treatments that involve hard tissue, such as cement removal in implant revisions, cartilage removal, laminectomy and drilling guidance holes for screw fixations. The presented depth control systems can prove to be valuable for dentistry (drilling cavities, plaque removal), mining (not penetrating fragile layers of earth), food industry (cutting, filling and seasoning), and rescue missions (careful removal of debris).

Samenvatting

Orthopedie is een medisch specialisme dat zich bezighoudt met de behandeling van het steun- en bewegingsapparaat. Voor een groot aantal orthopedische behandelingen is het noodzakelijk te boren of te zagen in bot. Hierbij worden starre boormachines of oscillerende zagen gebruikt. Het vervangen van deze instrumenten door een waterstraalinstrument kan voordelen bieden. Zo zal een waterstraal altijd scherp blijven en treedt geen thermische schade op door verhitting van het botweefsel. Tevens biedt waterstraaltechnologie de mogelijkheid om een flexibel instrument te ontwikkelen waarmee plekken in gewrichten bereikbaar worden die met star instrumentarium niet bereikbaar zijn. Het doel van deze thesis is een flexibel arthroscoopisch waterstraal instrument ontwikkelen dat kan boren in botweefsel.

De beoogde toepassing van het waterstraalinstrument is het uitvoeren van beenmergstimulatiebehandelingen. Beenmergstimulatiebehandelingen worden uitgevoerd bij patiënten waarbij het kraakbeen is beschadigd door een trauma. Tijdens deze behandeling wordt het beschadigde kraakbeen verwijderd. Vervolgens worden gaten met een diepte tussen 2 tot 4 mm aangebracht in het bot, waardoor bloedingen ontstaan. De bloedingen dragen bij aan het herstel van zowel het kraakbeen als het bot, waardoor de pijn van de patiënt afneemt.

Voor het ontwikkelen van een flexibel arthroscoopisch waterstraalinstrument is het volgende stappenplan doorlopen:

1. De haalbaarheid aantonen om met waterstralen te kunnen boren in bot.
2. Het achterhalen welke gat-afmetingen resulteren in optimaal herstel voor de patiënt.
3. De boordiepte controleren.
4. Ontwikkeling van een prototype.

De volgende paragrafen bespreken elke stap die doorlopen is, waarbij verwijzingen worden aangehaald naar de betreffende hoofdstukken. Stap 3 is het primaire onderzoek van deze thesis, aangezien de patiënt-veiligheid hiermee het meest is gemoeid. De voornaamste uitdaging in het controleren van de boordiepte is de inhomogeniteit van het botweefsel. Hierdoor is de verspanende werking van de waterstraal niet constant in elk deel van het bot, waardoor boordieptes van elkaar kunnen verschillen.

In Hoofdstuk 2 wordt de haalbaarheid voor het gebruik van enkel waterstralen om in bot te boren onderzocht (stap 1). Met een industriële waterstraalmachine worden gaten aangebracht in varkens-, schapen-, geiten- en humaan bot. Uit het onderzoek blijkt dat het gebruik van abrasieven (harde deeltjes toegevoegd aan de waterstraal), die schadelijk kunnen zijn voor patiënten, niet noodzakelijk is om in bot

te kunnen boren. “Pure” waterstralen volstaan hiervoor. De minimale waterdruk om bot te verspanen verschilt per dier, bot en locatie. Hieruit blijkt dat de botstructuur invloed heeft op de boordiepte. De geboorde gaten zijn conisch van vorm. Deze vorm is geschikt voor beenmergstimulatiebehandelingen en het voorboren van schroefgaten.

In Hoofdstuk 3 zijn de afmetingen van de gaten onderzocht die na een beenmergstimulatiebehandeling resulteren in het optimale herstel van bot en kraakbeen. Uit een systematische review blijkt dat variatie in chirurgische techniek geen overtuigende invloed heeft op de uitkomst van de beenmergstimulatiebehandeling. Voor het slagen van een behandeling dient het beschadigde kraakbeen verwijderd te worden en moeten gaten worden aangebracht tussen de 2 en 4 mm diep (totdat bloedingen of vetdruppels ontstaan) met een afstand tussen de gaten van 3 tot 4 mm. Door middel van een dierenstudie op geiten is onderzocht of diepere gaten of meer gaten met een kleinere diameter leidt tot een beter herstel van het bot en kraakbeen. Uit de uitkomst van deze studie blijkt dat het aanpassen van de diepte of diameter van de gaten het herstel niet verbetert. Met betrekking tot de dieptecontrole tijdens het waterstraalboren betekent dit dat een boordiepte tussen de 2 en 4 mm volstaat.

In Hoofdstuk 4 wordt de oorzaak van de inconsistente gatdiepte achterhaald tijdens het waterstraalboren in bot. Daarnaast worden twee methoden aangedragen waarmee de boordiepte gecontroleerd kan worden. De botdichtheid is de botstructureigenschap die de het meest correleert met de boordiepte. Wanneer de botdichtheid bekend is kan de boordiepte worden voorspeld. Instellingen van de waterstraalmachine kunnen worden aangepast om de invloed van de natuurlijke variaties in botdichtheid in het bot te compenseren, om zo te kunnen boren tot de beoogde diepte. De voornaamste instellingen van de waterstraalmachine die de boordiepte beïnvloeden zijn de waterdruk, de diameter van de waterstraal en de waterstraaltijd. Aan de hand van drie studies is een wiskundig model geconstrueerd waarmee de boordiepte nauwkeurig bepaald kan worden aan de hand van de waterstraalinstellingen en de botdichtheid. Mits de botdichtheid bekend is, is hiermee controle over de boordiepte verkregen. De voornaamste uitdaging in deze methode van dieptecontrole ligt in het vaststellen van de botdichtheid. Hiervoor is specialistische medische beeldvorming apparatuur benodigd.

Een tweede methode om de boordiepte te controleren is waterstraalinstellingen gebruiken die net krachtig genoeg zijn om te kunnen boren in bot. Een orthopedisch chirurg kan de boordiepte geleidelijk toe laten nemen door een korte waterstraalpuls toe te dienen. Hierbij is visuele feedback via de artroscopen noodzakelijk. Bij deze dieptecontrole methode is de chirurg de controller, waardoor dit proces trager en onnauwkeuriger zal verlopen dan met de eerste dieptecontrole methode.

Het voordeel van deze methode is dat de chirurg volledige controle heeft, en het waterstraalinstrument eenvoudig en compact gehouden kan worden door het ontbreken van extra (controle) componenten.

Een derde methode om de boordiepte te controleren wordt aangedragen in Hoofdstuk 5. Twee waterstralen worden uitgelijnd om op een specifiek punt samen te komen. Boven dit punt zijn de waterstralen krachtig genoeg om door bot te boren. Op het samenkomstpunt resulteert de botsing tussen de twee waterstralen in een spray. Deze spray is niet krachtig genoeg om bot te kunnen verspanen. Hiermee is controle over de boordiepte bereikt. Experimenten met deze controlemethode hebben aangetoond dat de boordiepte-nauwkeurigheid voor beenmergstimulatiebehandelingen voldoende is. Een nadeel van het gebruik van twee waterstralen is dat de afmetingen van het instrument toenemen. Dit maakt manoeuvreren in gewrichten lastiger ten opzichte van de eerder aangedragen methoden.

In Hoofdstuk 6 wordt een vierde methode om de boordiepte te controleren aangedragen. Een sensor bij de nozzle registreert de boordiepte, waarna de waterstraal wordt stopgezet wanneer een vooraf ingestelde boordiepte is bereikt. De waterstraal kan zowel bij de nozzle als de pomp worden stopgezet. Experimenten met prototypes tonen aan dat de boordiepte-nauwkeurigheid van deze controlemethode volstaat voor het uitvoeren van beenmergstimulatiebehandelingen. Een nadeel van deze controlemethode is dat een sensor de afmetingen van het instrument toe doet nemen, wat nadelig kan zijn tijdens het positioneren van het instrument in een gewricht.

Om een ontwerper van een medisch waterstraalinstrument ontwerprijheid te geven (stap 4), is een studie verricht naar de invloed van de totale toegevoegde volume aan water op het volume aan verwijderd bot. Het totale volume aan water en de botdichtheid correleert met hoeveelheid aan bot dat wordt verspaand. Dit betekent dat de waterstraaldiameter, druk en waterstraaltijd elkaar kunnen compenseren om een bepaald volume aan bot te verwijderen. Dit geeft een ontwerper een ontwerprijheid in keuzes die gemaakt dienen te worden. Zo kan bij de toepassing voor minimaal invasieve chirurgie een lagere druk en kleinere waterstraal diameter en een langere waterstraaltijd bijdragen aan de reductie van de afmetingen.

Het verder ontwikkelen van een minimaal invasief waterstraalinstrument vergt meer onderzoek op ten minste vijf gebieden. Ten eerste dient onderzocht te worden of waterstraalboren klinisch veilig is. Ten tweede dient een methode ontwikkeld te worden waardoor de nozzle op zijn plek blijft tijdens het waterstraalboren. Te veel instabiliteit kan leiden tot schade aan het omliggende weefsel. Een derde onderzoek dient zich te richten op het reduceren van de lengte die benodigd is om de nozzle aan de flexibele slang te bevestigen. Dit zal de benodigde flexibiliteit

van het instrument ten goede komen. Ten vierde zullen experimenten op kadavers uitgevoerd moeten worden om in kaart te brengen in welke mate de boorcapaciteit afneemt bij het gebruik van de prototypes met afmetingen die geschikt zijn voor minimaal invasieve chirurgie. Ten slotte dient de ergonomie onderzocht te worden, zodat de chirurg op intuïtieve wijze het instrument kan besturen. Enig onderzoek naar de vijf aangedragen onderwerpen is reeds verricht. Hieruit blijkt dat geen van de uitdagingen onoverkomelijk zijn.

Dit onderzoek heeft aangetoond dat beenmergstimulatiebehandelingen mogelijk uitgevoerd kunnen worden met waterstraaltechnologie. Het onderzoek kan als opstapje dienen voor de toepassing van waterstraaltechnologie voor andere behandelingen, zoals implantaat revisies, chirurgie aan kraakbeen en pezen, en het voorboren van gaten in bot voor schroefbevestigingen. De aangedragen methoden om de boordiepte te kunnen controleren kunnen gebruikt worden in de tandheelkunde (boren, plakverwijdering), mijnbouw (boren tot specifieke diepte), voedselindustrie (snijden, vullen met kruiden) en reddingsmissies (verwijderen van puin).

Chapter 1

Introduction

Introduction

Orthopedic surgery is a surgical discipline that is concerned with the treatment of the musculoskeletal system. Many orthopedic treatments involve cutting, drilling, sawing, piercing or other forms of machining bones, joints and ligaments of the human body. To perform these actions on bone tissue, the use of water jet technology can provide several advantages over the use of conventional surgical instruments. First, water jet technology is a non-thermal machining method [1], whereas conventional drilling, cutting or sawing instruments heat up the surrounding healthy tissue above 55 degrees Celsius [2, 3]. Temperatures above 55 degrees Celsius will lead to necrosis and impaired healing of the healthy tissue [4-6]. Secondly, a water jet instrument can be made compliant or flexible, which allows increased maneuverability in tight joint spaces during surgery. The increased maneuverability allows anatomic locations to be reached that cannot be treated by conventional rigid instruments. Thirdly, a water jet allows selective tissue removal due to differences in mechanical properties between the tissues. Relative stronger tissues, such as cortical bone, can be preserved, whilst the adjacent relative softer material, such as trabecular bone or periprosthetic interface tissue, are affected by water jets. The selectivity in tissue machining can be adjusted during surgery by changing machine settings such as the pressure or the diameter of the water jet. Fourth, a surgical water jetting instrument can be dimensioned slender and snake-like, allowing key hole surgery (arthroscopic surgery) to be performed instead of open surgery. Arthroscopy leads to a faster recovery for the patient. Fifth, the debris particles that are created during drilling or sawing with water jets can be minimized by using small diameter (0.1 mm) water jet compared to the debris sizes (order of magnitude several mms) of conventional saw or drill surgical tools. As a result, more healthy tissue is left intact, which can improve the patient's recovery. A sixth reason why water jet technology can be beneficial over standard instruments is the contactless interaction between the tissue and the instrument. The lack of contact will result in a constant performance since the water jet instrument does not suffer from wear or become blunt. Finally, a single water jet instrument can be used for several tasks (with)in orthopedic treatments, such as cutting tendons, dissecting soft tissue and drilling, cutting or milling of bone. Currently, for each of these actions different instruments are required. Switching between the different applications that a single water jet instrument can perform only requires a single setting to be changed at the pump: the water jet pressure. Consequently, this single universal instrument can save costs and optimizes surgical workflow.

The advantages of an arthroscopic water jet instrument are abundant, yet such a device has not been developed nor researched. Therefore, the focus of this thesis is on the feasibility, safety and development of a water jet instrument that is capable to machine bone tissue. Four topics will be introduced in this introduction section.

First, for the development of the intended arthroscopic water jet instrument a specific target operation – bone debridement and marrow stimulation - is introduced. The execution of this procedure can greatly benefit from using water jets.

Second, the basics of water jetting are explained, providing background knowledge and initial design decisions. Third, an overview of current research of water jets in surgery is given. With this background information, in the final paragraph, the aim of this thesis and action plan on the development of an arthroscopic water jet instrument is laid out.

Bone debridement treatments

To elucidate the advantages of using water jets, the bone treatment is briefly delineated. Bone debridement treatments are the preferred method for treating damaged cartilage (osteochondral defects) in joints that is caused by trauma [7-9]. Systematic reviews show a clinical success rate of 86% for bone debridement in the knee and ankle [10, 11]. To achieve regeneration of the cartilage, the damaged cartilage tissue and the underlying calcified cartilage is debrided using a rigid curette (Figure 1, left) [9]. Then, 2-4 mm deep holes are made in the bone tissue to induce bleeding (microfracturing, Figure 1, center). A cloth of blood, containing mesenchymal cells, will cover the defect in the bone and cartilage (Figure 1, right). The mesenchymal cells adapt to the surroundings, thereby regenerating both the subchondral plate and the cartilage. Though the patient's pain is relieved, the renewed cartilage is of lower quality than the original, making it more prone to wear.

Currently, rigid instruments such as curettes, awls, K-wires and drill bits are used to cause the microfracturing of the calcified bone surface (Figure 1 and 2). Due to the limited space to maneuver in a joint space, sculling and hammering

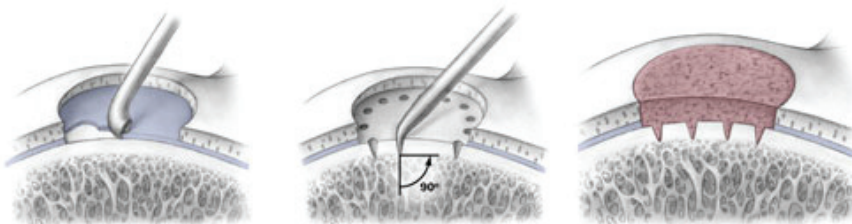


Figure 1. The consecutive steps of the bone debridement treatment. First, the damaged cartilage and calcified cartilage is removed with a curette (left). Then, small holes are made using an awl (center). The microfractures induce bleeding, which covers the defect, thereby contributing to the regeneration of the cartilage (right). Images courtesy of Mithoefer [12].



Figure 2. An arthroscopic image of the debridement of calcified cartilage. The joint space is limited, making it difficult to treat the tissue. Additionally, the tight space occasionally requires the rigid instruments to be sculled or hammered to achieve debridement and microfracturing, which can cause unwanted damage to surrounding healthy tissue. Image courtesy of Steadman [9].

on the instrument is frequently required to complete the treatment. For more complex situations, drill bits are used. As a result, the current rigid instruments can damage surrounding tissue either by inducing local pressure points (sculling), by unintentionally shooting out (hammering), by heat necrosis (drilling) [13], or impair healing caused by loose bone fragments [14].

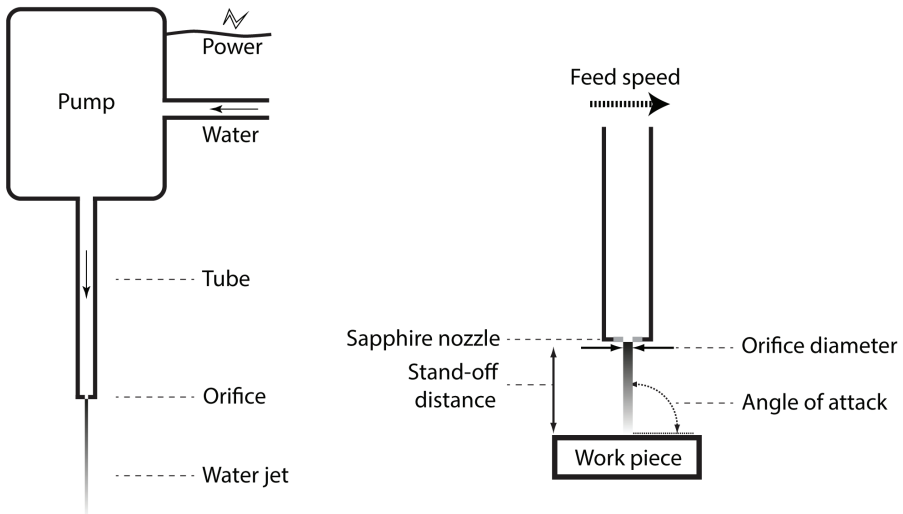


Figure 3. Simplification of a water jet system. Left: the pump creates a pressure by using energy and water. Tubing guides the water towards an orifice, where the water jet is created. Right: a close-up of the nozzle, indicating various machine settings.

Water jet machining basics

To create a water jet, water is to be pressurized and let out at one or multiple locations from its embodiment. In general, a pump is used to create the water pressure. The water is directed towards the location of interest using tubing. An orifice, usually a part of a sapphire or steel nozzle, is used to create a coherent water jet (Figure 3). Water is either provided by a source (tap), or the used water is being filtered and led back to the pump.

Various machine settings influence the machining capacity of a water jet: the suspension, pressure, orifice diameter, cutting speed or drilling time, angle of attack, stand-off distance and the nozzle design. In the following paragraphs the machine settings are briefly discussed.

Suspension

Globally speaking, three suspension types can be distinguished [15]. The most simple form is a pure water jet (PWJ) where only the energy of the water jet is used for cutting or drilling (Figure 4, left). PWJ is primarily used in the industry for cutting paper, cardboard, food or thin plastic, such as dashboards for cars [15, 16]. For machining harder materials such as glass or steel, an abrasive water jet (AWJ) is required [15, 16] (Figure 4, center). Abrasives are hard solid particles that are added to the water jet stream. The particles acquire the velocity of the water jet, and provide the majority of the machining capacity by rapid erosion [17]. The third suspension type is slurry abrasive water jetting (SAWJ), where the abrasives are mixed with the

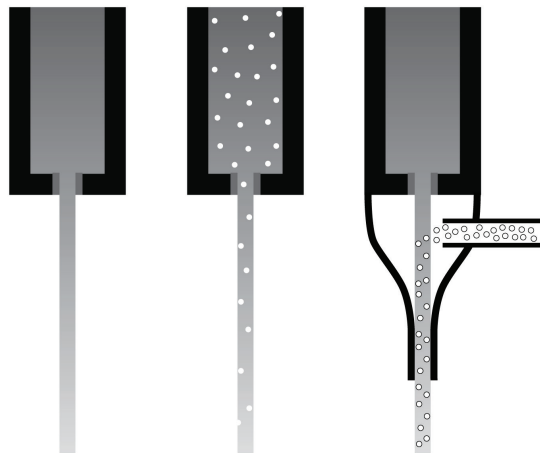


Figure 4. Three suspension types. Left: pure water jet (PWJ). Center: slurry abrasive water jet (SAWJ). Right: abrasive water jet (AWJ).

water before the fluid is accelerated through an orifice [15] (Figure 4, right).

PWJ machines stand out in simplicity, since no additional parts other than a pump, tubing and an orifice are required to achieve water jet cutting. AWJ machines are more powerful but also more complex than PWJ machines, since a precisely set-up abrasive feed mechanism is required. An advantage of a SAWJ machine is the absence of an abrasive feeder, allowing the nozzle head to be smaller. However, uniformly mixing the abrasives and an increased wear of the orifice and tubing can be challenging.

For bone debridement treatments, PWJ is considered the better option. This will be explained as follows. First, though biocompatible abrasives do exist [1, 18], no abrasive has been clinically approved, as to the best of the knowledge of the author. Second, PWJ technology allows instruments to be designed significantly smaller than when AWJ technology is used because an abrasive feed system is not required. Third, a PWJ system requires the least number of components compared to the other two options, which is advantageous for maintenance, sterilization, fabrication and minimizing costs.

Pressure and orifice diameter

The pressure and orifice diameter influence the machining capacity of a water jet in a similar way: when increased, the power of the water jet becomes greater, thereby increasing its destructive power [15, 19-22]. The water pressure directly affects the velocity of the water jet stream at the orifice, and thus the total volume of water per unit time (which can be considered equivalent to the power) that hits the material (see detailed formula's and explanation in Chapter 4). The orifice diameter quadratically affects the volume of water that is directed towards the material and thus will increase the water jet's destructive power quadratically [17]. Besides the increase in cutting or drilling depth, a wider water jet will increase the kerf width or hole diameter [19]. To a certain extent, the pressure and orifice diameter can compensate each other with respect to the destructive power of a water jet. For designers, this offers the freedom to adjust either one to accommodate specific requirements for specific medical treatments. For example, for minimal invasive surgery the dimensions of an instrument are to be minimized. In that case, a water jet instrument can be equipped with small orifice diameter in combination with a high water pressure.

Feed speed and jet time

The feed speed is the velocity in which the water jet transverses relative to the target material [15, 16]. For water jet drilling, the velocity is 0. The time that the water jet is directed towards a single point is called the drilling or jet time. Both the feed speed or the jet time affect the total energy that is directed towards the material,

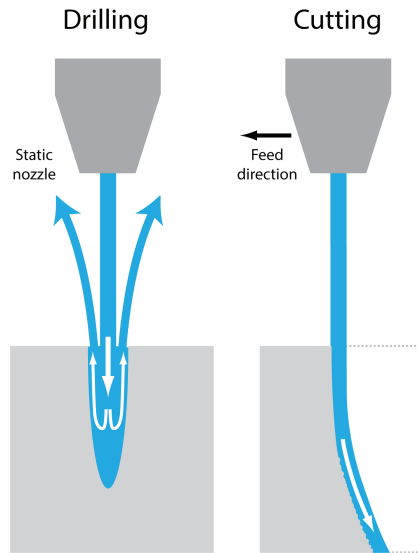


Figure 5. Drilling versus cutting. When drilling, turbulence is introduced due to interference with the excess water in the hole, impairing the drilling capacity compared to water jet cutting, where the jet is always directed towards the material.

which are highly correlated to the total volume of material that is removed. Increasing the cutting speed results in a shorter exposure of a specific part the material to the water jet, resulting in shallower depths [19, 20]. Increasing the drilling/jet time increases the exposure of the material to the water jet, resulting in deeper holes [23]. The mechanism of material removal for water jet cutting and drilling are different. When drilling, the excess water in the hole and the incoming water jet interfere with each other, causing turbulence and incoherency in the water jet which negatively affects the machining capacity. As a result, the coherent water jet does not directly interact with the sides of the hole that is being drilled, whereas for water jet cutting the destructive jet continuously erodes the material due to its feed speed (Figure 5). For industrial or medical application of water jets, research on water jet drilling is scarce.

Stand-off distance, angle of attack and nozzle design

The stand-off distance, angle of attack and the nozzle design affect the machining capacity of a water jet [15, 17]. The stand-off distance is the distance from the orifice to the target (Figure 3) [15]. In this space, the water jet has to travel through air or fluid, thereby losing energy with increasing distance. This decreases the depth of the cut or hole. The angle of attack is the angle between the water jet and the surface of the target material, which affects the interaction between the water

jet and the material [17]. The extent of the effect in machining capacity of the angle of attack depends on the material properties of a material (primarily its toughness) [17]. Therefore, it is difficult to quantify this effect by a general rule of thumb or linear relation. The design and material of the nozzle can have a critical impact on the coherency of a water jet. A stronger coherency of a water jet will result in a smaller target area that has to sustain the total power of the water jet. As a result, the energy density (W/m^2) of the water jet is larger [24]. This allows tougher or harder materials to be machined to a greater depth. Parameters that affect the coherency of the water jet are the length and shape of the inlet, the dimensions of the chamber in front of the orifice, the smoothness of the trajectory that the water has to follow towards the orifice, the material of the nozzle and the material of the orifice.

Mechanical properties of target material

The mechanical properties of the target material have the largest influence on the water jet's machining capacity. The maximum tension, compression and bending strengths, the modulus of elasticity, hardness and specific impact viscosity show a strong correlation with the water jet power required to machine the material [17]. In general, an increase in material strength requires more water jet machining capacity. Therefore, knowledge on the material properties is critical to choose adequate machine settings and nozzles.

For bone tissue, mechanical properties have been thoroughly investigated [25-27]. The composition and structure of the bone significantly affect its mechanical properties [28]. Since the bone structure adapts to the load it is to bear, variations in mechanical properties between and within a bone arise. This affects the local machinability of the bone with a water jet, causing variations in drilling depth. So far, interaction between a water jet and a bone with various bone structures have not been investigated, which is a prerequisite for the safe application of water jet drilling in any type of bone.

Water jets in surgery and current research

Water jet technology was first introduced in the mining industry in the 1930's [15]. Fifty years later, the technology progressed towards clinical applications. The first water jet surgery was reported in 1982 to perform liver resections [29]. Since then, water jet technology found its application in treatments of soft tissue, such as neurosurgery [30-32], surgery of the prostate [33], liver [34] and skin [35, 36], hydrosurgical debridement of wounds [37-39] and preparing skin grafts [40]. In

these treatments, the ability to spare tougher tissues such as nerves and veins whilst removing the target tissue is the primary advantage of using water jets. Commercial surgical water jet products such as the Erbejet [41] and Versajet [39, 42] are used in clinical, experimental or trial settings.

Water jet surgery of hard tissue requires more water jet power than surgery of soft tissue due to differences in mechanical properties such as the tensile strength and modulus of elasticity. In 2000, the first preliminary tests were performed in the field of orthopedic surgery by cutting bones and bone cement [43, 44]. More recently, prosthesis revisions and robot assisted bone surgery was investigated [45, 46].

For the development of a safe arthroscopic water jet instrument that is able to machine bone tissue, current research falls short on the various aspects. Previous research rigid industrial water jet set-ups were used to cut through bone tissue, which is different from a clinical situation where a compliant water jet instrument is to be manipulated and guided by the surgeon. Additionally, experimental water jet set-ups that were used to machine bone tissue in previous studies used cutting enhancing solid particles named abrasives. However, abrasives have never been approved for safe clinical use, whereas pure water jets that require a saline solution have been applied numerous in medicine and is considered safe [35, 36, 39, 47-49]. Nevertheless, commercially available pure water jet systems that can machine bone tissue do not exist. Furthermore, existing research has focused solely on water jet cutting, which is a different mechanism of material removal compared to drilling (see paragraph Water jet basics). As a result, the applicability of prior knowledge is limited. Furthermore, when water jet drilling, control over the drilling depth is required to ensure the patient's safety, which is not the case when cutting since a jet absorber can be placed behind the material to avoid an overshoot. The interaction of a water jet has never been investigated with varying bone structures that are caused by the bone's natural inhomogeneity. Since bone structures differ within and between patients, the relation between bone structure and machining capacity is a prerequisite to ensure the patient's safety. Finally, to summarize, the advantages of using a water jet instrument for arthroscopic orthopedic surgery are numerous, but research on this topic is scarce.

Aim

The aim of this thesis is to develop a compliant arthroscopic surgical instrument for bone debridement treatments that is based on water jet technology, with a focus on ensuring safety by gaining control over the drilling depth that is thwarted by the interaction between heterogeneous bone tissue and a water jet. The following

research questions are to be addressed for the development of such an instrument:

1. Is it possible to drill holes in articular bone tissue using pure water jets?
2. What hole dimensions in the bone debridement treatments result in optimal healing for the patient?
3. What water jet machine settings are to be used to drill holes in bone tissue to a specific depth?
4. How can the drilling depth be controlled considering the heterogeneity of the bone tissue?
5. What remaining challenges need to be addressed for arthroscopic water jet drilling?

Outline of this thesis

In Chapter 2 of this thesis, the feasibility of using pure water jets to drill in bone tissue is investigated and the minimum required water pressure is determined. In Chapter 3, optimal hole dimensions for bone debridement are considered by performing a literature review and a study with a caprine animal model. The dimensions are important input for the design of the water jet instrument. To achieve these optimal hole dimensions, control over the drilling depth is required. This can be solved in a feed forward system fed by preoperative knowledge on the local bone material properties, a feedback control loop system where the surgeon or instrument inhibits an overshoot, or a system that inherently limits the depth of drilling. In Chapter 4, feed forward system is discussed first as this would meet the conditions for a slender surgical instrument best. For this, the influence of primary machine settings on the drilling depth is determined. This influence is presented in predictive equations that allow precise drilling to a predetermined depth when the local bone structural properties are known. Furthermore, the chapter discusses the influence of the bone structure on the efficiency of a water jet, which could affect the minimum requirements of the irrigation system to remove superfluous water in the joint space. Although the feed forward concept is favored from an engineering perspective, the determination of local bone structural properties a priori in a clinical setting can be impractical and difficult to implement. Therefore, Chapter 5 describes a method that inherently limits the drilling depth, regardless the bone structural properties. This offers full drilling depth control, but at the cost of increase complexity of the design. In Chapter 6, the research questions are answered by discussing the previous chapters. Additionally, a further elaboration is made concerning depth control systems, the general applicability drilling depth control, the miniaturization of an arthroscopic water jet instrument and the future challenges for further development.

References

1. Schmolke, S., et al., Temperature measurements during abrasive water jet osteotomy. *Biomedizinische Technik*, 2004. 49(1-2): p. 18-21.
2. Eriksson, A.R., T. Albrektsson, and B. Albrektsson, Heat caused by drilling cortical bone. Temperature measured in vivo in patients and animals. *Acta Orthopaedica Scandinavica*, 1984. 55(6): p. 629-31.
3. Palmisano, A.C., et al., Comparison of cortical bone drilling induced heat production among common drilling tools. *Journal of orthopaedic trauma*, 2015. 29(5): p. e188-e193.
4. Moritz, A.R. and F.C. Henriques, Studies of Thermal Injury: II. The Relative Importance of Time and Surface Temperature in the Causation of Cutaneous Burns. *Am J Pathol*, 1947. 23(5): p. 695-720.
5. Eriksson, A.R. and T. Albrektsson, Temperature threshold levels for heat-induced bone tissue injury: a vital-microscopic study in the rabbit. *J Prosthet Dent*, 1983. 50(1): p. 101-7.
6. Lundskog, J., Heat and bone tissue. An experimental investigation of the thermal properties of bone and threshold levels for thermal injury. *Scand J Plast Reconstr Surg*, 1972. 9: p. 1-80.
7. Buckwalter, J.A., Articular cartilage: injuries and potential for healing. *Journal of Orthopaedic & Sports Physical Therapy*, 1998. 28(4): p. 192-202.
8. Giannini, S. and F. Vannini, Operative treatment of osteochondral lesions of the talar dome: current concepts review. *Foot & Ankle International*, 2004. 25(3): p. 168-175.
9. Steadman, J.R., W.G. Rodkey, and J.J. Rodrigo, Microfracture: surgical technique and rehabilitation to treat chondral defects. *Clin Orthop Relat Res*, 2001(391 Suppl): p. S362-9.
10. Zengerink, M., et al., Treatment of osteochondral lesions of the talus: a systematic review. *Knee Surgery, Sports Traumatology, Arthroscopy*, 2010. 18(2): p. 238-246.
11. Verhagen, R.A., et al., Systematic review of treatment strategies for osteochondral defects of the talar dome. *Foot and ankle clinics*, 2003. 8(2): p. 233-242.
12. Mithoefer, K., et al., Chondral resurfacing of articular cartilage defects in the knee with the microfracture technique. *Surgical technique. Journal of Bone and Joint Surgery-American Volume*, 2006. 88 Suppl 1 Pt 2: p. 294-304.
13. Murawski, C.D., L.F. Foo, and J.G. Kennedy, A Review of Arthroscopic Bone Marrow Stimulation Techniques of the Talus: The Good, the Bad, and the Causes for Concern. *Cartilage*, 2010. 1(2): p. 137-144.
14. van Bergen, C.J., P.A. de Leeuw, and C.N. van Dijk, Potential pitfall in the microfracturing technique during the arthroscopic treatment of an osteochondral lesion. *Knee Surgery, Sports Traumatology, Arthroscopy*, 2009. 17(2): p. 184-187.
15. Summers, D., *Waterjetting technology*. first ed. 1995: Taylor & Francis.
16. Momber, A.W. and R. Kovacevic, *Principles of abrasive water jet machining*. 1998, London: Springer.
17. Tikhomirov, R.A., et al., *High-pressure jetcutting*. 1992, New York: ASME Press. 197.
18. Honl, M., et al., The water jet as a new tool for endoprosthesis revision surgery - An in vitro study on human bone and bone cement. *Bio-Medical Materials and Engineering*, 2003. 13(4): p. 317-325.
19. Mohamed, M.A.K., *Waterjet cutting up to 900 MPa*. 2004, Universitat Hannover. p. 122.
20. Hoogstrate, A., *Towards high-definition abrasive waterjet cutting*. TU Delft, 2000.
21. Oweinah, H., *Leistungssteigerung des Hochdruckwasserstrahlschneidens durch Zugabe von Zusatzstoffen*. 1990: C. Hanser.
22. Imanaka, O. Experimental study of machining characteristics by liquid jets of high power density up to 108 Wcm⁻². in *Proc. 1st Int. Symp. Jet Cutting Tech.*, BHRA. 1972.
23. Akkurt, A., The effect of material type and plate thickness on drilling time of abrasive water jet drilling process. *Materials & Design*, 2009. 30(3): p. 810-815.
24. Chillman, A., M. Hashish, and M. Ramulu, Energy Based Modeling of Ultra High-Pressure Waterjet Surface Preparation Processes. *Journal of Pressure Vessel Technology-Transactions of the Asme*, 2011. 133(6).
25. Reilly, D.T., A.H. Burstein, and V.H. Frankel, The elastic modulus for bone. *J Biomech*, 1974. 7(3): p. 271-5.
26. Reilly, D.T. and A.H. Burstein, The elastic and ultimate properties of compact bone tissue. *J Biomech*, 1975. 8(6): p. 393-405.
27. Zioupos, P. and J.D. Currey, Changes in the stiffness, strength, and toughness of human cortical bone with age. *Bone*, 1998. 22(1): p. 57-66.
28. Day, J.S., *Bone Quality: The Mechanical Effects of Microarchitecture and matrix properties*. 2005, Optima Grafische Publicatie: Rotterdam.
29. Papachristou, D.N. and R. Barthers, Resection of the liver with a water jet. *British journal of Surgery*, 1982. 69(2):

- p. 93-94.
30. Keiner, D., et al., Water jet dissection in neurosurgery: an update after 208 procedures with special reference to surgical technique and complications. *Operative Neurosurgery*, 2010. 67: p. ons342-ons354.
 31. Balak, N., Quadrantectomy for resection of spinal ependymomas with a new classification of unilateral approaches regarding bone drilling and the use of a new tool: The Balak ball-tipped water jet dissector. *Interdisciplinary Neurosurgery*, 2016. 5: p. 18-25.
 32. Oertel, J., et al., Waterjet dissection in the brain: review of the experimental and clinical data with special reference to meningioma surgery. *Neurosurgical Review*, 2003. 26(3): p. 168-174.
 33. De la Maza, S.F., et al., Early clinical experience with water-jet dissection (hydro-jet) during nerve-sparing radical retropubic prostatectomy. *Minimally Invasive Therapy & Allied Technologies*, 2002. 11(5-6): p. 257-264.
 34. Rau, H.G., A.P. Duessel, and S. Wurzbacher, The use of water-jet dissection in open and laparoscopic liver resection. *HPB*, 2008. 10(4): p. 275-280.
 35. Hreha, P., et al., Water Jet Technology Used in Medicine. *Tehnicki Vjesnik-Technical Gazette*, 2010. 17(2): p. 237-240.
 36. Taghizadeh, R., S.P. Mackay, and P.M. Gilbert, Treatment of rhinophyma with the Versajet (TM) hydrosurgery system. *Journal of Plastic Reconstructive and Aesthetic Surgery*, 2008. 61(3): p. 330-333.
 37. Allan, N., et al., The Impact of Versajet (Tm) Hydrosurgical Debridement on Wounds Containing Bacterial Biofilms. *Wound Repair and Regeneration*, 2010. 18(6): p. A88-A88.
 38. Gravante, G., et al., Versajet hydrosurgery versus classic escharectomy for burn debridement: A prospective randomized trial. *Journal of Burn Care & Research*, 2007. 28(5): p. 720-724.
 39. Klein, M.B., et al., The Versajet (TM) water dissector: A new tool for tangential excision. *Journal of Burn Care & Rehabilitation*, 2005. 26(6): p. 483-487.
 40. Bibbo, C., VERSAJET (TM) Hydrosurgery Technique for the Preparation of Full Thickness Skin Grafts and the Creation of Retrograde Split Thickness Skin Grafts. *Journal of Foot & Ankle Surgery*, 2010. 49(4): p. 404-407.
 41. Tschan, C.A., et al., First experimental results with a new waterjet dissector: Erbejet 2. *Acta Neurochirurgica*, 2009. 151(11): p. 1473-1482.
 42. Gravante, G., G. Esposito, and A. Montone, Versajet((R)) hydrosurgery in burn wound debridement - Revised. *Burns*, 2008. 34(2): p. 299-299.
 43. Honl, M., et al., Water jet cutting of bone and bone cement. A study of the possibilities and limitations of a new technique. *Biomedizinische Technik*, 2000. 45(9): p. 222-227.
 44. Honl, M., et al., The use of water-jetting technology in prostheses revision surgery - First results of parameter studies on bone and bone Cement. *Journal of Biomedical Materials Research*, 2000. 53(6): p. 781-790.
 45. Kraaij, G., et al., Waterjet cutting of periprosthetic interface tissue in loosened hip prostheses: An in vitro feasibility study. *Medical engineering & physics*, 2015. 37(2): p. 245-250.
 46. Suero, E.M., et al., Robotic guided waterjet cutting technique for high tibial dome osteotomy: A pilot study. *Int J Med Robot*, 2017.
 47. Pascone, M., G. Papa, and A. Ranieri, Use of a novel hydrosurgery device in surgical debridement of difficult-to-heal wounds. *Wounds-a Compendium of Clinical Research and Practice*, 2008. 20(5): p. 139-146.
 48. Shekarraz, B., J. Upadhyay, and M.A.S. Jewett, Nerve-sparing retroperitoneal lymphadenectomy using hydro-jet dissection: Initial experience. *Journal of Endourology*, 2004. 18(3): p. 273-276.
 49. Yeh, C.C., Y.S. Lin, and K.F. Huang, Resurfacing of Total Penile Full-Thickness Burn Managed With the Versajet (TM) Hydrosurgery System. *Journal of Burn Care & Research*, 2010. 31(2): p. 361-364.

Chapter 2

Feasibility of using pure water jets for bone drilling

Sections:

Pure waterjet drilling of articular bone: an in vitro feasibility study

Pure waterjet drilling of articular bone: an in vitro feasibility study

*Steven den Dunnen, Gert Kraaij, Christian Biskup,
Gino M.M.J. Kerkhoffs, Gabrielle J.M. Tuijthof*

*“Pure waterjet drilling of articular bone: an in vitro feasibility study”
Strojniski vestnik - Journal of Mechanical Engineering, vol. 59, p 425-432, 2013*

The clinical application of waterjet technology for machining tough human tissues, such as articular bone, has advantages, as it produces clean sharp cuts without tissue heating. Additionally, water supply is possible via flexible tubing, which enables minimally invasive surgical access. This pilot study investigates whether drilling bony tissue with pure waterjets is feasible.

Water pressures between 20 and 120 MPa with an orifice of 0.6 mm were used to create waterjets to drill blind borings in the talar articular surface of cadaveric calcaneus bones of humans, sheep, goats and pigs. A stand-off distance between 2.5 and 5.5 mm and a jet time of 5 seconds were chosen. The depth of the holes was measured using a custom-adapted dial gauge.

At least 30 MPa of water pressure is required to penetrate the human and goat specimens, and 50 MPa for the pig and sheep specimens. Overall, the machined holes were conically shaped and increased in depth with an increase of pressure. Above certain pressure levels, pure waterjets can be used for machining holes in articular bone, thereby opening a window for further research on pure waterjet drilling in orthopedics.

Introduction

Since its first successful application in the 1970's by Hashish, waterjet technology has been applied in many industries [1] such as cutting cardboard, metals and frozen food [2,3]. For medical applications, differences in material properties of human organs allow precise dissection of soft tissue without damaging stronger tissues such as nerves or veins [4-6]. Especially the absence of tissue heating [7] and the always sharp and clean cut has led to further exploration of waterjet technology for application in orthopedic surgery [8-13]. Research in this field primarily involved cutting cortical bone with abrasive (small solid particles) waterjets for the preparation for arthroplasty [8-10, 13-15].

Additionally, waterjetting allows for water supply via flexible tubings which opens possibilities for minimally invasive surgical access. The focus of this study will be on the latter application for which it is important to investigate the feasibility of pure waterjets to drill holes in articular bone. Drilling holes in bones is frequently performed in for example microfracturing treatments and screw fixations [16,17]. Knowledge from previous studies cannot be used to determine the feasibility of pure waterjet drilling in articular bone as this differs completely from abrasive waterjet cutting. Differences lie in the interaction between the waterjet and the material, which causes the penetration depth using pure waterjet drilling to be less than for abrasive waterjet cutting. When cutting, the waterjet is translated over the material with a set feed speed (Fig. 1). The waterjet first strikes the edge of the material and exits at the opposite side. When drilling, the waterjet does not continue its path

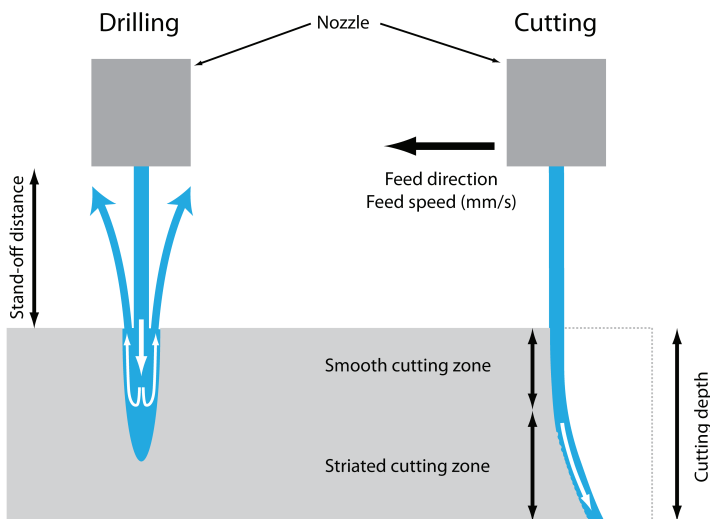


Figure 1. The difference in waterjet flow direction between waterjet drilling and cutting.

through all the material, but changes its trajectory 180 degrees after reaching the bottom of the hole (Fig. 1) [18,19]. Therefore, interference with the incoming waterjet is inevitable [2,3]. This leads to a disruption of the integrity of the waterjet and a turbulent flow in the boring, causing the impact pressure and kinetic energy to diminish [2,18,20].

To improve the cutting capacity of water jets, previous research involved the addition of abrasives to the waterjet [21]. Special biocompatible abrasives have been proposed and tested in a lab settings [8,15], but so far no clinical trials have been performed to verify their safe use. Other than that, articular bone toughness is presumably less than diaphyseal cortical bone. Therefore, an abrasive suspension might not be necessary to penetrate the articular bone. Since pure waterjets contribute to patients safety, pure waterjets are investigated in this study.

The aim of this study is to determine the feasibility of pure waterjet drilling in articular bone, and indicate the minimum water pressure required to penetrate articular bone. Sub goals are a) determination of the variation in the minimum penetration pressure. This variation can also be expected amongst the patients receiving surgical treatment and is therefore of concern for patient safety; b) global analysis of the shape of holes in bone, because specific hole profiles are desired for certain orthopedic treatments.

Materials and methods

A theoretical overview is set up regarding a) the main parameters that influence the machining capacity of a pure waterjet and b) the expected consecutive steps of the waterjet-material interaction when drilling a hole in articular bone. Based on this, starting conditions for the pilot study were chosen and interpretation of the results were facilitated.

Besides the mechanical properties of the material, the two dominant parameters for the machining capacity of a waterjet are the velocity and the volume of the water that is hitting the object [2]. An increase in either one of these parameters will increase the kinetic energy of the waterjet, which is transferred to the material on impact. Assuming water is incompressible, the relation between the waterjet velocity v_{liquid} [m/s] and the water pressure P [N/m²] and density ρ [kg/m³] is given by Bernoulli's equation:

$$v_{liquid} = \mu_v \cdot \sqrt{\frac{2P}{\rho}} \quad (1)$$

The velocity coefficient μv depends on the waterjet setup that is used, but is usually between 0.86 and 0.97 [22]. As the μv and ρ remain constant, the waterjet velocity is dependent solely on the water pressure. Therefore, pressure was chosen to be varied.

When drilling in articular bone, the waterjet needs to penetrate cartilage, subchondral bone and trabecular bone, consecutively. Each layer has a specific composition and material properties [23]. Mechanical properties that play a significant role in the effectiveness of waterjet machining are, in order of importance, the tensile strength, compressive strength, modulus of elasticity and hardness [3]. An increase in any of these properties will increase the strength of the material and thus the resistance to a waterjet. The tensile strength at the tissue level for articular cartilage, cortical bone and trabecular bone in human femora are approximately 30 MPa [24], 120 MPa [25,26] and 20 MPa [27,28], respectively. Even though these numbers on itself cannot be used to predict whether a waterjet can penetrate the bone tissue, the subchondral bone layer will most likely offer the highest resistance.

The cartilage is expected to be machined most easily as the modulus of elasticity and the hardness is lower than for trabecular bone [26,29]. Summarizing, the feasibility of drilling articular bone with pure water greatly relies on the ability to penetrate the subchondral plate. Increasing the water pressure will increase the waterjet's ability to penetrate this bone layer.

Waterjet drilling of bony tissue was performed on an industrial waterjet cutting system (Fig. 2a) equipped with a high pressure intensifier pump DU 400-4/PL. The cutting table was controlled by a Berger Lahr NC control system Posab 3300, which also regulated the waterjet time.

A waterjet nozzle diameter (Fig. 2b) of 0.6 mm and a jet time of five seconds was used in all experiments. The diameter of the machined holes created by this nozzle

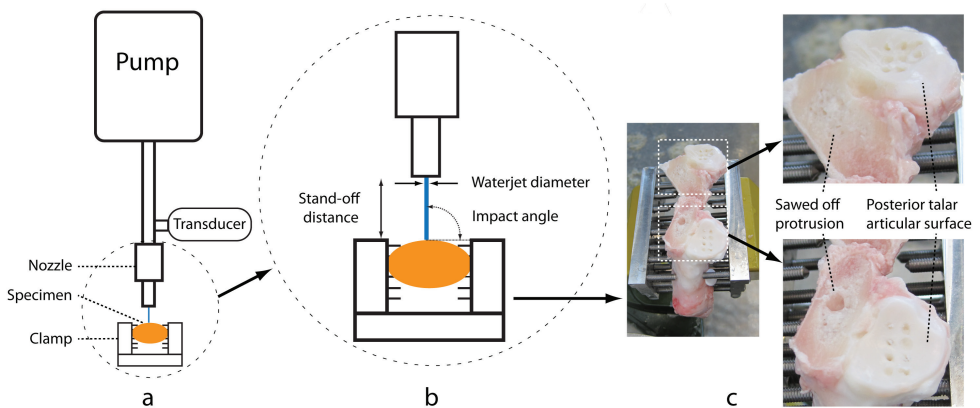


Figure 2. a) Overview of the experimental setup, b) potential waterjet settings, c) two bone specimens fixated in a clamp.

were most comparable to the 1.3 mm diameter holes that are frequently created in orthopedic microfracturing. Based on the experiments of Honl et al. [10], the water pressure was varied between 20 and 120 MPa. The genuine pressure was measured directly in front of the water jet cutting head at a sample frequency of 50 Hz by a WIKA high pressure transducer (type 891.23.610).

Fresh frozen calcanei of four mammals were obtained: five goat, six sheep, four pig and five human bones. The animals were chosen as they are frequently used for orthopedic animal-experiments due to their similar weight, metabolism [30,31] and bone volume fraction [32-34] as humans. The specimens were removed from the frozen storage 30 minutes before the experiment and sprinkled over with a 0.9% saline solution, thereby preserving the cartilage tissue and allowing the bone to come to room temperature before waterjet drilling. To prevent collision with the waterjet nozzle, protrusions were sawed off (Fig. 2c).

Holes were drilled in the posterior articular facet of the calcanei, at least 5 mm from the rim of the surface area to prevent drilling in cortical bone (Fig. 2c). A specially adapted clamp allowed for perpendicular alignment of the bone surface and the waterjet. Individually adjustable pins at the sides of the clamp provided a firm grip on the specimens (Fig. 2c). To prevent location based bias, holes were machined in a random order of sequence per calcaneus. Depending on the size of the articular surface six to nine holes were drilled at least 4 mm apart in each specimen. As perpendicular drilling enables the deepest cuts in cortical bone drilling [10], an impact angle of 90 degrees was used for all experiments (Fig. 2b). The stand-off distance between the nozzle and the specimen was set at 3 mm using a spacer. In practice, this led to a stand-off distance between 2.5 and 5.5 mm due to the curved articular surface of the bones.

The depth of the machined blind holes was measured with a dial-gauge where the standard 1 mm wide sensory tip was replaced by a 0.3 mm wide tip made out of pivot steel wire. The adaptation increased the measurement depth to 30 mm and decreased the minimum required hole diameter. The 0.3 mm tip was small enough to reach the bottom of the holes, but could not enter natural cavities in the undrilled trabecular bone. To prevent the trabecular bone from being damaged by the wire, the insertion force was kept between 0.2 and 0.3 N by using a spring. Three measurements were performed on each hole, and re-measurement was performed if the variation was larger than 0.25 mm.

The cartilage thickness was measured by inserting the dial gauge equipped with a sharp pin into an intact cartilage layer. The sharp pin penetrated the layer of cartilage, but was stopped by the harder subchondral bone plate. The distance covered by the pin was assumed equal to the thickness of the cartilage. For each mammal, this measurement was performed on two bone specimens at three different locations.

One specimen of each animal was scanned with a Scanco microCT80 scanner to examine the internal damage caused by the water jet and examine the shape of the

drilled holes. This allowed 20 holes to be examined, which was considered sufficient to determine a consistent trend in hole shape. Cartilage tissue damage was examined with a Keyence VHX-100 digital microscope equipped with a Keyence VHZ-35 lens.

The actual water pressures were calculated with a custom written Matlab routine. The hole-depth and the cartilage thickness measurements were averaged and rounded off to 0.1 mm. As the adapted dial-gauge measured the combined depth of the hole in the bone and the cartilage, the average thickness of the cartilage layer was subtracted to discriminate between pure bone waterjet drilling and cartilage waterjet drilling. For each specimen, the penetration pressure threshold was determined by the lowest pressure where a hole depth larger than 0 mm was drilled.

Table 1. Outcomes of experiment for each mammal calcaneus bone.						
	Average Cartilage Thickness (mm)	Total number holes drilled	No holes (depth of 0 mm)	Piercing holes	Immeasurable due to cavity in bone (>30 mm)	Average pressure to penetrate subchondral plate (MPa (SD*))
Goat	1.0	34	5	10	0	36 (5.9)
Sheep	0.8	48	19	2	0	62 (8.5)
Pig	1.2	32	15	0	0	56 (5.8)
Human	1.8	32	10	0	5	37 (10)

*SD: standard deviation

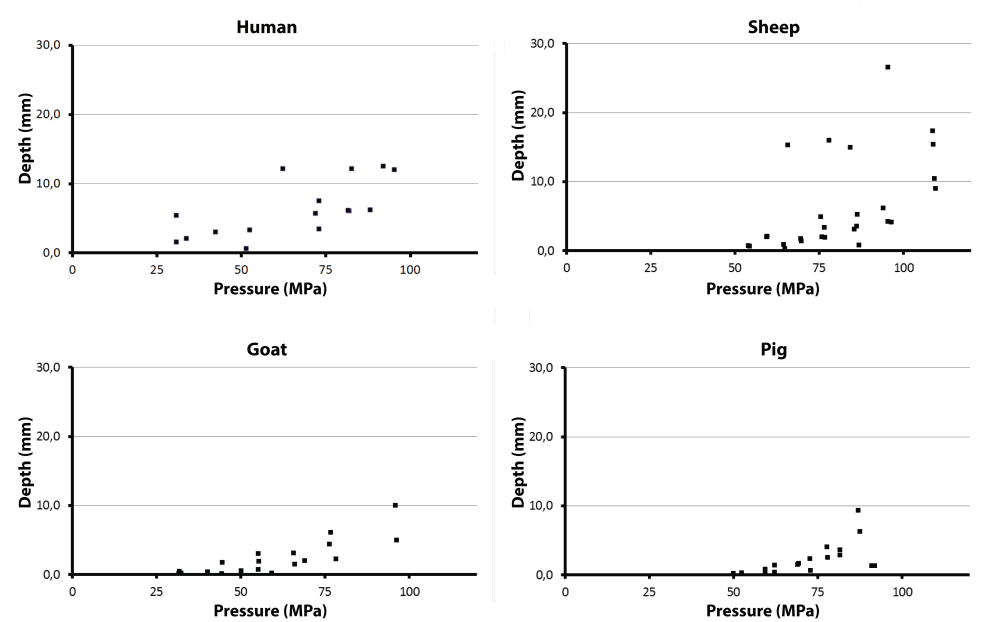


Figure 3. The outcomes of the waterjet pressure versus the depth of the machined hole for four different mammal calcaneus bones.

Results

Pure waterjets can be used for machining holes in subchondral bone. The minimum-threshold pressure for drilling in subchondral bone of human, goat, sheep and pig calcaneus bone were 37 (SD 10), 36 (SD 5.9), 62 (SD 8.5) and 56 MPa (SD 5.8) respectively (Table 1). In general, the cutting depth increases with pressure (Fig. 3). The gradual rise in depth is most apparent for goat and pig specimens, while sheep and human bone show a more scattered plot.

Observations showed that pressures below the minimum-thresholds caused a continuous waterjet reflection at an angle of approximately 30 degrees to the surface. This induced dents in the cartilage, which were approximately 50% larger in diameter (from 2 to 3 mm) compared to holes that penetrated bone. The reflection angle to the surface increased when the waterjet did penetrate bone. Besides exiting at the hole, water escaped at the sawed-off protrusion (Fig. 2a and 4).

For the majority of the specimens, a pressure of 30 MPa was sufficient to penetrate the cartilage up to the subchondral plate (Table 1). The μ CT-scans showed consistently that the waterjets create cone-shaped holes running from the subchondral plate into trabecular bone (Fig. 4).

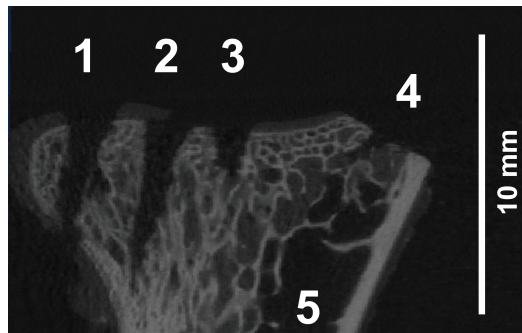


Figure 4. A slice of a μ CT scan of goat bone with three machined holes; 1) full penetration of the bone, 2) and 3) cone shaped holes, 4) the sawed-off protrusion, and 5) a natural cavity in the bone.

Discussion

The pilot study demonstrated that waterjet drilling with pure waterjets can machine blind holes in articular bone. The minimum water pressure ranged between 36 (average goat) to 62 MPa (average sheep). Variation in minimum water pressure

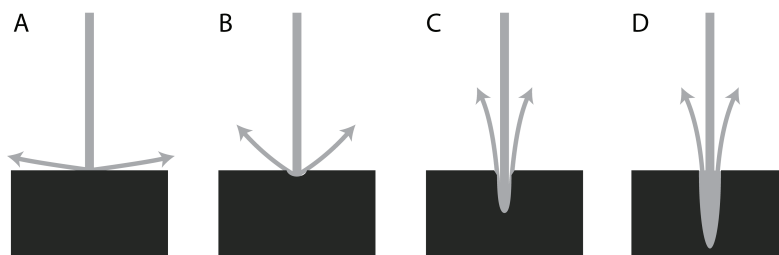


Figure 5. Different stages of waterjet drilling; a) reflection tangential to the surface, b) small cavity changes reflection angle, c) incoming and outgoing waterjets start to interfere, widening the hole beyond the waterjet diameter, and d) hole depth and diameter are further increased (based on [2,3,18,19]).

between the animals and between specimens indicate that one pressure will result in a variance of hole depth. These variations can be caused by differences in bone volume fraction and thicknesses of cartilage, subchondral and trabecular bone layers. An increase in bone volume fraction or the thickness of the subchondral bone layer results in stronger bone [32,35] that is more resilient to waterjets. For waterjet drilling with similar pressures, human and sheep bone show a larger deviation in hole depth compared to goat and pig specimens (Fig. 3). A possible cause for the larger deviation can be the consistency in origin, forage, treatment and age of the animals, which has a great influence on the mechanical properties of bone [36,37]. The goat and pig bone specimens were acquired from cattle that was nurtured under similar circumstances. For human and sheep cadaveric bone specimens, the age and gender were unknown, thereby contributing to the larger difference in depths for similar pressures.

The results support Equation 1 which indicates that an increase of hole depth is expected by an increase of water pressure. Impact pressures, frictional drag and shockwaves are all intensified at higher pressures, which contribute as well to the forming of a deeper hole [3,38].

The larger dents in the cartilage when the subchondral plate was not penetrated can be explained by the difference in material properties between the bone layers in combination with the reflection angle of the waterjet after impact. During the drilling process, the reflection angle increases with the hole depth (Fig. 5a to d). When the minimal penetration pressure threshold is not met, the energy of the waterjet is insufficient to machine the subchondral plate. Instead of continuing its original path, the water spreads tangential to the surface (Fig. 5a) [3,18], which damages the surrounding cartilage. When the pressure threshold is met, this phenomenon is only present for a split second, thereby leaving an smaller dent.

The four μ CT scans gave a view of the shape on 20 holes that were machined by pure waterjets. This does not allow for generalization, but does demonstrate a consistent trend. The holes showed a decrease in diameter with an increase of depth (Fig. 4). The conical shape of the holes can be explained by the variances in the

intensity of the interfering incoming and outgoing water jets. At the top of the hole, the incoming jet enters the water-filled cavity, resulting in disturbances in the water flow and a decrease in the waterjet velocity (Fig. 5). The waterjets' energy is dissipated by pushing the superfluous water towards the circumference and the exit of the hole. This results in a widening of the hole (Figs. 5c and d). At greater hole depths, the waterjets' energy has been partially dissipated, causing the superfluous water to be pushed out at a lower velocity. As a result, the hole diameter at the bottom of a hole increases at a slower pace compared to the shallow depths. This conical shape is potentially useful in orthopedic treatment such as screw fixation or bone marrow stimulation.

The pre-programmed CNC controlled nozzle caused some holes to be drilled too close to the rim of the bone, where the bone is thinner than 5 mm. This primarily occurred in goat bone, which had the smallest dimensions compared to the other calcaneal bones. In these cases, the bone was fully penetrated (piercing hole) and could not be measured (Table 1, column piercing hole). The missing values of the piercing holes are not considered to have a great effect on the outcomes of this study. For human specimens, 5 holes could not be measured because the holes were deeper than the maximum of 30mm the adapted dial-gauge could measure (Table 1). In these cases, the water pressures were considerably higher than the minimum pressure for penetrating articular bone and therefore do not affect the conclusions of this study. Nevertheless, an increase of the sample size and smaller water pressure increments could have contributed to a higher accuracy in determining the minimum pressure threshold.

The sawed-off protrusion might have caused an increase in hole depth. When a slug of water reaches the bottom of a hole, it tries to find the path with the least resistance towards an exit. For waterjet drilling in non-porous materials, the primary exit is the hole itself (Figs. 1 and 5c to d). The open trabecular structure in combination with a sawed-off protrusion allowed the water to leave at a secondary exit, thereby partially taking away the interference between the incoming and outgoing jets. Consequently, the drilled holes in this pilot experiment are expected to be deeper than when drilling bone that is complete, which is favorable from the safety point of view.

Fluctuations in the water pressure caused by the intermittently reciprocating plungers [12] can have caused variations in the hole depths, but they were considered marginal compared to the variations in material characteristics of the bone.

The experiment showed a range of pressures and a resulting range of in depth which clearly indicates the influence of bone material properties. These results show that pig bone is most difficult to be machined, which can be considered for future experiments to investigate waterjet settings that can penetrate any type of articular bone. For clinical safety, controlling the depth of a waterjet machined hole is an issue that needs to be addressed. Solely using pressure to control the depth is insufficient

due to the heterogeneous characteristics of the bone tissue. To this extent, an additional safety system that shuts off the waterjet after penetrating the suchondral plate is recommended. Nonetheless, piercing bone is unlikely as in orthopedics the majority of the holes are drilling towards the center of a bone where the bone is thicker.

Conclusion

Machining blind holes in bone by using waterjet technology is feasible without adding abrasives. A minimum pressure threshold needs to be overcome before any damage is inflicted. This threshold differs for every animal tested. A waterjet pressure of 60 MPa is sufficient to inflict damage to the majority of articular bone tissue and should be considered as a starting point for future research. The conical shape of the holes makes pure waterjet drilling in bone interesting for orthopedic treatments.

Acknowledgements

Prof. Dr.-Ing. Fr.-W. Bach, head of the Institute of Materials Science in Hannover, receives our acknowledgement for the use of the facilities at the Water Jet Laboratory Hannover. We are grateful to A.C. Kok, I.N. Sierevelt and J.R.A. Dukker for their help in respectively the preparations of the experiment, statistics and fabrication of experimental equipment. Finally, we would like to thank dr. ir. B. van Rietbergen and dr. ir. L. Mulder (Eindhoven University of Technology) for using the μ CT scanner and providing μ CT imaging related support.

This work was supported by the Technology Foundation Stichting voor de Technologische Wetenschappen (STW), Applied Science Division of NWO, and the technology program of the Ministry of Economic Affairs, The Netherlands (grant number 10851). The sponsor had no involvement in the study design, analysis or interpretation of the data.

References

1. Hashish, M., Duplessis, M.P. (1978). Theoretical and Experimental Investigation of Continuous Jet Penetration of Solids. *Journal of Engineering for Industry-Transactions of the ASME*, vol. 100, no. 1, p. 88-94.
2. Summers, D. (1995). *Waterjetting technology*. Taylor & Francis, London.
3. Tikhomirov, R.A., Petukhov, E.N., Babanin, V.F., Starikov, I.D., Kovalev, V.A. (1992). *High-pressure jetcutting*. ASME Press, New York.
4. Cadavid, R., Jean, B., Wustenberg, D. (2009). On the selection of the nozzle geometry and other parameters for cutting corneal flaps with waterjets. *Biomedizinische Technik*, vol. 54, no. 3, p. 134-41.
5. Bibbo, C. (2010). Versajet (TM) Hydrosurgery Technique for the Preparation of Full Thickness Skin Grafts and the Creation of Retrograde Split Thickness Skin Grafts. *Journal of Foot & Ankle Surgery*, vol. 49, no. 4, p. 404-407.
6. Tschan, C.A., Keiner, D., Muller, H.D., Schwabe, K., Gaab, M.R., Krauss, J.K., Sommer, C., Oertel, J. (2010). Waterjet dissection of peripheral nerves: An experimental study of the sciatic nerve of rats. *Neurosurgery*, vol. 67, suppl. 2, p. 368-376.
7. Schmolke, S., Pude, F., Kirsch, L., Honl, M., Schwieger, K., Kromer, S. (2004). Temperature measurements during abrasive water jet osteotomy. *Biomedizinische Technik*, vol. 49, no. 1- 2, p. 18-21.
8. Honl, M., Rentzsch, R., Muller, G., Brandt, C., Bluhm, A., Hille, E., Louis, H., Morlock, M., (2000). The use of water-jetting technology in prostheses revision surgery - First results of parameter studies on bone and bone Cement. *Journal of Biomedical Materials Research*, vol. 53, no. 6, p. 781-790.
9. Honl, M., Rentzsch, R., Schwieger, K., Carrero, V., Dierk, O., Dries, S., Louis, H., Pude, F., Bishop, N., Hille, E., Morlock, M., (2003). The water jet as a new tool for endoprosthesis revision surgery - An in vitro study on human bone and bone cement. *Bio-Medical Materials and Engineering*, vol. 13, no. 4, p. 317-325.
10. Honl, M., Schwieger, K., Carrero, V., Rentzsch, R., Dierk, O., Dries, S., Pude, F., Bluhm, A., Hille, E., Louis, H., E., Morlock, M., (2003). The pulsed water jet for selective removal of bone cement during revision arthroplasty. *Biomedizinische Technik*, vol. 48, no. 10, p. 275-280.
11. Schwieger, K., Carrero, V., Rentzsch, R., Becker, A., Bishop, C., Hille, E., Louis, H., Morlock, M., Honl, M. (2004). Abrasive water jet cutting as a new procedure for cutting cancellous bone - In vitro testing in comparison with the oscillating saw. *Journal of Biomedical Materials Research Part B-Applied Biomaterials*, vol. 71B, no. 2, p. 223- 228.
12. Bach, F.-W., Biskup, C., Kremer, G., Schmolke, S. (2007). Investigation of the AWIJ-Drilling Process in Cortical Bone. *Proceedings of the 2007 American WJTA Conference and Expo*, 1-D.
13. Hloch, S., Valicek, J., Kozak, D. (2011). Preliminary Results of Experimental Cutting of Porcine Bones by Abrasive Waterjet. *Tehnicki Vjesnik-Technical Gazette*, vol. 18, no. 3, p. 467-470.
14. Honl, M., Rentzsch, R., Lampe, F., Muller, V., Dierk, O., Hille, E., Louis, H., Morlock, M., (2000). Water jet cutting of bone and bone cement. A study of the possibilities and limitations of a new technique. *Biomedizinische Technik*, vol. 45, no. 9, p. 222-227.
15. Kuhlmann, C., Pude, F., Bishop, C., Krömer, S., Kirsch, L., Andreae, A., Wacker, K., Schmolke, S., (2005). Evaluation of potential risks of abrasive water jet osteotomy in-vivo. *Biomedizinische Technik. Biomedical engineering*, vol. 50, no. 10, p. 337.
16. Steadman, J.R., Rodkey, W.G., Rodrigo, J.J. (2001). Microfracture: surgical technique and rehabilitation to treat chondral defects. *Clinical Orthopaedics and Related Research*, vol. 391, p. S362-369.
17. Asnis, S.E., Kyle, R.F. (1996). *Cannulated Screw Fixation: Principles and Operative Techniques*. Springer, New York.
18. Orbanic, H., Junkar, M. (2004). An experimental study of drilling small and deep blind holes with an abrasive water jet. *Proceedings of the Institution of Mechanical Engineers Part B-Journal of Engineering Manufacture*, vol. 218, no. 5, p. 503-508.
19. Ohlsson, L., Ivarson, A., Magnusson, C., Powell, J. (1992). Optimisation of the piercing or drilling mechanism of abrasive water jets. *Fluid Mechanics and Its Applications*, vol. 13, p. 359-370.
20. Leach, S., Walker, G. (1966). The application of high speed liquid jets to cutting. *Philosophical Transactions of the Royal Society of London*, vol. 260A, no. 1110, p. 295-308.
21. Hashish, M. (1989). An Investigation of Milling with Abrasive-Waterjets. *Journal of Engineering for Industry-Transactions of the ASME*, vol. 111, no. 2, p. 158-166.
22. Momber, A.W., Kovacevic, R. (1998). *Principles of Abrasive Water Jet Machining*. Springer, London.
23. An, Y.H., Draughn, R.A. (2000). *Mechanical testing of bone and the bone-implant interface*. CRC Press, Boca

- Raton.
24. Kempson, G.E. (1982). Relationship between the tensile properties of articular cartilage from the human knee and age. *Annals of Rheumatic Diseases*, vol. 41, no. 5, p. 508- 11.
 25. Reilly, D.T., Burstein, A.H. (1975). The elastic and ultimate properties of compact bone tissue. *Journal of Biomechanics* , vol. 8, no. 6, p. 393-405.
 26. Burstein, A.H., Reilly, D.T., Martens, M. (1976). Aging of bone tissue: mechanical properties. *Journal of Bone and Joint Surgery-American Volume*, vol. 58, no. 1, p. 82-86.
 27. Kuhn, J.L., Goldstein, S.A., Ciarelli, M.J., Matthews, L.S. (1989). The limitations of canine trabecular bone as a model for human: a biomechanical study. *Journal of Biomechanics*, vol. 22, no. 2, p. 95- 107.
 28. Odgaard, A., Hvid, I., Linde, F. (1989). Compressive axial strain distributions in cancellous bone specimens. *Journal of Biomechanics*, vol. 22, no. 8-9, p. 829-35.
 29. Athanasiou, K.A., Rosenwasser, M.P., Buckwalter, J.A., Malinin, T.I., Mow, V.C. (1991). Interspecies Comparisons of Insitu Intrinsic Mechanical-Properties of Distal Femoral Cartilage. *Journal of Orthopaedic Research*, vol. 9, no. 3, p. 330-340.
 30. Lane, J.G., Massie, J.B., Ball, S.T., Amiel, M.E., Chen, A.C., Bae, W.C., Sah, R.L., Amiel, D., (2004). Follow-up of osteochondral plug transfers in a goat model: a 6-month study. *The American Journal of Sports Medicine* , vol. 32, no. 6, p. 1440-50.
 31. Newman, E., Turner, A.S., Wark, J.D. (1995). The potential of sheep for the study of osteopenia: current status and comparison with other animal models. *Bone*, vol. 16, no. 4 Suppl, p. 277S- 284S.
 32. Teo, J.C.M., Si-Hoe, K.M., Keh, J.E.L., Teoh, S.H. (2007). Correlation of cancellous bone microarchitectural parameters from microCT to CT number and bone mechanical properties. *Materials Science and Engineering: C*, vol. 27, no. 2, p. 333-339.
 33. Siu, W., Qin, L., Cheung, W.H., Leung, K. (2004). A study of trabecular bones in ovariectomized goats with micro- computed tomography and peripheral quantitative computed tomography. *Bone*, vol. 35, no. 1, p. 21-26.
 34. Hildebrand, T., Laib, A., Muller, R., Dequeker, J., Rueggsegger, P. (1999). Direct three-dimensional morphometric analysis of human cancellous bone: Microstructural data from spine, femur, iliac crest, and calcaneus. *Journal of Bone and Mineral Research*, vol. 14, no. 7, p. 1167-1174.
 35. Bevil, G., Eswaran, S.K., Gupta, A., Papadopoulos, P., Keaveny, T.M. (2006). Influence of bone volume fraction and architecture on computed large-deformation failure mechanisms in human trabecular bone. *Bone*, vol. 39, no. 6, p. 1218-1225.
 36. Crenshaw, T.D., Peo, E.R., Jr., Lewis, A.J., Moser, B.D., Olson, D. (1981). Influence of age, sex and calcium and phosphorus levels on the mechanical properties of various bones in swine. *Journal of Animal Science*, vol. 52, no. 6, p. 1319-29.
 37. Zioupos, P., Currey, J.D. (1998). Changes in the stiffness, strength, and toughness of human cortical bone with age. *Bone*, vol. 22, no. 1, p. 57-66.
 38. Chen, L., Siores, E., Wong, W.C.K. (1996). Kerf characteristics in abrasive waterjet cutting of ceramic materials. *International Journal of Machine Tools & Manufacture*, vol. 36, no. 11, p. 1201- 1206.

Chapter 3

Bone debridement treatments: optimal hole dimensions to improve cartilage regeneration

Sections:

Is technique performance a prognostic factor in bone marrow stimulation of the talus?

No effect of hole geometry in microfracture for talar osteochondral defects

Is technique performance a prognostic factor in bone marrow stimulation of the talus?

*Aimee C. Kok, Steven den Dunnen, Gabrielle J.M. Tuijthof, C. Niek van Dijk,
Gino M.M.J. Kerkhoffs*

*“Is Technique Performance a Prognostic Factor in
Bone Marrow Stimulation of the Talus?”*

The Journal of Foot & Ankle Surgery, vol. 51, p 777-782, 2012

Although results of bone marrow stimulation in osteochondral defects of the talus (OCDT) have been satisfactory, the technique performance has not yet been subjected to review as a prognostic factor.

The aim of this systematic review is to determine whether variation within technique influences outcome of bone marrow stimulation for OCDT.

Electronic databases were searched for articles on OCDT treated with bone marrow stimulation techniques, providing a technique description. Six articles on microfracture were included (198 patients). Lesion size averaged 0.9 cm² to 4.5 cm², and follow-up varied from 2 to 6 years.

Key elements were removal of unstable cartilage, hole depth variation between 2 and 4 mm until bleeding or fat droplets occurred, and a distance between the created holes of 3 to 4 mm. The success rate (excellent/good results by any clinical outcome score) was 81%. There is a vast similarity in the technique with similar outcomes as in previous general reviews; therefore variation in technique as currently described in the literature does not seem to influence the outcome of bone marrow stimulation for OCDT.

Whether the instruments used or the hole depth and geometry influence clinical outcome remains to be determined. Microfracture is safe and effective for OCDTs smaller than 15 mm. However, in this review, only 81% of patients obtained satisfactory results. Larger clinical trials are needed with clearly defined patient groups, technique descriptions, and reproducible outcome measures to provide insight in the specific indications and the preferred technique of bone marrow stimulation.

Introduction

An osteochondral defect is a lesion involving articular cartilage and subchondral bone often caused by a traumatic event. Osteochondral lesions of the talus (OCDT) are reported in more than 6% of acute ankle sprains [8, 40], up to 25% in chronic lateral ankle instability [15], and up to 50% of acute ankle fractures [41]. Symptoms are deep ankle pain on weight bearing and prolonged joint swelling. When conservative treatment does not lead to satisfactory results, arthroscopic debridement and bone marrow stimulation are simple and cost-effective operative treatments with a lower morbidity rate and a faster return to activity than open surgery [9, 14, 19, 41, 49]. Bone marrow stimulation is performed during arthroscopy by drilling the subchondral bone [1, 31, 38] or by using an arthroscopic awl to create microfracture holes [2, 46]. The subsequent bleeding induces an intrinsic healing process involving mesenchymal stem cells located in bone marrow, which results in fibrocartilage formation in the defect [44].

The results of bone marrow stimulation in OCDT have been satisfactory in 61% and up to 86% of patients [48, 49]. Recent studies in both the talus and the knee joint have analysed the influence of possible prognostic factors, such as lesion size [14, 20], location [14, 43], age [14, 30, 46], or body weight [20, 25] to account for the rate of therapy failure, but many results are contradictory and remain inconclusive [14, 33].

To our knowledge, there are no studies or reviews that have taken the specific operative technique of bone marrow stimulation into account. Because it is an invasive procedure, it is important to investigate the execution of the technique and the possible effects of its variation on the outcome [12, 45]. This includes the choice for either drilling or using an awl, because differences in biological reaction between drilling and the use of an awl have been observed in animal studies because of heat necrosis and impacted bone fragments [10, 12]. Also, we believe that paying greater attention to each separate step in the bone marrow stimulation procedure is important because each step has a different biological significance. This will be discussed in greater detail in the methods section.

The primary aim of this systematic review was to analyse the technique variation of bone marrow stimulation for treatment of osteochondral defects of the talus. Our hypothesis was that there is variation in the key steps of the technique performance with the key steps defined as debridement, introduction of the holes, and confirmation of adequate bleeding. We expected variation in the extent of debridement, instruments used, and dimensions and dispersion of the holes, as well as introduction of additional steps to the procedure. This allowed us to determine whether the technique itself is a prognostic factor for treatment outcome.

Materials and methods

Electronic databases (Cochrane Central Register of Controlled Trials, MEDLINE, EMBASE [classic]) were used for searching for clinical studies on microfracture or debridement and drilling published between 1946 and September 2010. Search terms for title and abstract were “microfracture,” “subchondral drilling,” “subchondral arthroplasty,” (also as MeSH term), or “Pridie drilling.” The references of eligible articles were screened by hand for additional articles.

Full-text articles with original patient groups were included when a clear description of the type of bone marrow stimulation treatment and details on the technique were given. Descriptive articles without patient groups, animal studies, articles on microfracture outcomes without a clear description of the technique, and case reports were excluded. All English, Dutch, German, French, and Italian articles were included (Fig. 1).

All articles were independently screened by two reviewers (A.K. and S.D.) by title and abstract. If the article was possibly eligible or the nature of the article was unclear, the full text was consulted. Any disagreement on inclusion or exclusion between the reviewers was resolved by discussion. Third-party adjudication was not necessary. The level of evidence was assessed by both reviewers using the Levels of

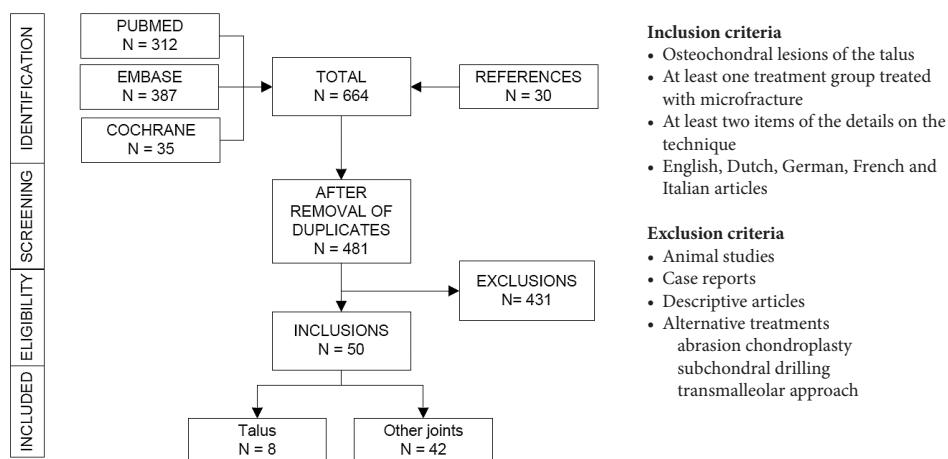


Figure 1. Flowchart outlining the article selection process. From the 664 identified articles, 50 articles remained after screening the title and abstract for eligibility and duplicate removal. In 42 articles, bone marrow stimulation was performed on other joints (knee, hip, shoulder) or the hallux. Six studies used awls to perform bone marrow stimulation. The remaining 2 studies used drilling with Kirschner wires. We excluded these 2 studies from further review because of a large risk of selection bias.

Evidence for Primary Research Question Chart of the Centre for Evidence-Based Medicine (Oxford, UK) as adapted by the Journal of Bone and Joint Surgery [3]. Included articles were scored on each of the items displayed in Table 2. The included articles were scored on the key elements of the technique, which were taken from the original article by Steadman et al [46], based on the key features to elicit the biological reaction that should take place. Sufficient debridement of the lesion is the first of the essential steps in this technique, first described by Magnuson [34]. Debridement of loose flaps prevents residual tissue to hamper the development of repair tissue. In addition to this mechanical factor, the removal can also decrease the inflammatory response within the joint that is caused by the damaged tissue. Debridement can decrease symptoms, but will not prevent the deterioration of the lesion [28]. Additional procedures at this stage are first the removal of the calcified tissue, if the base of the lesion has calcified. Removing this calcified layer first will improve the bonding of the repair tissue [18]. The preparation of a perpendicular rim creates a stable and defined defect that is surrounded by healthy cartilage as a solid scaffold for the repair tissue.

The formation of repair tissue is induced by the introduction of pluripotent mesenchymal stem cells from the subchondral vascular bone marrow. Defects that do not involve the subchondral bone plate and the boundary between the cartilage and the bone are secluded from this pool. This is the reason that abrasion of the base of the lesion alone is likely to not induce healing of the lesion [27, 36]. Also, it is known that pure chondral defects do not show intrinsic healing, because the subchondral bone plate is still intact. By penetrating the subchondral bone plate, an access is created, whether this is with an awl or by drilling. Too extensive debridement of the subchondral bone creates a risk of bone overgrowth and a thinner repair cartilage.

When placing the holes, it is important to leave sufficient space between the holes to prevent the intermediate bone from becoming unstable [35]. Also, the depth of the holes should be ample because shallow holes will not bleed and thus do not cause an influx of mesenchymal stem cells.

PASW Statistics 18.0.5 (IBM Corporation, Somers, NY) was used for data collection and analysis. Participants were patients with osteochondral defects of the talus who were treated by means of debridement and subsequent microfracture or subchondral drilling after failure of conservative therapy. Diagnosis was made by clinical evaluation and confirmed by conventional radiograph, MRI, and/or CT scan. The ankle joint was free of concomitant diseases, such as osteoarthritis, rheumatic arthritis, and associated injuries. Failure rate was defined as the necessity of reoperation because of persistent complaints, and/or a score below 70 points using the American Orthopaedic Foot and Ankle Society's Ankle Hindfoot Score (AOFAS-AHS). When there were different therapies performed in one study, data were extracted of the bone marrow stimulation groups only. In the event that articles did not provide the data necessary for our analysis, the missing data were requested

Table 1. Characteristics of the patient groups that received bone marrow stimulation of the included articles																	
Author/year of publication	Level of evidence	Cases (ankles)	M:F	Age in years (range)	Follow-up in months (range)	Cases lost to follow-up	Lesion size in cm²	Location lesion (N=, %)						% traumatic			
								Medial			Lateral				Central	Posterior	Medial and lateral
								Anterior	Central	Posterior	Anterior	Central	Posterior				
Becher et al. 2010	Level IV	45	25:20	40 (16-74)	70 (16-115)	6	0.5 – 2.0	9 (18%)	30 (67%)	12 (24%)	6 (12%)	11 (24%)	-	4 (9%)	69%		
Choi et al. 2009	Level III	51	37:14	35 (13-66)	44 (16-70)	0	1 (0.3-2.3)	18 (35%)	18 (35%)	-	-	6 (12%)	-	-	NA		
Gobbi et al. 2006	Level II	9 (10)	6:3	24 (17-28)	53 (24-119)	0	4.5 (1.5-8)**	-	3 (30%)	-	-	7 (70%)	-	-	NA		
Guo et al. 2010	Level IV	32	26:6	22 (12-52)	32 (12-59)	4	11.6 ± 3.5**	-	27 (84%)	-	-	5 (16%)	-	-	NA		
Lee et al. 2010	Level IV	35	27:8	35 (17-50)	33 (21-48)	0	0.9 (0.6–1.4)	-	29 (83%)	-	-	6 (17%)	-	-	86%		
Saxena et al. 2007	Level IV	26	18:8	36 (18-44)	32 (24-55)*	0	NA	9 (34%)	3 (12%)	-	12 (46%)	-	1 (4%)	-	NA		
Weighted averages				33 (12-74)			0.3 - 4.5		67 %			27%			80%		

* Study characteristics of the whole patient populations, including other study groups.

** Two studies only included patients with either lesions smaller or larger than 1.5 cm².

Article	Instrument	Dimensions	Dispersion	Debridement	Check	Technique and Additional Remarks
Becher et al. 2010	Arthroscopic awl	2-4 mm deep	3 to 4 mm apart	Limited synovectomy	Fat droplets	n/a
Choi et al. 2009	Microfracture awl	Multiple perforations, perpendicular to the joint surface	n/a	Removal of cartilage cap and excision of the lesion	Unstable chondral fragments, calcified layer.	Referring to Steadman et al [36]. Abrasion arthroplasty in case of loss of subchondral bone until a stable, smooth articular surface was created.
Gobbi et al. 2006	Microfracture awl	Multiple perforations, perpendicular to the joint surface	3 to 4 mm apart	Unstable chondral fragments, calcified layer.	Fat droplets and blood	Referring to Steadman et al [36]
Guo et al. 2010	Microfracture awl	approximately 4 mm deep	n/a	Yes	Bleeding	n/a
Lee et al. 2010	Arthroscopic awl	3-4 mm deep	3 to 4 mm apart	All unstable cartilage and fibrous tissues.	Fat droplets and blood	Sharp, perpendicular margins. Peripheral to centre in a spiral pattern with different angles.
Saxena et al. 2007	Chondropick	n/a	n/a	Yes	n/a	Caution to leave the subchondral bone plate intact.

* Items in the treatment performance were based on the original article by Steadman et al (12). In all studies, synovectomy or debridement was performed. Several additional recommendations or remarks were made by the authors. Two studies referred directly to the original article by Steadman et al in the technique description.

by correspondence with the authors. An overview of the requested data and the response is given in the Appendix.

A total of 664 articles were found (Fig. 1). Four hundred thirty-one articles were excluded for the following reasons: the article was not about microfracture in the sense of a therapy for osteochondritis dissecans (N=217), did not contain a technique description (N=52), was an abstract or congress report (N=20), was a descriptive article (N=116), was an animal study (N=16), or was an additional duplicate (N=10). Fifty articles on bone marrow stimulation met the inclusion criteria for further review. Forty-two articles concerned joints other than the ankle. The eight articles concerning osteochondral defects of the talus are reviewed here (Table 1). Six studies used awls to perform bone marrow stimulation. The remaining two studies used drilling with Kirschner wires [24]. We excluded these two studies from further review because we felt the results would run a large risk of bias because of the small number of studies.

Results

One randomized controlled trial, two prospective, and three retrospective case series were included (Table 1). The six included articles summarize the outcome of a total of 198 patients (199 ankles). Study size varied from 9 (10 ankles) to 51 patients, with a weighted average age of 34 (range: 13 to 74) years. The average follow-up varied from 2 to 6 years. The average of lesion size per study varied from 0.9 cm² to 4.5 cm². Two studies only included patients with either lesions smaller [32] or larger than 1.5 cm² [21]. In total, medial lesions were more prevalent than lateral lesions (70% and 27%, respectively). The remaining lesions were either centrally located or “kissing” lesions running from medial to lateral..

Technique

Technique descriptions in the different articles showed much similarity on the provided details of the bone marrow stimulation technique (Table 2). In all studies, synovectomy or debridement was performed. Hole depth was either 2 to 4 mm deep or not specified [17, 24, 41]. The distance between the holes, mentioned in three studies [5, 21, 32], was consistently between 3 and 4 mm. Authors from four studies visualized bleeding or fat droplets from the subchondral bone to confirm adequate treatment of the defect [5, 21, 22, 32]. Several additional recommendations were made: the preparation of a perpendicular rim to prevent the blood clot from detaching [32], complete and careful removal of the calcified layer on top of the subchondral plate [21] without damaging it [5], making holes perpendicular to the surface [13, 21], and

the sequence of the holes [32]. Two studies referred directly to the original article by Steadman et al [46] in the technique description [13, 21].

Clinical Outcome

Because of the heterogeneity of the studies, meta-analysis was not performed. Weighted averages were calculated from the clinical outcome scores and failure rates with respect to the number of procedures performed in the studies. The most prevalent outcome scale was the AOFAS-AHS [29], which was used in five studies [13, 21, 22, 32, 41]. The improvement on the last follow-up was significant in all studies (weighted average preoperative: 63, range 34 to 72; weighted average postoperative: 89, range 84 to 94). The visual analogue scale (VAS) [39] scores were used in three studies [5, 22, 32] (Table 3). VAS score for pain decreased from 6.8 (range 6.5 to 7) to 2.3 (range 2 to 2.51). Five studies divided the primary outcome into categories (excellent, good, moderate, poor) to evaluate the success rate of the procedure (4,32,34–36) (Table 3).

In total, 81% of the patients reached excellent to good results (range 66% to 96%), 13% retrieved a moderate result (range 2% to 29%), and the remaining 6% (range 0% to 10%) were considered a poor result. In the case of the AOFAS-AHS, “excellent” corresponded with an end score of > 90, “good” corresponded with a score between 80 and 90, “moderate” (or “fair”) corresponded with a score between 70 and 80, and a “poor” outcome was defined as a score below 70 or a failure of the therapy.

Failure Rate and Complications

The weighted average failure rate was 6% (range 0% to 19%, 13 out of 193 procedures; Table 3). In case of failure, bone marrow stimulation was performed again or a secondary therapeutic procedure was used, such as cartilage grafts, an ankle arthrodesis, or ankle prosthesis. Failure occurred on average 2 to 3 years after the initial surgery. The only reported complication was persistent pain after 24 months in one bilateral case [21]. Five studies reported no complications [5, 13, 22, 32, 41].

Prognostic Factors

Age or sex did influence the treatment outcome significantly in four and two studies, respectively. Anterior lesions had better clinical results in two studies when compared with central or posterior lesions [22, 41]. Anterior-medial lesions resulted in better AOFAS-AHS scores when compared with lateral lesions (44 vs. 56) and a faster return to activities (14 vs. 18 to 20 weeks). This was not seen with lesions located on the medial side of the talus [41]. Two studies show two separate prognostic factors that are not mentioned in the other four studies. Becher et al [5] found that degenerative chondral defects result in lower Hannover Scoring System

Table 3. Available preoperative and postoperative VAS and AOFAS scores in the microfracture studies with the categorical clinical outcome in the scoring system used (excellent, good, moderate, and poor) and the failure rate as a percentage of the respective patient group*

Article	VAS		AOFAS			Overall clinical outcome				Failure N=/total (%)		
	Preoperative	Postoperative	Preoperative	Postoperative		Scoring system	Excellent %	Good %	Moderate %		Poor %	
Becher et al. 2010	6.5	2.4	P < .001		NA	HSS	49	31	10	10	4/39 (10%)	
Choi et al. 2009	NA			87 ± 8	63 ± 17	P < .001	AOFAS	29	37	29	5	2/51 (5%)
Gobbi et al. 2006	NA			84	34	P < .001	AOFAS	NA				1/10 (10%)
Guo et al. 2010	7.0 ± 1.4	2.5 ± 2.5	P < .001	89 ± 11	72 ± 4	P < .001	AOFAS	-----87-----		3	10	6/32 (19%)
Lee et al. 2010	7 (5-8)	2 (0-5)	P < .05	90 (73-100)	63 (52-77)	P < .05	AOFAS	46	43	11	0	0/35 (0%)
Saxena et al. 2007	NA			94 ± 6	55 ± 8	P < .001	AOFAS	74	22	2	2	0/26 (0%)
Weighted averages	6.8 (range 6.5-7)	2.3 (range 2.2-5)		89 (range: 84-94)	63 (range 34-72)			81%		13%	6%	6%

Abbreviations: AOFAS, American Orthopaedic Foot and Ankle Society; HHS, Hannover Scoring System; VAS, visual analogue scale.

* Weighted averages were calculated based on the size of the patient groups per article.

(HSS) scores than traumatic osteochondral defects (60 vs. 86, $p < .001$) and VAS scores. The explanation would be that in osteochondral defects without signs of joint degeneration the cartilage around the defect is intact, whereas in degenerative lesions caused by posttraumatic loss of joint cartilage thickness in the presence of existing degenerative joint disease, the condition of the surrounding cartilage will also be inferior.

There are several prognostic factors that show conflicting results. Body mass index (BMI) was found to have a lower clinical outcome in patients with a BMI above 25 kg/m² on the HSS (84 vs. 75) and the

VAS scores for pain (1.6 vs. 3.0), with 18 patients below and 27 patients above 25 kg/m² [5]. Lee et al found no difference with 21 patients below 25 kg/m², but a smaller amount of patients above 25 kg/m² (N=14). Lastly, symptoms present more than one year resulted in lower scores for clinical outcome (AOFAS 86 vs. 93, $p < .05$) [32]. However, another study showed no significant influence of symptom duration [13].

Discussion

The aim of this systematic review was to determine whether variation in the technique influences the outcome of bone marrow stimulation in OCDT. It is shown that there is a high level of similarity in the descriptions of the technique performance. Unstable cartilage is removed; 2 to 4 mm deep holes are made with a distance of 3 to 4 mm between the holes and perpendicular to the surface in a spiral pattern from the outer rim to the centre of the defect. Additionally, a perpendicular rim is prepared to prevent the blood clot from detaching, and the calcified layer on top of the subchondral plate is completely but carefully removed.

An important difference between our study and that of previous reviews is that we selected articles specifically based on the description of the essential steps of the bone marrow stimulation technique. The high level of consistency in the disclosed details of the technique in our review does not allow for further analysis of the effect of different surgical techniques as a prognostic factor for outcome. However, it does show the clinical outcome of a consistent treatment strategy that is performed with specific attention drawn to the correct dimensions and placement of the microfracture holes. It provides insight into the possible influence of the correct effectuation of the microfracture technique on the variability of outcome with bone marrow stimulation. The characteristics of the study population are similar to those of studies that did not use this inclusion criterion (age, male/female ratio, length of follow-up, lesion size and location [16], aetiology [4, 31, 37, 40]). Also, the 81% success rate in our review was comparable with the success rates reported in previous reviews and studies: 81%

[4, 42], 87% [48], and 85% [47, 49], although obviously the experience and skills of the surgeon would influence outcome.

Because of the nature of the technique and the biological response it aims to elicit, it is vital that the key elements of the technique are accurately executed. However, recent literature suggests that the nature of the key elements as defined in the method section might be more delicate than the current guidelines advise, for example, 2 vs. 4 mm drill holes resulted in a different outcome in a recent animal study [11]. This has yet to be investigated in clinical studies.

Also, there is a difference in mechanism between the use of a microfracture awl and the drilling of a Kirschner wire. Both methods are arthroscopic procedures and are therefore relatively minimally invasive. The flexible Kirschner wire allows for drilling in different angles in a high congruent joint like the ankle. The rigid, angled awls allow for treatment “around the corner” and a better control for creating holes at the desired depth and perpendicular to the surface [6, 7], but these are difficult to use in posterior defects and hold the risk of damaging the tibial edge by wedging the instrument if used with too much force. There are no large comparative clinical studies available that compare drilling with microfracture. In the initial eligible studies, two different bone marrow stimulation techniques were used: the drilling of Kirschner wires or the use of an awl to puncture the subchondral plate. The first was described in only two studies and was excluded because of the risk of selection bias [17, 24]. However, both studies on drilling did indicate less satisfactory results compared with the included microfracture studies. This might be explained by the small amount of studies and the use of different outcome questionnaires. Both drilling studies used several different scoring systems and were not comparable. In Ferkel et al [17], the AOFAS postoperative score was 84 (range 34 to 100) and lesions were evaluated according to the grading on arthroscopy. This resulted in significant differences in clinical outcome between the lesions with intact cartilage (Cheng-Ferkel grade A-C) and those with (partially) detached cartilage (Cheng-Ferkel grade D-E).

Aside from microfracture and drilling, there is a vast amount of other surgical treatment options that use a different approach (retrograde drilling, bone marrow stimulation using a transmalleolar approach), or a different technique to elicit bleeding (abrasion arthroplasty) or that use grafts (osteochondral autograft transplantation, autologous chondrocyte implementation). It was not within the scope of this review to investigate the technique of these other treatment modalities for primary OCDT. Bone marrow stimulation is still the preferred treatment for primary OCDT [49], and although several attempts have been made to provide an algorithm for the choice of treatment, there is a lack of high-quality comparative studies to determine the appropriate treatment for each individual patient based on patient characteristics, lesion type, and other prognostic factors. When synthesizing these possible prognostic factors, we were confronted with several conflicting results in the current literature.

A BMI < 25 kg/m² [5, 32], anterior lesions [13, 22, 41], duration of symptoms less than one year [13, 32], and traumatic aetiology [5, 13] showed better clinical results in some articles, but were insignificant in others. Also, because we needed to exclude many articles based on the lack of a technique description, the number of studies that investigate a particular prognostic factor is very limited. Hence, we were unable to formulate any strong conclusions because of a lack of power.

However, there were two results that followed from our analysis. First, in two studies a larger lesion size negatively influenced outcome in the patient cohort, but did not provide data on the microfracture group only [13, 22]. However, Choi et al did report that in the patient cohort receiving either microfracture or abrasion arthroplasty, lesions smaller than 1.5 cm² showed significantly higher AOFAS scores at 48-month follow-up and a 90% good to excellent result, compared with 20% in lesions with a larger surface area. Two studies included only patients with lesions either smaller or larger than 1.5 cm² [21, 32]. Outcome was not comparable, but failure rates were 0% and 10%, respectively. Considering that lesion size is often overestimated or underestimated [42], the use of a grading system is a valid alternative. Adequate measurement of lesion dimensions is important to determine the appropriate therapeutic intervention for OCDT [23, 26].

Second, it has been previously suggested that advanced age is considered a relative contraindication [46] because of the diminished quality of bone and limited revalidation possibilities [30]. This review contains five articles with patients more than 50 years of age and up into the seventh decade, with four showing no differences in clinical outcome between patients younger than 50 years of age and those older [5, 13, 22, 32].

This review has limitations. Because of the selection criteria, only 6 studies were included, with a relatively small number of patients. The majority of articles were retrospective case series with limited statistical analysis. The articles that were excluded for this review showed a similar quality. The lack of strong evidence is a known problem in the literature for treatment osteochondral defects in the talus [33]. In our opinion, this not only shows the need for higher quality studies, but also underlines the necessity to supply more information on the exact nature of the intervention to improve reproducibility and allow for in-depth comparison of study groups in surgical interventions.

In conclusion, there is a large degree of similarity described in the literature in regard to bone marrow stimulation in the treatment of osteochondral lesions of the talus. Microfracture is a safe and effective therapy for OCDT with a diameter smaller than 15 mm. The percentage of total success of bone marrow stimulation of this defined and homogenous treatment procedure as defined by any clinical outcome score was 81%, which shows persistent improvement on an average follow-up of 70 months up to 14 years in one study. The failure rate was 6%. However, whether the instruments used or the hole depth and geometry influence clinical outcome remains

to be determined in clinical studies because these have not yet been investigated.

Larger, randomized clinical trials with homogeneous patient groups, an adequate description of the surgical intervention(s), elaborate lesion description and grading, and reproducible outcome measures would provide the opportunity to construct a founded theory for the indication for the use of bone marrow stimulation and prognostic factors. This would be valuable in the pre-selection of patients, which would increase the success rate by referring patients who have a high risk of treatment failure with another therapy regimen.

Acknowledgements

This work was supported by the Technology Foundation STW, the Applied Science Division of NWO, the technology program of the Ministry of Economic Affairs, The Netherlands, and the Marti-Keunig Eckhart Foundation, Lunteren, The Netherlands. The investigation was also supported by the Ministry of Economic Affairs of The Netherlands, and the Marti-Keunig Eckhart Foundation, Lunteren, The Netherlands.

References

- Alexander AH, Lichtman DM. Surgical Treatment of Transchondral Talar-Dome Fractures (Osteochondritis Dissecans): Long-Term Follow-up. *J Bone Jt. Surg Am.* 2008;62:646–652.
- Alford JW, Cole BJ. Cartilage restoration, part 2: techniques, outcomes, and future directions. *Am. J. Sports Med.* 2005;33:443–60.
- Anon. The Journal of Bone and Joint Surgery Instructions for Authors. Available at: <http://www.jbjs.org/public/instructionsauthors.aspx#LevelsEvidence>. Accessed July 1, 2011.
- Baker CL, Morales RW. Arthroscopic Treatment of Transchondral Talar Dome Fractures: A Long-term Follow-up Study. 1999;15:197–202.
- Becher C, Driessen A, Hess T, Giuseppe U, Nicola L. Microfracture for chondral defects of the talus: maintenance of early results at midterm follow-up. 2010:656–663.
- Bergen CJA Van, Leeuw PAJ De, Dijk CN Van. Treatment of osteochondral defects of the talus Traitement des lésions ostéochondrales de l'astragale. 2008:398–408.
- Bhosale AM, Richardson JB. Articular cartilage: Structure, injuries and review of management. *Br. Med. Bull.* 2008;87:77–95.
- Bosien WR, Staples OS RS. Residual disability following acute ankle sprains. *Bone Jt. Surg Am.* 1955;37:1237–1243.
- Buckwalter JA. Articular cartilage: injuries and potential for healing. *J Orthop Sport. Phys Ther.* 1998;28:192–202.
- Chen H, Chevrier A, Hoemann CD, Sun J, Ouyang W, Buschmann MD. Characterization of subchondral bone repair for marrow-stimulated chondral defects and its relationship to articular cartilage resurfacing. *Am. J. Sports Med.* 2011;39:1731–1740.
- Chen H, Hoemann CD, Sun J, Chevrier A, McKee MD, Shive MS, Hurtig M, Buschmann MD. Depth of subchondral perforation influences the outcome of bone marrow stimulation cartilage repair. *J Orthop Res.* 2011;29:1178–1184.
- Chen H, Sun J, Hoemann CD, Lascau-Coman V, Ouyang W, McKee MD, Shive MS, Buschmann MD. Drilling and microfracture lead to different bone structure and necrosis during bone-marrow stimulation for cartilage repair. *J Orthop Res.* 2009;27:1432–1438.
- Choi WJ, Park KK, Kim BS, Lee JW. Osteochondral lesion of the talus: is there a critical defect size for poor outcome? *Am J Sport. Med.* 2009;37:1974–1980.
- Chuckpaiwong B, Berkson EM, Theodore GH. Microfracture for osteochondral lesions of the ankle: outcome analysis and outcome predictors of 105 cases. *Arthroscopy.* 2008;24:106–112.
- DIGiovanni BF, Fraga CJ, Cohen BE, Shereff MJ. Associated injuries found in chronic lateral ankle instability. *Foot ankle Int.* 2000;21:809–15.
- Elias I, Zoga AC, Morrison WB, Besser MP, Schweitzer ME, Raikin SM. Osteochondral lesions of the talus: localization and morphologic data from 424 patients using a novel anatomical grid scheme. *Foot Ankle Int.* 2007;28:154–161.
- Ferkel RD, Zanotti RM, Komenda GA, Sgaglione NA, Cheng MS, Applegate GR, Dopirak RM. Arthroscopic treatment of chronic osteochondral lesions of the talus: long-term results. *Am. J. Sports Med.* 2008;36:1750–1762.
- Frisbie DD, Trotter GW, Powers BE, Rodkey WG, Steadman JR, Howard RD, Park RD, McIlwraith CW. Arthroscopic subchondral bone plate microfracture technique augments healing of large chondral defects in the radial carpal bone and medial femoral condyle of horses. *Vet. Surg. VS Off. J. Am. Coll. Vet. Surg.* 1999;28:242–255.
- Giannini S, Ruffilli A, Pagliuzzi G, Mazzotti A, Evangelisti G, Buda R, Faldini C. Treatment algorithm for chronic lateral ankle instability. *Muscles. Ligaments Tendons J.* 2014;4:455–60.
- Giannini S, Vannini F. Operative treatment of osteochondral lesions of the talar dome: current concepts review. *Foot Ankle Int.* 2004;25:168–175.
- Gobbi A, Francisco RA, Lubowitz JH, Allegra F, Canata G. Osteochondral lesions of the talus: randomized controlled trial comparing chondroplasty, microfracture, and osteochondral autograft transplantation. *Arthroscopy.* 2006;22:1085–1092.
- Guo Q, Hu Y, Jiao C, Yu C, Ao Y-F. Arthroscopic treatment for osteochondral lesions of the talus: analysis of outcome predictors. *Chin. Med. J. (Engl).* 2010;123:296–300.
- Han SH, Lee JW, Lee DY, Kang ES. Radiographic changes and clinical results of osteochondral defects of the

- talus with and without subchondral cysts. *Foot ankle Int.* 2006;27:1109–1114.
24. Hunt SA, Sherman O. Arthroscopic treatment of osteochondral lesions of the talus with correlation of outcome scoring systems. *Arthrosc. - J. Arthrosc. Relat. Surg.* 2003;19:360–367.
 25. Japour C, Vohra P, Giorgini R, Sobel E. Ankle arthroscopy: follow-up study of 33 ankles--effect of physical therapy and obesity. *J Foot Ankle Surg.* 1996;35:199–209.
 26. John HJ, Carag A V, Moon JPTKS. Role of arthroscopic microfracture for cystic type osteochondral lesions of the talus with radiographic enhanced MRI support. 2011:858–862.
 27. Johnson LL. Arthroscopic abrasion arthroplasty: a review. *Clin. Orthop. Relat. Res.* 2001:S306-17.
 28. Kim HK, Moran ME, Salter RB. The potential for regeneration of articular cartilage in defects created by chondral shaving and subchondral abrasion. An experimental investigation in rabbits. *J Bone Jt. Surg Am.* 1991;73:1301–15.
 29. Kitaoka HB, Alexander IJ, Adelaar RS, Nunley JA, Myerson MS, Sanders M. Clinical rating systems for the ankle-hindfoot, midfoot, hallux, and lesser toes. *Foot ankle Int.* 1994;15:349–353.
 30. Kreuz PC, Erggelet C, Ph D, Steinwachs MR, Ph D, Krause SJ, Lahm A, Ph D, Niemeyer P, Ghanem N, Uhl M, Ph D, Südkamp N, Ph D, Able T. Is Microfracture of Chondral Defects in the Knee Associated With Different Results in Patients Aged 40 Years or Younger? *Arthroscopy.* 2006;22:1180–1186.
 31. Kumai BYT, Takakura Y, Higashiyama I, Tamai S. Arthroscopic Drilling for the Treatment of Osteochondral Lesions of the Talus. *J Bone Jt. Surg Am.* 1999;81:1229–1235.
 32. Lee KB, Bai LB, Chung JY, Seon JK. Arthroscopic microfracture for osteochondral lesions of the talus. *Knee Surg Sport. Traumatol Arthrosc.* 2010;18:247–253.
 33. Loveday D, Clifton R, Robinson A. Interventions for treating osteochondral defects of the talus in adults. *Cochrane Database Syst Rev.* 2010:CD008104.
 34. Magnussen RA, Dunn WR, Carey JL, Spindler KP. Treatment of Focal Articular Cartilage Defects in the Knee A Systematic Review. 2008:952–962.
 35. Mithoefer K, Williams RJ, Warren RF, Potter HG, Spock CR, Jones EC, Wickiewicz TL, Marx RG. Chondral Resurfacing of Articular Cartilage Defects in the Knee with the Microfracture Technique. 2010.
 36. Nakajima H, Goto T, Horikawa O, Kikuchi T, Shinmei M. Characterization of the cells in the repair tissue of full-thickness articular cartilage defects. *Histochem. Cell Biol.* 1998;109:331–338.
 37. Ogilvie-Harris DJ, Sarrosa EA. Arthroscopic treatment after previous failed open surgery for osteochondritis dissecans of the talus. *Arthroscopy.* 1999;15:809–812.
 38. Parisien JS. Arthroscopic treatment of osteochondral lesions of the talus. *Am J Sport. Med.* 1986;14:211–217.
 39. Revill SI, Robinson JO, Rosen M, Hogg MI. The reliability of a linear analogue for evaluating pain. *Anaesthesia.* 1976;31:1191–1198.
 40. Robinson D, Nevo Z. Articular cartilage chondrocytes are more advantageous for generating hyaline-like cartilage than mesenchymal cells isolated from microfracture repairs. *Cell Tissue Bank.* 2001;2:23–30.
 41. Saxena A, Eakin C. Articular talar injuries in athletes: results of microfracture and autogenous bone graft. *Am J Sport. Med.* 2007;35:1680–1687.
 42. Schäfer D, Boss A, Hintermann B. Accuracy of arthroscopic assessment of anterior ankle cartilage lesions. *Foot Ankle Int.* 2003;24:317–20.
 43. Schimmer RC, Dick W, Hintermann B. The role of ankle arthroscopy in the treatment strategies of osteochondritis dissecans lesions of the talus. *Foot Ankle Int.* 2001;22:895–900.
 44. Shapiro F, Koide S, Glimcher MJ. Cell origin and differentiation in the repair of full-thickness defects of articular cartilage. *J Bone Jt. Surg Am.* 1993;75:532–553.
 45. Slabaugh MA, Hess DJ, Bajaj S, Farr J, Cole BJ. Management of Chondral Injuries Associated With Patellar Instability. *YOTSM.* 2010;18:115–122.
 46. Steadman JR, Rodkey WG, Rodrigo JJ. Microfracture: surgical technique and rehabilitation to treat chondral defects. *Clin Orthop Relat Res.* 2001:S362-9.
 47. Tol JL, Struijs PA, Bossuyt PM, Verhagen RA, van Dijk CN. Treatment strategies in osteochondral defects of the talar dome: a systematic review. *Foot ankle Int. / Am. Orthop. Foot Ankle Soc. [and] Swiss Foot Ankle Soc.* 2000;21:119–126.
 48. Verhagen R a, Struijs P a, Bossuyt PM, van Dijk CN. Systematic review of treatment strategies for osteochondral defects of the talar dome. *Foot Ankle Clin.* 2003;8:233–42, viii–ix.
 49. Zengerink M, Struijs PAA, Tol JL, van Dijk CN. Treatment of osteochondral lesions of the talus: A systematic review. *Knee Surgery, Sport. Traumatol. Arthrosc.* 2010;18:238–246.

No effect of hole geometry in microfracture for talar osteochondral defects

Aimée C. Kok, Gabrielle J. M. Tuijthof, Steven den Dunnen, Jasper van Tiel, Michiel Siebelt, Vincent Everts, C. Niek van Dijk, Gino M. M. J. Kerkhoffs
“No Effect of Hole Geometry in Microfracture for Talar Osteochondral Defects”
Clinical Orthopaedics and Related Research, vol. 471 (11), p 3653-3662, nov 2013

Background: Debridement and bone marrow stimulation is an effective treatment option for patients with talar osteochondral defects. However, whether surgical factors affect the success of microfracture treatment of talar osteochondral defects is not well characterized.

Questions/purpose: We hypothesized (i) holes that reach deeper into the bone marrow-filled trabecular bone allow for more hyaline-like repair; and (ii) a larger number of holes with a smaller diameter result in more solid integration of the repair tissue, less need for new bone formation, and higher fill of the defect.

Methods: Talar osteochondral defects that were 6 mm in diameter were drilled bilaterally in 16 goats (32 samples). In eight goats, one defect was treated by drilling six 0.45 mm diameter holes in the defect 2 mm deep; in the remaining eight goats, six 0.45 mm diameter holes were punctured to a depth of 4 mm. All contralateral defects were treated with three 1.1 mm diameter holes 3 mm deep, mimicking the clinical situation, as internal controls. After 24 weeks, histologic analyses were performed using Masson-Goldner/Safranin-O sections scored using a modified O'Driscoll histologic score (scale 0–22) and analysed for osteoid deposition. Before histology, repair tissue quality and defect fill were assessed by calculating the mean attenuation repair/healthy cartilage ratio on Equilibrium Partitioning of an Ionic Contrast agent (EPIC) micro CT (μ CT) scans. Differences were analysed by paired comparison and Mann-Whitney U tests.

Results: Significant differences were not present between the 2 mm and 4 mm deep hole groups for the median O'Driscoll score ($p = 0.31$) and the median of the μ CT attenuation repair/healthy cartilage ratios ($p = 0.61$), nor between the 0.45-mm diameter and the 1.1-mm diameter holes in defect fill ($p = 0.33$), osteoid ($p = 0.89$), or structural integrity ($p = 0.80$).

Conclusions: The results indicate that the geometry of microfracture holes does not influence cartilage healing in the caprine talus.

Introduction

Debridement and bone marrow stimulation is a simple, cost-effective operative treatment for osteochondral defects with lower morbidity and faster return to activity than open cartilage restoration surgery [7, 8, 14, 16, 43, 52]. Systematic reviews have shown a current clinical success percentage of 86%. The affect of patient and defect specific prognostic factors such as lesion size [14, 16], location[14, 44], age [14, 24, 47], or body weight [15, 22] is inconclusive owing to the absence of well-designed prospective studies [22, 23]. The exact mechanisms of the healing process are unknown, which makes prediction of clinical outcome difficult [40, 50].

There is little, and only experimental, research on whether improvements in surgical technique can enhance the healing process of damaged cartilage surfaces. One animal study suggests that the depth of subchondral perforation influences the degree of fill and quality of repair tissue [9]. Other research indicates that there is a difference in bone structure and degree of bone necrosis between drilling and microfracture [11, 33].

A recent systematic literature review showed a large degree of similarity in current surgical techniques for microfracture [23], including use of K-wires [2, 26, 35] or awls [47], removal of unstable cartilage, hole depth between 2 and 4 mm until bleeding or fat droplets occur, and hole spread with a distance of 3 to 4 mm. These recommendations are similar to the originally presented technique by Steadman et al. [47]. Additional recommendations are creation of a stable rim, placement of the holes perpendicular to the surface, and removal of the calcified layer at the base of the defect [12, 17, 27]. To the best of our knowledge, there are no published studies

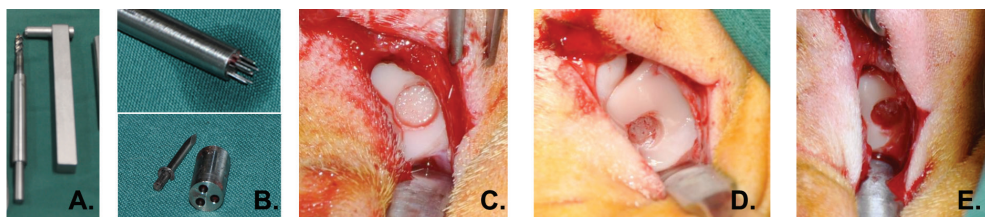


Figure 1. A 6-mm diameter osteochondral defect was drilled in the talus of both hind legs. In the same session, one defect subsequently was treated with six 0.45-mm diameter puncture holes of either 2 mm or 4 mm depth. The contralateral defect was treated with three puncture holes made by a 0.045 (1.1 mm diameter) K-wire capped to a depth of 3 mm to simulate the dimensions of the current clinically applied microfracture awls. (A) The customized drill guide was designed to create a 3-mm deep defect. (B) The microfracture tools used to standardize the diameter and distance between the holes are shown. (C) The 6-mm diameter, 3-mm depth created defect was made without bleeding from the defect before treatment. (D) The defect was treated with six 0.45-mm diameter holes with punctuate bleeding from the holes. (E) The contralateral defect was treated with three holes of 0.045 K-wires (1.1 mm diameter).

regarding whether hole size or distance between the defects influences the degree and quality of the repair tissue.

The aim of our study was to determine the influence of hole geometry, when performing microfracture treatment in the talus, on the quality of the repair cartilage and the filling grade of the defect in a goat model. We formulated two hypotheses: (i) holes that reach deeper into the bone marrow-filled trabecular bone result in better quality repair tissue; and (ii) a larger number of holes with a smaller diameter result in a more solid integration of the repair tissue, less need for new bone formation, and higher fill of the defect.

Materials and methods

Sixteen female Dutch milk goats (*Capra hircus sana*), 4 years of age, with an average weight of 69 kg (range 44–86 kg), were used in this study. Screening for pregnancy and disease was performed before entering the trial. The goats were kept in group housing starting one week before and continuing until one week after surgery to minimize stress. The number of goats was determined from a sample size calculation performed using a power of 90% and two-sided significance level of 5% between groups. A 10% SD of the histology score was described by O'Driscoll et al. [32]; therefore, a minimal effect of 15% was considered clinically significant [4, 25]. Our study protocol was approved by the local animal welfare committees (ORCA102287).

Talar defects are predominantly osteochondral defects, unlike the knee where chondral defects most often are seen [3, 12, 14, 19, 49]. The primary surgical treatment for both is microfracture [7, 52]. To best represent the clinical situation we created an osteochondral talar defect. The dimensions of the created defect depth and diameter and the distance between the microfracture holes in this study were scaled down using the respective ratio between a critical-size osteochondral defect in the human (15 mm diameter) and in the smaller goat talus (6 mm diameter) [12,

Table 1. Treatment group specifications

<i>Number of specimens</i>	<i>Talus</i>	<i>Number of holes</i>	<i>Diameter</i>	<i>Depth</i>
8 goats (16 defects)	Randomized talus (8 defects)	6	0.45 mm	2 mm
	Contralateral talus (8 defects)	3	1.1. mm	3 mm
8 goats (16 defects)	Randomized talus (8 defects)	6	0.45 mm	4 mm
	Contralateral talus (8 defects)	3	1.1. mm	3 mm

21]. Therefore, defect depth was 3 mm, reaching just underneath the sub chondral bone plate [13] but sufficiently shallow to avoid pre-emptive spontaneous bleeding (Fig. 1). One defect in each goat served as a reference mimicking standard clinical microfracture dimensions: three holes of 1.1 mm diameter and 3 mm deep (Table 1). The contralateral defect served to test our hypotheses. To investigate the effect of microfracture hole depth, this defect was treated with microfracture awls penetrating only the subchondral bone plate (2 mm) in half of the goats, whereas in the other half, the holes reached the centre of the talus (4 mm) (Table 1). To determine the effect of the microfracture hole diameter and number, the contralateral defects of the goats were treated with six holes of 0.45-mm diameter, keeping the total treatment surface area constant (Table 1).

All operative procedures were performed in a standardized manner by the first author (ACK), one experienced orthopaedic surgeon (GMMJK), and an assistant (Appendix 1). A posterolateral surgical approach was used to access the talus [6]. Through a 6 mm diameter cannulated drill guide, the osteochondral defect was drilled in the tali of both hind legs perpendicular to the talar surface under continuous cooling with saline. The defect was placed at the centre of the talar dome as designated by one surgeon for all goats. After debridement, the goats were treated according to a randomization scheme (Table 1; Fig. 1) using custom-made surgical templates. The joint capsule and subcutaneous tissue were closed with interrupted 2-O absorbable sutures and the skin was closed with an absorbable continuous intracutaneous suture. The animals were encouraged to perform immediate weight bearing and were transferred to a farm off-site after primary wound closure to complete follow-up under daily observation with neither food nor exercise restriction.

After 24 weeks, the goats were euthanized. All tali were collected, photographed, and stored at 4° C in phosphate-buffered saline 1% with aspartic, serine, and cysteine proteases inhibitors (complete ULTRA Mini Tablets; Roche Diagnostics Corporation, Indianapolis, IN, USA).

To compare the microscopic quality of the repair tissue between the 2 mm and the 4 mm groups, histologic analysis was performed. Second, osteoid formation and repair tissue integration were compared in the 1.1 mm and 0.45 mm diameter groups to establish any differences in integration and bone formation between these groups. All tali were cut into 20 x 20-mm blocks around the defect, leaving the entire depth of the talus intact. The blocks were fixed in 4% formaldehyde in a 0.1 mol/L phosphate buffer, dehydrated, and embedded in methylmethacrylate. At a quarter into and at the centre of the defect, 5 µm slices were sectioned and stained alternately with hematoxylin and eosin, Safranin-O, and Masson-Goldner trichrome. Collagen fibres were examined using polarized light to assess the structure of the repair tissue. Hyaline cartilage will show organization of the fibres, whereas fibrous tissue does not.

To quantify our cartilage quality assessment, a modified form of the score described by O'Driscoll et al. was used (Appendix 2) [32]. The original score by

O'Driscoll et al. contains four main categories: nature of predominant tissue, structural characteristics, freedom from cellular changes of degeneration, and freedom from degenerative changes of the adjacent cartilage, which give a maximum total score of 24 points. The subitem cartilage thickness was not scored, because the repair tissue in the defects was never thinner than the healthy cartilage surrounding the defects. Therefore, a maximum of 22 points could be scored in this study. Each sample was scored twice with a one month interval by one blinded observer (ACK). Differences between the scores at the two times were resolved by an experienced histologist (VE). The entire defect was represented by an average O'Driscoll score, which was calculated using the values at a quarter and at the centre of the defect.

To quantitatively assess glycosaminoglycan (GAG) content [36], sections from the centre of the defect were stained with Safranin-O without any counterstaining and digitally analysed using a Leica microscope (Leica, Wetzlar, Germany) with a 518-nm wavelength filter and evaluated using imaging software [39]. The normalized average Safranin-O intensity (SOI) ratio of the repair tissue compared with the healthy reference cartilage region in the same sections then was calculated. A ratio close to one suggests a cartilage quality of the repair tissue close to that of healthy cartilage.

Osteoid formation was assessed on regular slices using the Masson-Goldner sections from the centre and categorized into three groups: (1) no osteoid formation; (2) slight, less than 20% of the defect; or (3) substantial osteoid formation, greater than 20% of the defect.

Repair tissue integrity was quantified by a subitem of the O'Driscoll score into three categories: (1) full integration; (2) slight disruptions including cysts; or (3) severe disruptions.

To compare the quality of the repair tissue between the 2-mm and 4-mm deep groups, a non contrast-enhanced micro-CT scan (μ CT) and an equilibrium partitioning of an ionic contrast agent (EPIC) through μ CT (EPIC- μ CT) scan were acquired of each entire talus using an μ CT scanner (Skyscan1076; Skyscan, Kontich, Belgium) [34, 51] before histologic analysis. The EPIC- μ CT was acquired after the tali had been saturated for 24 hours in a 40% Hexabrix 360 dilution (Guebet BV, Gorinchem, The Netherlands) [51]. The following scan settings were used: isotropic voxel size of 18 μ m; voltage of 70 kV; current of 111 μ A; 0.5-mm aluminium filter; and 198° with a 0.4° rotation step. Using Skyscan analysis software (Skyscan), a normalized attenuation (grey value) ratio was calculated between a region of cartilage repair tissue and a region of healthy cartilage on the opposite side of the talus. A normalized attenuation ratio close to one indicates that the quality of the repair tissue is close to that of healthy cartilage.

To compare the effect on repair tissue volume between the 4 mm and 2 mm deep holes the cartilage repair tissue volume was determined as a percentage of the total tissue volume of a three-dimensional volume of 8 x 8 x 8-mm around the centre of the defect. Two observers (ACK, SdD) individually determined the repair tissue

volume using image software [39], and disagreements between the observers were solved by discussion resulting in a single value per sample (Fig. 2).

All surgical wounds healed without infection. Two complications occurred after surgery: one temporary pressure neuropathy of the peroneal nerve, which sub sided completely within 12 hours, and one persistent swelling of both hind legs causing impeded mobilization. Supportive treatment was given using cooling gel. One goat was terminated early at 22 weeks follow-up for a bilateral front hoof problem causing walking difficulty and pain. There were no apparent problems with the hind legs. The last two weeks at the end of the follow-up period were expected to have had minimal influence on the overall healing tendency. Therefore, these tali were included for analysis. All other 15 goats completed follow-up without difficulty.

The modified O'Driscoll scores including subitems, attenuation ratios, and repair tissue volume percentages from the EPIC- μ CT, the Safranin-O intensity ratios, and the osteoid formation categories were analysed nonparametrically as a result of skewed distribution of the data and the small sample sizes. Paired analysis between the experimental and control sides of each goat was performed to decrease the influence of repair variability between the goats. In addition, the differences between the talus treated with the experimental treatment and the contralateral talus were calculated per goat using Mann-Whitney U tests ($p = 0.05$). The EPIC- μ CT attenuation ratios correlated significantly with the SOI ratio for the experimental groups ($R^2 = 0.5$; $p = 0.05$) and the control defects ($R^2 = 0.7$; $p = 0.006$). In one μ CT of the 2 mm group, an artefact was seen on the defect. This sample and its matching control were excluded for this specific analysis.

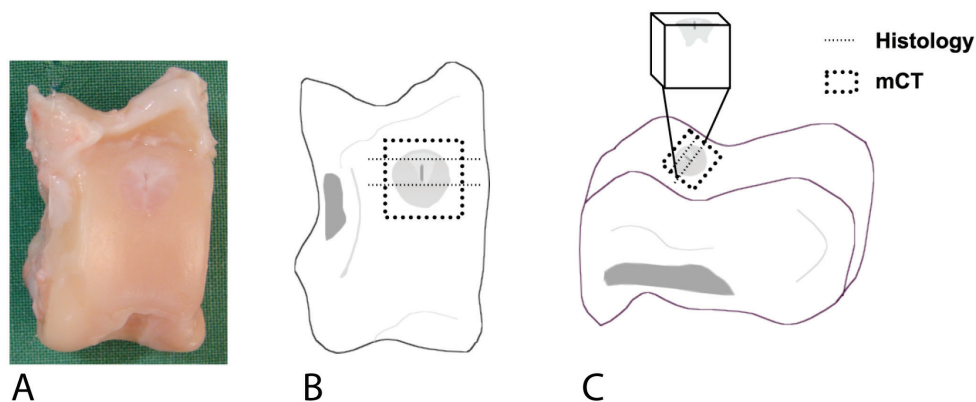


Figure 2. (A) A photograph of the talus with the treated defect is shown. The schematic representations of the same talus in the (B) cranial and (C) lateral views show the two locations of histologic analysis (dotted lines) and the 8 x 8 x 8-mm region of interest in the ICT of which the percentage of repair tissue area was calculated.

Results

We found no clinically significant relationship between repair tissue quality and the depth of microfracture holes. The median difference in the modified O'Driscoll score between the treatment and control legs per goat per group was 1.3 (range: -1.3 to 4.3) for the 2 mm group and -0.9 (range: -4.3 to 2.0) for the 4 mm group (Table 2). This difference was statistically significant ($p = 0.04$). All sections contained predominantly fibrous cartilage repair tissue with diminished Safranin-O staining and disorganized collagen structures on polarized light microscopy. The majority of the defect surfaces showed smooth surfaces (18 samples; Fig. 3). One goat in the 2 mm group had large residual defects with a cleft in the centre in both tali (Fig. 3). No cause could be identified from the operation or the postoperative period. Thirteen samples showed progressive hypocellularity near the surface in a zonal distribution compared with deeper zones near the sub chondral bone plate (six controls, three in the 2 mm group and four in the 4 mm group; Fig. 3).

Digital analysis of the Safranin-O intensity showed five samples in the control group and two in the 4 mm experimental group with uniform Safranin-O distribution with moderate staining. The other defects showed only patches of staining (Fig. 3). The difference in SOI ratio per goat per group was the same, 0.2, for the 2 mm and the 4 mm groups. This was not significant (Table 2). No significant difference was present between the attenuation ratio of the 2 mm group (range: -0.2 to 0.4) or the 4 mm group (range: 0.0 to 0.8) (Table 2). In all scans the repair tissue was largely saturated with the contrast agent (average grey value 84/255, 33%) indicating a relatively low GAG content, compared with the relatively low saturation (average grey value 53/255, 21%), indicating high GAG content for the healthy adjacent cartilage (Fig. 4).

We also found no relationship between defect fill or repair tissue integrity between the 2 mm and 4 mm groups. On histology, the O'Driscoll score subitem "structural integrity" was not significantly different between the 2 mm and 4 mm groups nor was the osteoid formation (Table 3). Six samples showed severe disruption

Table 2. Results per depth group. Results are presented as median values with ranges between brackets

	2 mm			4 mm			Difference between groups
	Randomized talus	Control	Difference	Randomized talus	Control	Difference	
MODS	12.5 (10.8–15.3)	12.0 (9.0–13.0)	1.3 (-1.25 to 4.3)	11.5 (9.8–16.0)	12.6 (11.5–14.3)	-0.9 (-4.3 to 2.0)	2.4* ($p = 0.04$)
SOI ratio	1.8 (1.4–2.7)	1.7 (1.1–4.7)	0.2 (-3.0 to 1.3)	1.5 (0.9–2.4)	1.4 (1.0–2.3)	0.2 (1.2 to 0.5)	0 (NS)
μ CT attenuation ratio	1.6 (1.5–1.8)	1.6 (1.4–1.7)	0.01 (-0.2 to 0.4)	1.6 (1.3–2.1)	1.5 (1.3–1.8)	0.03 (0.3–0.8)	0.02 (NS)

*Difference between 2-mm and 4-mm groups is significant ($p = 0.04$); NS = not significant ($p > 0.05$).; MODS: modified O'Driscoll score; SOI: Safranin-O intensity ratio.

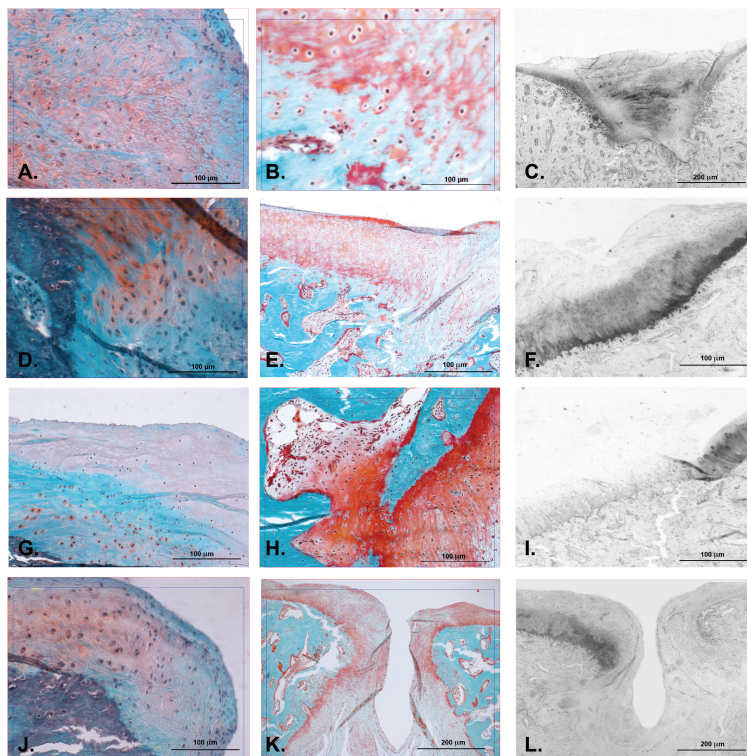


Figure 3. An example of a best case result is shown with (A) moderate Safranin-O staining with evenly distributed GAG (original magnification, x400), (B) Masson-Goldner staining with little osteoid formation (original magnification, x200); and (C) Safranin-O without counterstains used for digital Safranin-O intensity with moderate staining and evenly distributed GAGs, and a smooth surface without disruptions or cysts in the repair tissue. An example of a moderate result is shown with (D) Safranin-O staining with patches of moderate staining and also unstained tissue (original magnification, x400); (E) Masson-Goldner staining with several osteoid isles visible underneath the repair tissue (black arrows) (original magnification, x200); and (F) Safranin-O without counterstains showing patches of moderate staining and also unstained tissue, are shown. Overall, the staining is less than the healthy tissue (*repair tissue, white arrow = adjacent cartilage), and the repair tissue has not bonded to the healthy tissue (black arrow). An example of a worst case result is shown with (G) Safranin-O staining with a strong zonal distribution of Safranin-O and an irregular surface (original magnification, x400); (H) Masson-Goldner staining with large osteoid formations (original magnification, x200); and (I) Safranin-O without counterstains used for digital Safranin-O intensity (SOI), with a large difference in SOI between the repair tissue staining as shown (*repair tissue; white arrow = adjacent cartilage). The repair tissue has not bonded to the adjacent cartilage (black arrow). (J) Safranin-O staining of a sample with a cleft in the center shows similar results to the moderate case with moderate Safranin-O staining (original magnification, x400). (K) A few osteoid isles can be seen on the sample with Masson-Goldner staining (original magnification, x200). (L) There was uneven Safranin-O distribution and detachment of the healthy cartilage on the Safranin-O without counterstains digital analysis.

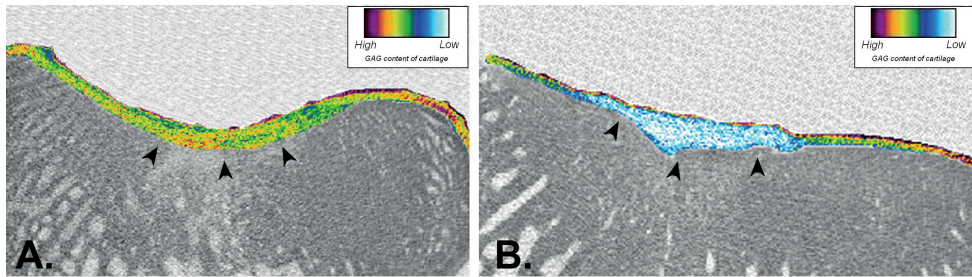


Figure 4. Two samples of EPIC-ICT images are shown. The arrows indicate the repair tissue site in the cartilage. (A) The contrast influx is close to that of the adjacent cartilage, indicating a relatively similar GAG content. This results in an attenuation ratio (repair tissue: healthy reference) close to 1. (B) In this sample the attenuation ratio is lower owing to the low attenuation in the repair tissue caused by the lower negative charge density.

Table 3. Results per diameter group			
Diameter	Ø 0.45 mm	Ø 1.1 mm	Difference
Structural integrity (O'Driscoll Score)			
Normal	1 (6%)	4 (25%)	NS
Slight disruption	10 (63%)	9 (36%)	
Severe disruption	5 (31%)	3 (19%)	
Osteoid formation			
None	1 (6%)	2 (13%)	NS
Moderate	8 (50%)	8 (50%)	
Severe	7 (44%)	6 (38%)	
Repair tissue volume (%)			
Median (Range)	23% (10-40%)	29% (10-75%)	-3% (ns)

NS: not significant ($p > 0.05$).

of tissue integrity, evenly distributed over both experimental groups and the control groups (Fig. 3). No significant difference was present in repair tissue volume on the EPIC- μ CT scans (range: 10%–75%; Table 3).

Discussion

The aim of our study was to determine the effect of depth and diameter of holes created with microfracture bone marrow stimulation on repair tissue quality and the filling grade of the defect. We found that hole depth and hole diameter did not influence the defect fill or the structural integrity of repair tissue. To our knowledge,

there are no previous comparative studies that have investigated hole diameter to compare with these results.

Our study has some limitations. Despite the efforts to standardize the protocol, a large variation was present in quality of repair tissue and defect fill even though we used a sample size calculation that was based on previous studies [4, 6, 25, 31]. The variation might be because the goats were not restricted in mobilization causing some goats to mobilize at a different pace [1]. However, signs of disturbed healing resulting from too fast or hampered mobilization (e.g., limping, swelling) were not seen. In addition, there was a large range in weight in our animals (range: 47–90 kg). However, this proved to be attributable to two outliers, whereas 14 of 16 goats weighed 60 to 80 kg.

The results of repair response compared with non-weight bearing locations (e.g., the trochlea), which correspond to less hyaline repair tissue [20]. Additionally, talar cartilage is known to be stiffer and denser with a higher GAG and lower water content [48]. This changes the physical properties of the cartilage and its response to cyclic loading. Further clinical research is needed to investigate whether the biomechanical differences also might influence the healing response, clinical outcome, and controversial prognostic factors in the two most predominantly used joints for bone marrow stimulation [29, 45]. This should be taken into account when applying our results to the knee, especially because we used an animal model to answer our research question. Extrapolating results from an animal study to a clinical situation should be done cautiously.

In many cartilage studies smaller, mainly rabbit models have been used [8, 11, 13, 45]. We chose a goat model because this allows creation of larger defects (6 mm in diameter) that do not heal spontaneously [21]. In addition, the two outliers were similar to those of the other goats. We do not expect this to have influenced our results, because the literature is controversial regarding the effect of weight on the outcome of microfracture [5, 23, 27].

Another limitation is the use of the smaller joint (the ankle) rather than the knee. This limited the extremes in microfracture hole depth between the treatment groups in the current study. All other animal studies used the knee [11, 21, 28, 45, 46]. The maximum depth for the microfracture holes in the talus was 4 mm when using a 3 mm deep osteochondral defect and without penetrating the centre of the talus. Other studies used depths between 2 and 6 mm [10, 11, 28]. In addition, the knee is connected to a shaft bone containing a large reserve of bone marrow [37], whereas the talus is dependent on the external vascular supply and the cells present in the trabecular bone [38]. These differences might have limited the number of cells that could be recruited from deeper areas. However, the talus is a more congruent joint and such a confined space might protect the blood clot from detaching during initial weight bearing. Immediate weight bearing on the defects also could have enhanced cortical and trabecular bone structure of the goat is similar to human bone and the

proportion of cartilage to subchondral bone [13, 46]. In addition, some studies had a shorter follow-up (range: 1–56 days) [10, 11, 46], which is less analogous to the clinical situation. Clinical studies of the ankle use a follow-up period that generally ranges from several months to years [5, 12, 18, 26, 27, 29, 43, 52].

Concerning our first hypothesis, the differences we observed in terms of the O'Driscoll score for cartilage repair were on the border of statistical significance favouring 2 mm deep holes over 4 mm deep holes, but did not reach the threshold of 15% defined elsewhere as clinically significant [42, 46]. A study using a rabbit model indicated that deeper compared with shallower drilling (6 mm versus 2 mm) elicited a cartilage repair tissue with a more hyaline character in the repair matrix [10]. We did not find this in our study. The predominantly fibrous repair tissue that we observed was similar to that in other cartilage repair studies using the microfracture technique [8, 28, 52]. This also caused a considerable saturation level of the repair tissue in the EPIC- μ CT of the repair tissue, resulting from the relatively low GAG content. More subtle zonal differences in the repair tissue as seen in the Safranin-O slices remained undetected. Further research is needed to determine the right saturation protocol of fibrous tissue to enhance the potential of EPIC- μ CT analysis of cartilage repair tissue.

Concerning our second hypothesis, no differences were found between 0.45 mm diameter microfracture holes and 1.1 mm diameter holes in the “structural integrity” subitem of the O'Driscoll score, repair tissue volume, or osteoid formation (Table 3). Another study also used the O'Driscoll score to assess 6-mm diameter defects in goats treated with subchondral drilling (mean score: 11.3; SD 7) [28]. A couple studies reported limited bonding to the subchondral bone and adjacent cartilage and only 30% to 50% defect fill [8, 28]. The modified O'Driscoll score in our study was higher and all samples showed good bonding to the subchondral bone, bonding to the adjacent cartilage on at least one side, and higher overall defect fill (Fig. 3; Table 3).

The study has several strengths. First, a high level of standardization was achieved by the use of specifically designed surgical templates to minimize variation in hole diameter, depth, and hole dispersion. Second, the minimally invasive approach decreased the operative burden on the animal and reduced the chance of postoperative complications. Third, the animals were used as their own controls to compensate for the high variability between goats. A control group with an untreated defect was deemed an unnecessary increase of used animals, because previous studies have shown the significant lack of healing of these defects [6, 28]. Fourth, samples were analysed according to the guidelines for cartilage assessment in animal studies [20]. For cartilage assessment, the modified O'Driscoll score was used [32] because it is validated in animal models [30, 41]. Supporting the modified O'Driscoll score, two semiautomatic quantitative techniques were used as an internal reference: μ CT and digital Safranin-O analysis. The use of μ CT also offered a three-dimensional volume in which bone and cartilage repair could be assessed in the entire defect.

Using these tools and approaches, we found no clinically significant difference in the cartilage repair tissue quality or degree of defect fill of talar osteochondral defects treated with different sized microfracture holes or holes with different depths.

Acknowledgements

We thank K. W. Meyer, P. Sinnige, G. Vink, and J. Tiehatten for practical assistance; J. Hogervorst, M. van Duin, and D. Nagel for help with the histologic analyses; and A. Jonker for assistance with the digital analyses.

Appendix 1

Substances used during operative treatment and euthanasia

1. General anesthesia
10 mg/kg ketamine (Alfasan International BV, Woerden, The Netherlands)
1.5 mg atropine (Centrafarm Services BV, Etten-Leur, The Netherlands)
10–20 mg etomidate intravenously (B. Braun Melsungen AG, Melsungen, Germany) on effect per goat
250 µg fentanyl bolus intravenous injection (Hameln pharmaceuticals gmbh, Hameln, Germany) and repetition based on heart rate
15 mg midazolam bolus injection intravenously (Dormicum; Roche Nederland BV, Woerden, The Netherlands) and repetition on heart rate
1%–2.0% isoflurane (Nicholas Piramal Limited, London, UK) per inhalation
2. Epidural injection
0.1 mg/kg morphine in 4 mL NaCl 0.9%
3. Postoperative pain medication
One 75-µg/hour Duragesic patch (Janssen Cilag BV, Tilburg, The Netherlands)
0.02 mg/kg meloxicam subcutaneously once daily, 5 days maximum
4. Euthanasia
10 mg/kg ketamine (Alfasan International BV)
1.5 mg atropine (Centrafarm Services BV)
10 mg xylazine intramuscularly (Sedazine1; ASTfarma, Oudewater, The Netherlands)
20 mg/kg pentobarbital natrium intravenously (Euthasol 20%; ASTfarma)

Appendix 2

Modified O'Driscoll score as used in this article

Characteristics	Points
Nature of predominant tissue	
Cellular morphology	
Hyaline articular cartilage	4
Incompletely differentiated mesenchyme	2
Fibrous tissue or bone	0
Safranin-O staining of the matrix	
Normal or nearly normal	3
Moderate	2
Slight	1
None	0
Structural characteristics*	
Surface regularity	
Smooth and intact	3
Superficial horizontal lamination	2
Fissures 25 to 100 percent of the thickness	1
Severe disruption, including fibrillation	0
Structural integrity	
Normal	2
Slight disruption, including cysts	1
Severe disintegration	0
Bonding to the adjacent cartilage	
Bonded at both ends of graft	2
Bonded at one end, or partially at both ends	1
Not bonded	0
Freedom from cellular changes of degeneration	
Hypocellularity	
Normal cellularity	3
Slight hypocellularity	2
Moderate hypocellularity	1
Severe hypocellularity	0
Chondrocyte clustering	
No clusters	2
<25 percent of the cells	1
25-100 percent of the cells	0
Freedom from degenerative changes in adjacent cartilage	
Normal cellularity, no clusters, normal staining	3
Normal cellularity, mild clusters, moderate staining	2
Mild or moderate hypocellularity, slight staining	1
Severe hypocellularity, poor or no staining	0

* The subitem "Thickness of repair tissue" was left out because all repair tissue was always thicker than the adjacent cartilage and therefore could not be scored accurately. (Modified score of O'Driscoll et al. published with permission from O'Driscoll SW.

Adapted from Table II in O'Driscoll SW, Keeley FW, Salter RB.

References

1. Adams MA. The mechanical environment of chondrocytes in articular cartilage. *Biorheology*. 2006;43:537–545.
2. Alexander AH, Lichtman DM. Surgical Treatment of Transchondral Talar-Dome Fractures (Osteochondritis Dissecans): Long-Term Follow-up. *J Bone Jt. Surg Am*. 2008;62:646–652.
3. Aroen A, Heir S, Loken S, Engebretsen L, Reinholt FP. Healing of articular cartilage defects. An experimental study of vascular and minimal vascular microenvironment. *J Orthop Res*. 2006;24:1069–1077.
4. Beardmore AA, Brooks DE, Wenke JC, Thomas DB. Effectiveness of local antibiotic delivery with an osteoinductive and osteoconductive bone-graft substitute. *J Bone Jt. Surg Am*. 2005;87:107–112.
5. Becher C, Driessen A, Hess T, Giuseppe U, Nicola L. Microfracture for chondral defects of the talus : maintenance of early results at midterm follow-up. 2010:656–663.
6. van Bergen CJ a, Kerkhoffs GMMJ, Marsidi N, Korstjens CM, Everts V, van Ruijven LJ, van Dijk CN, Blankevoort L. Osteochondral Defects of the Talus: A Novel Animal Model in the Goat. *Tissue Eng. Part C. Methods*. 2013;19.
7. Van Bergen CJA, de Leeuw PAJ, van Dijk CN. Treatment of osteochondral defects of the talus. *Rev Chir Orthop Reparatrice Appar Mot*. 2008;94:398–408.
8. Buckwalter JA. Articular cartilage: injuries and potential for healing. *J Orthop Sport. Phys Ther*. 1998;28:192–202.
9. Chen H, Chevrier A, Hoemann CD, Sun J, Ouyang W, Buschmann MD. Characterization of subchondral bone repair for marrow-stimulated chondral defects and its relationship to articular cartilage resurfacing. *Am. J. Sports Med*. 2011;39:1731–1740.
10. Chen H, Hoemann CD, Sun J, Chevrier A, McKee MD, Shive MS, Hurtig M, Buschmann MD. Depth of subchondral perforation influences the outcome of bone marrow stimulation cartilage repair. *J Orthop Res*. 2011;29:1178–1184.
11. Chen H, Sun J, Hoemann CD, Lascau-Coman V, Ouyang W, McKee MD, Shive MS, Buschmann MD. Drilling and microfracture lead to different bone structure and necrosis during bone-marrow stimulation for cartilage repair. *J Orthop Res*. 2009;27:1432–1438.
12. Choi WJ, Park KK, Kim BS, Lee JW. Osteochondral lesion of the talus: is there a critical defect size for poor outcome? *Am J Sport. Med*. 2009;37:1974–1980.
13. Chu CR, Szczodry M, Bruno S. Animal models for cartilage regeneration and repair. *Tissue Eng Part B Rev*. 2010;16:105–115.
14. Chuckpaiwong B, Berkson EM, Theodore GH. Microfracture for osteochondral lesions of the ankle: outcome analysis and outcome predictors of 105 cases. *Arthroscopy*. 2008;24:106–112.
15. Giannini S, Ruffilli A, Pagliuzzi G, Mazzotti A, Evangelisti G, Buda R, Faldini C. Treatment algorithm for chronic lateral ankle instability. *Muscles. Ligaments Tendons J*. 2014;4:455–60.
16. Giannini S, Vannini F. Operative treatment of osteochondral lesions of the talar dome: current concepts review. *Foot Ankle Int*. 2004;25:168–175.
17. Gobbi A, Francisco RA, Lubowitz JH, Allegra F, Canata G. Osteochondral lesions of the talus: randomized controlled trial comparing chondroplasty, microfracture, and osteochondral autograft transplantation. *Arthroscopy*. 2006;22:1085–1092.
18. Hangody L, Kish G, Modis L, Szerb I, Gaspar L, Dioszegi Z, Kendik Z. Mosaicplasty for the treatment of osteochondritis dissecans of the talus: two to seven year results in 36 patients. *Foot Ankle Int*. 2001;22:552–558.
19. Hjellev K, Solheim E, Strand T, Muri R, Brittberg M. Articular cartilage defects in 1,000 knee arthroscopies. *Arthroscopy*. 2002;18:730–734.
20. Hoemann C, Roberts S, Saris D.B.F, Creemers L., Mainil-Varlet P, Methot S., (...), Buschmann M.D. KR. International cartilage repair society (ICRS) recommended guidelines for histological endpoints for cartilage repair studies in animal models and clinical trials. *Cartilage*. 2011;2:153–172.
21. Jackson DW, Lalor PA, Aherman HM, Simon TM. Spontaneous repair of full-thickness defects of articular cartilage in a goat model. A preliminary study. *J Bone Jt. Surg Am*. 2001;83–A:53–64.
22. Japour C, Vohra P, Giorgini R, Sobel E. Ankle arthroscopy: follow-up study of 33 ankles--effect of physical therapy and obesity. *J Foot Ankle Surg*. 1996;35:199–209.
23. Kok AC, Dunnen S, Tuijthof GJ, van Dijk CN, Kerkhoffs GM. Is technique performance a prognostic factor in bone marrow stimulation of the talus? *J Foot Ankle Surg*. 2012;51:777–782.
24. Kreuz PC, Erggelet C, Ph D, Steinwachs MR, Ph D, Krause SJ, Lahm A, Ph D, Niemeyer P, Ghanem N, Uhl M, Ph D, Südkamp N, Ph D, Able T. Is Microfracture of Chondral Defects in the Knee Associated With Different

- Results in Patients Aged 40 Years or Younger? *Arthroscopy*. 2006;22:1180–1186.
25. Kruyt MC, Dhert WJ, Oner FC, van Blitterswijk CA, Verbout AJ, de Bruijn JD. Analysis of ectopic and orthotopic bone formation in cell-based tissue-engineered constructs in goats. *Biomaterials*. 2007;28:1798–1805.
26. Kumai BYT, Takakura Y, Higashiyama I, Tamai S. Arthroscopic Drilling for the Treatment of Osteochondral Lesions of the Talus. *J Bone Jt. Surg Am*. 1999;81:1229–1235.
27. Lee KB, Bai LB, Chung JY, Seon JK. Arthroscopic microfracture for osteochondral lesions of the talus. *Knee Surg Sport. Traumatol Arthrosc*. 2010;18:247–253.
28. Lind M, Larsen A, Clausen C, Osther K, Everland H. Cartilage repair with chondrocytes in fibrin hydrogel and MPEG polylactide scaffold: an in vivo study in goats. *Knee Surg Sport. Traumatol Arthrosc*. 2008;16:690–698.
29. Loveday D, Clifton R, Robinson A. Interventions for treating osteochondral defects of the talus in adults. *Cochrane Database Syst Rev*. 2010:CD008104.
30. Moojen DJ, Saris DB, Auw Yang KG, Dhert WJ, Verbout AJ. The correlation and reproducibility of histological scoring systems in cartilage repair. *Tissue Eng*. 2002;8:627–634.
31. Newton PO, Lee SS, Mahar AT, Farnsworth CL, Weinstein CH. Thoracoscopic multilevel anterior instrumented fusion in a goat model. *Spine (Phila Pa 1976)*. 2003;28:1614–9; discussion 1620.
32. O'Driscoll SW, Keeley FW, Salter RB. Durability of regenerated articular cartilage produced by free autogenous periosteal grafts in major full-thickness defects in joint surfaces under the influence of continuous passive motion. A follow-up report at one year. *J. Bone Joint Surg. Am*. 1988;70:595–606.
33. Orth P, Goebel L, Wolfram U, Ong MF, Graber S, Kohn D, Cucchiari M, Ignatius A, Pape D, Madry H. Effect of subchondral drilling on the microarchitecture of subchondral bone: analysis in a large animal model at 6 months. *Am J Sport. Med*. 2012;40:828–836.
34. Palmer AW, Guldborg RE, Levenston ME. Analysis of cartilage matrix fixed charge density and three-dimensional morphology via contrast-enhanced microcomputed tomography. *Proc Natl Acad Sci U S A*. 2006;103:19255–19260.
35. Parisien JS. Arthroscopic treatment of osteochondral lesions of the talus. *Am J Sport. Med*. 1986;14:211–217.
36. Pastoureaux P, Leduc S, Chomel A, De Ceuninck F. Quantitative assessment of articular cartilage and subchondral bone histology in the meniscectomized guinea pig model of osteoarthritis. *Osteoarthr. Cartil*. 2003;11:412–423.
37. Pittenger MF, Mackay AM, Beck SC, Jaiswal RK, Douglas R, Mosca JD, Moorman MA, Simonetti DW, Craig S, Marshak DR. Multilineage potential of adult human mesenchymal stem cells. *Science (80-.)*. 1999;284:143–147.
38. Prasarn ML, Miller AN, Dyke JP, Helfet DL, Lorich DG. Arterial anatomy of the talus: a cadaver and gadolinium-enhanced MRI study. *Foot Ankle Int*. 2010;31:987–993.
39. Rasband WS. *ImageJ*. 1997-202011.
40. Redman SN, Oldfield SF, Archer CW. Current strategies for articular cartilage repair. *Eur Cell Mater*. 2005;9:23–32.
41. Rutgers M, van Pelt MJP, Dhert WJA, Creemers LB, Saris DBF. Evaluation of histological scoring systems for tissue-engineered, repaired and osteoarthritic cartilage. *Osteoarthr. Cartil*. 2010;18:12–23.
42. Saris DB, Dhert WJ, Verbout AJ. Joint homeostasis. The discrepancy between old and fresh defects in cartilage repair. *J Bone Jt. Surg Br*. 2003;85:1067–1076.
43. Saxena A, Eakin C. Articular talar injuries in athletes: results of microfracture and autogenous bone graft. *Am J Sport. Med*. 2007;35:1680–1687.
44. Schimmer RC, Dick W, Hintermann B. The role of ankle arthroscopy in the treatment strategies of osteochondritis dissecans lesions of the talus. *Foot Ankle Int*. 2001;22:895–900.
45. Shapiro F, Koide S, Glimcher MJ. Cell origin and differentiation in the repair of full-thickness defects of articular cartilage. *J Bone Jt. Surg Am*. 1993;75:532–553.
46. Simon TM, Aberman HM. Cartilage regeneration and repair testing in a surrogate large animal model. *Tissue Eng Part B Rev*. 2010;16:65–79.
47. Steadman JR, Rodkey WG, Rodrigo JJ. Microfracture: surgical technique and rehabilitation to treat chondral defects. *Clin Orthop Relat Res*. 2001:S362–9.
48. Treppo S, Koepf H, Quan EC, Cole AA, Kuettner KE, Grodzinsky AJ. Comparison of biomechanical and biochemical properties of cartilage from human knee and ankle pairs. *J Orthop Res*. 2000;18:739–748.
49. Widuchowski W, Widuchowski J, Trzaska T. Articular cartilage defects: study of 25,124 knee arthroscopies. *Knee*. 2007;14:177–182.
50. Williams Iii RJ, Brophy RH. Cartilage repair procedures: clinical approach and decision making. *Instr Course Lect*. 2008;57:553–561.
51. Xie L, Lin AS, Levenston ME, Guldborg RE. Quantitative assessment of articular cartilage morphology via EPIC-microCT. *Osteoarthr. Cartil*. 2009;17:313–320.
52. Zengerink M, Struijs PAA, Tol JL, van Dijk CN. Treatment of osteochondral lesions of the talus: A systematic

review. *Knee Surgery, Sport. Traumatol. Arthrosc.* 2010;18:238–246.

Chapter 4

Water jet drilling in bone: the influence of the primary machine settings and the bone architecture on the hole dimensions

Sections:

Waterjet drilling in porcine bone: The effect of the nozzle diameter and bone architecture on the hole dimensions

How do jet time, pressure and bone volume fraction influence the drilling depth when water jet drilling in porcine bone?

The influence of water jet diameter and bone structural properties on the efficiency of pure water jet drilling in porcine bone

Waterjet drilling in porcine bone: the effect of the nozzle diameter and bone architecture on the hole dimensions

Steven den Dunnen, Lars Mulder, Gino M.M.J. Kerkhoffs, Jenny Dankelman,
Gabrielle J.M. Tuijthof

“Waterjet drilling in porcine bone: the effect of the nozzle diameter and bone architecture on the hole dimensions”

Journal of the Mechanical Behavior of Biomedical materials, vol. 27, p 84-93, 2013

Using waterjets instead of rigid drill bits for bone drilling can be beneficial due to the absence of thermal damage and a consequent sharp cut. Additionally, waterjet technology allows the development of flexible instruments that facilitate maneuvering through complex joint spaces. Controlling the drilling depth is of utmost importance to ensure clinical safety, but is challenging given the local variations in structural properties of the bone.

The goal of this study was to deduct a descriptive mathematical equation able to predict the hole depth and diameter based on the local structural properties of the bone at given waterjet diameters.

210 holes were drilled in porcine femora and tali with waterjet diameters (D_{nozzle}) of 0.3, 0.4, 0.5 and 0.6 mm at a pressure of 700 bar and a 5 second jet time. Hole depths (L_{hole}), diameters (D_{hole}) and bone architectural properties were determined using microCT scans.

The most important bone architectural property is the bone volume fraction (BV/TV), resulting in the significant predictive equations: $L_{\text{hole}} = 34.3 * D_{\text{nozzle}}^2 - 17.6 * BV/TV + 10.7$ ($R^2=0.90$, $p<0.001$), and hole $D_{\text{hole}} = 3.1 * D_{\text{nozzle}} - 0.45 * BV/TV + 0.54$ ($R^2 = 0.58$, $p=0.02$), with L_{hole} , D_{hole} and D_{nozzle} in mm.

Drilling to a specific depth in bone tissue with a known BV/TV is possible, thereby contributing to the safe application of waterjet technology in orthopedic surgery.

Introduction

Conventional, orthopedic drill bits for bone drilling increase the temperature of surrounding bone tissue [1, 2], which can lead to irreversible damage to bone cells (necrosis) and poor bone healing [3-5]. Temperatures above 90°C have been reported [1, 2, 6, 7], which is substantially higher than the lowest temperature at which necrosis occurs (52 °C) [8-10]. Using waterjets to drill in bones causes an increase of the surrounding tissue temperature of maximally 13 °C [11], which causes no thermal damage to bone cells. The machining capacity of waterjets provides several additional advantages over conventional drilling instruments. First, a constant sharp and clean cut is created due to the absence of contact between the instrument and the tissue. Second, the exit location of the waterjet from the instrument can be chosen arbitrarily, for example at the sides perpendicular to the instrument shaft. This allows multi-directional cutting or drilling. Third, waterjet technology allows the use of compliant or steerable instruments, while the water flows through flexible tubing. This increases the working space and facilitates maneuvering through complex joint spaces. Examples of surgical procedures where waterjet technology can make a valuable contribution are debridement and drilling of osteochondral defects, prostheses (re)fixations and predrilling of holes for screw fixations [12, 13].

Clinical safety is of utmost importance for the application of waterjet technology in orthopedic surgery. A key factor to guarantee safety is the ability to control the drilling depth and diameter, because unwanted damage to surrounding healthy tissues should be prevented at all times. As has been extensively investigated for industrial materials, the drilling capacity of waterjets is not solely defined by the machine settings, but also by the material properties of the object to which the jet is applied [14, 15]. This implies that the various waterjet drilling models that have been developed for industrial materials [16-18], cannot be applied for bone drilling due to its heterogeneous characteristics. Hence, the local variations in structural properties of bone cause variations in hole dimensions while waterjetting with the same machine settings. In the majority of the studies on machining bone with waterjets, cortical bone from the femoral or tibial diaphysis was used, which gave constant results in kerf depth due to the relative homogeneity of those bone types [19-22]. Other studies focused on fully cutting through bone to perform osteotomies [20-25] without addressing cutting depth control. Finally, the study by Bach et al. [19] that actually describes an investigation on bone drilling using abrasives, which are small drilling enhancing particles. This technique, however, has biocompatibility issues [26]. All in all, previous studies on machining bone with waterjets have not addressed the important influence of the bone's heterogeneous structure [19-27]. To determine how to safely drill holes with predetermined dimensions in bone, the influence of both waterjet settings and the heterogeneous structure of bone on hole geometry must be investigated separately. Therefore, the goal of this study was to

perform an experimental study to deduct a descriptive mathematical relationship that predicts the hole depth and diameter based on the local structural properties of the bone at given waterjet diameters.

Materials and methods

Study design considerations

The considerations regarding the study design will be discussed by providing a brief theoretical background of the key waterjet settings for waterjet drilling. Subsequently, bone properties that influence this drilling process are discussed, resulting in an overview of the waterjet settings that were varied and the bone properties that were measured.

Waterjet settings: nozzle diameter and water pressure

Water pressure P (N/m²), waterjet time and the waterjet diameter D (m) are the dominant waterjet settings that determine the drilling capacity. The resulting total mass of water fired at an object is considered the key parameter in the effectiveness of a waterjet [14, 15]. The mass flow rate \dot{m} (kg/s) combines the volume of added water and its density, and is given by:

$$\dot{m} = A \cdot v_{liquid} \cdot \rho \quad (1)$$

in which A is the cross sectional area of the waterjet (m²), v_{liquid} the water jet velocity (m/s) and ρ the fluid density (kg/m³). A and v_{liquid} can be varied by adjusting the nozzle diameter D_{nozzle} and pressure P respectively. Reformulation of Eq. 1 by calculating the surface area of the waterjet and integrating Bernoulli's equation for the waterjet velocity leads to:

$$\dot{m} = \frac{1}{4} \cdot \pi \cdot D_{nozzle}^2 \cdot \sqrt{\frac{2 \cdot P}{\rho}} \cdot \rho \quad (2)$$

An increase in D_{nozzle} or P will cause an increase in mass flow rate, thereby enhancing the drilling capacity. This study focuses on the influence of the waterjet diameter, because D_{nozzle} has a quadratic impact on the mass flow rate (Eq. 2). Furthermore, it gives control over the hole diameter [19], which is of great importance for orthopedic applications, for example when drilling pilot holes for screw fixations in bone. In arthroscopy, hole diameters between 0.6 and 1.2 mm are desired [12, 28]. A pilot study has shown that a water jet of diameter D_{nozzle} results in holes with diameters of approximately $2 \cdot D_{nozzle}$. Therefore, the following nozzle diameters were

used in this study: 0.3, 0.4, 0.5 and 0.6 mm.

Structural properties of bone: bone architecture

Structural properties of bone vary between subjects due to e.g. differences in age, diet, diseases and gender [29]. Even within a single bone, variations in structural properties are present due to the bone’s ability to adapt to the specific mechanical loading exerted on it [30]. The organization of bone trabeculae, often referred to as bone architecture, contributes substantially to the bone’s mechanical properties [31] and consequently to its machinability. The following structural parameters provide a good indication of the mechanical properties: bone volume fraction (BV/TV), trabecular thickness (Tb.Th), trabecular spacing (Tb.Sp), and non-metric measures such as degree of anisotropy (DA), plateness, structure model index (SMI) and connectivity density (Conn.D) [31–35] (Table 1). Consequently, these measures were studied to determine their influence on the drilling depth.

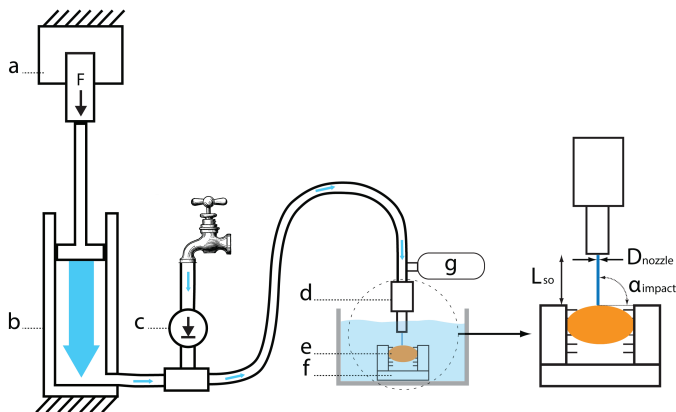


Figure 1. A schematic overview of the experimental waterjet setup. a: tensile tester. b: water filled cylinder. c: one way valve. d: waterjet nozzle. e: specimen. f: clamp. g: pressure sensor. L_{so} : stand-off distance. D_{nozzle} : nozzle diameter. α_{impact} : impact angle.

Table 1. The bone structural properties that were determined		
Bone architecture	Abbreviation	Description
Bone volume fraction	BV/TV	Fraction of mineralized bone per unit volume
Trabecular thickness	Tb.Th.	Mean trabecular thickness
Trabecular spacing	Tb.Sp.	Mean spacing between trabeculae
Degree of anisotropy	DA	Measure how highly orientated substructures are within a volume
Structure model index	SMI	Measure for plate- or rod-like geometry or trabecular structures
Plateness Middle/Longest	Plateness	Measure for prolate, oblate or spherical trabecular structures. Experimental, but does account for concave surfaces which the Structure Model Index does not.
Plateness Shortest/Longest		
Connectivity Density	Conn.D.	Measure how connected the trabeculae are in the network

When waterjet drilling in bone, the cartilage, subchondral bone and trabecular bone layers have to be penetrated, consecutively. To rule out the influence thickness variation of cartilage and subchondral bone, their thickness was measured at every drilling location.

Waterjet set-up

The waterjet drilling experiments were performed using a custom made waterjet set up as schematically depicted in Figure 1. To obtain water pressure, the piston of a cylinder (Holmatro HAC30S15, Glen Burnie, Maryland, USA) that is filled with tap water is pushed in by a tensile tester (HTS, Eden Prairie, Minnesota, United States of America) with a constant load of 295 kN (Figure 1a and 1b). Within 0.3 seconds the water in the cylinder is pressurized to 70 MPa and pushed out, passing a one way valve, via hoses and through the nozzle towards the bone specimen that is held steady by a clamp (Figure 1c to 1f). The water pressure as function of time was monitored with a KLPT-WH pressure transmitter (Koppen & Lethem, Newark, United Kingdom) to verify the time to build up pressure and pressure stability during the experiments (Figure 1g). When the cylinder was depleted, it was refilled by tap water, thereby pushing the piston out to its extended position. A one way valve prevented water from returning to the main water line (Figure 1c). A custom-made nozzle holder allowed sapphire nozzles with various waterjet diameters to be used (Figure 1d). The nozzle holder was stabilized using a frame that was placed in a watertight cabinet to protect the environment from splashing water and debris (Figure 2). To mimic arthroscopic surgery that uses saline to irrigate the joint, the nozzle and the bone specimen were submerged.

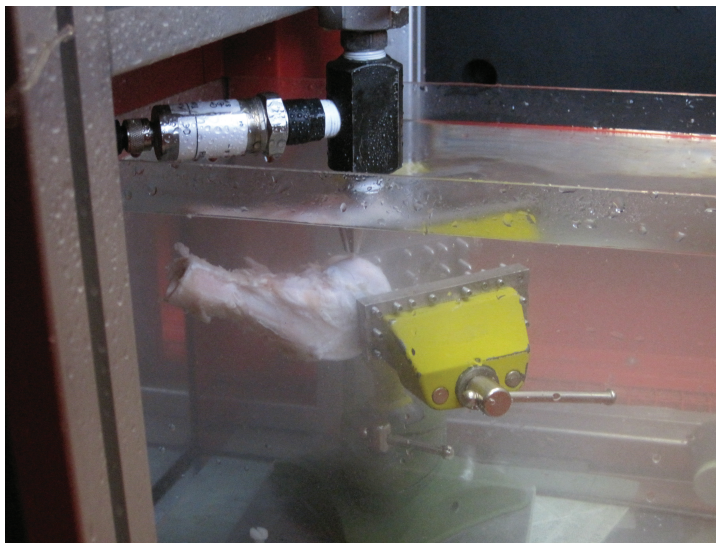


Figure 2. A porcine femur treated with a 0.3 mm nozzle.

Specimens

Ten fresh porcine tali and ten femoral condyles (3-4 months, approximately 40 kg) obtained from an animal experiment were used. Pig bone was chosen because pigs have a metabolism [36] and bone volume fraction [37, 38] comparable to humans. Bones from ankle and knee joint were chosen because the frequency of operative orthopedic procedures is highest in these joints[12]. The specimens were held frozen before and after the experiment. The specimens were thawed to room temperature 90 minutes prior to the experiment. During this time, a 0.9 % saline solution was sprinkled over the bones regularly to preserve the cartilage tissue. A clamp with pins, that allowed omni-directional rotation and height adjustment, provided a rigid grip on the specimens (Figure 1f and 2). A height gauge was used to align the specimens with a stand-off distance of 8 mm and a perpendicular impact angle to the joint surface (Figure 1). The fixated specimen was placed in an aquarium below the nozzle in the watertight cabinet (Figure 1 and 2). A low pressure waterjet (<2 bar) was used to align the target location on the bone with the waterjet. Subsequently, holes were drilled in the tibial surface of the talus and the femoral condyles with a five second waterjet. Holes were drilled in a random sequence order at least 5 mm from the rim of the articular surface area to prevent location based bias and drilling in cortical bone. Three holes were machined in the tali using nozzle diameters 0.4, 0.5 and 0.6 mm. In the femoral condyles, three holes were drilled using nozzle diameters 0.3, 0.4, 0.5 and 0.6 mm as the available articular surface was larger. Consequently, each nozzle diameter was tested 30 times per bone type.

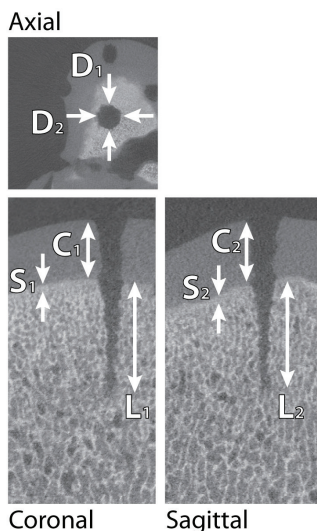


Figure 3. The measurements that were performed on the post-experimental μ CT scans. Each measurement was performed in two views by two individuals and then averaged. For the hole depth, the maximum measurement was used. $D_{1,2}$: hole diameter. $C_{1,2}$: cartilage thickness. $S_{1,2}$: subchondral plate thickness. $L_{1,2}$: hole depth.

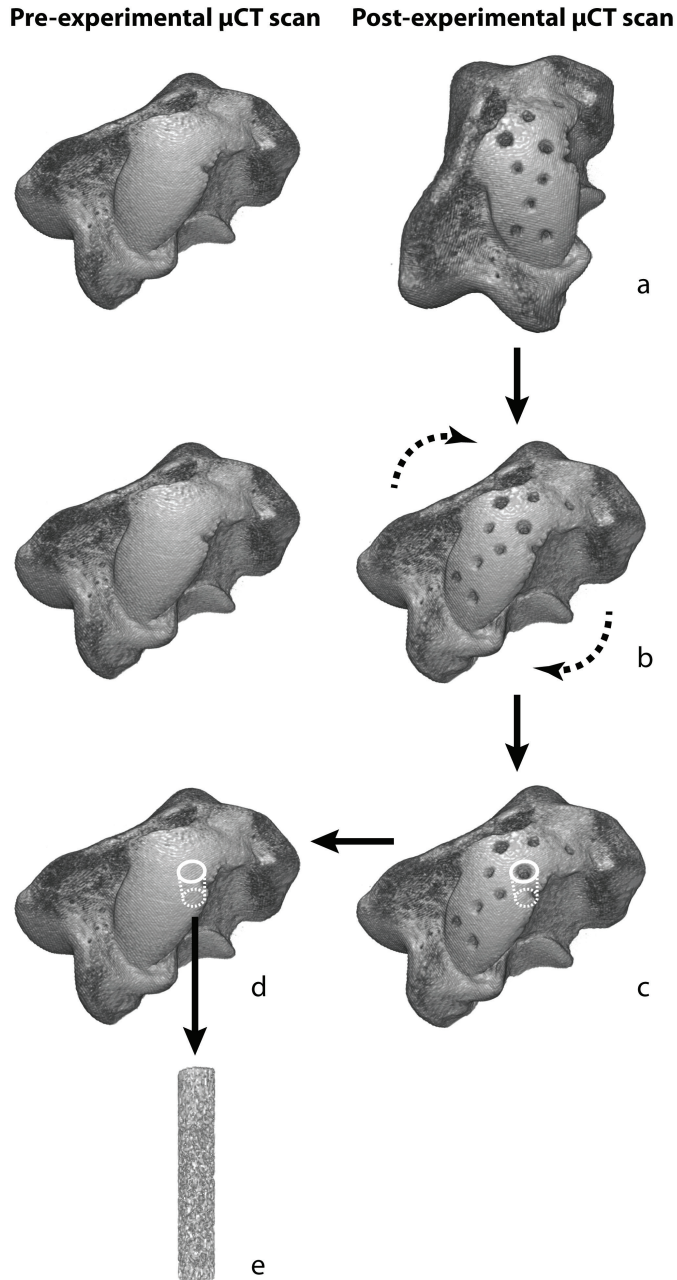


Figure 4. The method for determining the bone architectural properties of at each location where tissue was machined. (a) pre- and post-experimental μ CT scans were made. (b) The post experimental scan was registered to the pre-experimental scan. (c) a region of interest was defined at the drilling location. (d) the region of interest was copied to the pre-experimental scan. (e) the region of interest was isolated.

Measurements

Micro-Computed Tomography (μ CT) scans were made of each bone specimen before and after the experiment with a Scanco microCT 80 scanner (Scanco Medical AG, Brüttisellen, Switzerland) using a spatial resolution of 37 micrometer and identical slice thickness, a scan voltage of 70kVp and exposure time of 300ms. The hole depth, hole diameter at subchondral plate level, the thicknesses of the cartilage layer and the subchondral plate were measured in two different planes in the post-experimental μ CT scans with ImageJ version 1.46m [39, 40] and the Stack Alignment plugin (Align3 TP, version 2010/12/12) [41] (Figure 3). The hole diameter and layer thicknesses measurements were averaged. For the hole depth the maximum value was used. Each measurement was performed by two different persons and averaged. The thresholds for re-measurement for different outcomes between the two persons were 10% of the maximum hole depth, 0.3 mm for the hole diameter, 0.35 mm for the cartilage thickness and 0.15 mm for the subchondral plate thickness.

The bone architectural properties BV/TV, Tb.Th, Tb.Sp, Conn.D, DA, SMI and plateness (Table 1) at each location where tissue was machined were determined (Figure 4). To that end, the pre-and post-experimental μ CT scans were registered (Figure 4a and 4b) by applying an affine transformation matrix, determined using Amira version 5.3.3 (Visualization Sciences Group, Burlington, Miami, USA), to the post-experimental scan in the ImageJ plugin TransformJ Affine version 2.8.0 [42]. A cylindrical region of interest was defined around each hole in the post-experimental scan (Figure 4c). The diameter and depth of the cylindrical selection were equal to the diameter at the widest point and depth of the drilled hole. A minimum of 2 mm in diameter, which is equivalent to approximately four trabeculae, was kept to allow a proper determination of the bone architecture [43]. A selection of the exact bone tissue that was drilled was determined by copying the cylindrical selection from the post-experimental scan to the pre-experimental scan with the Region of Interest (ROI) Manager in ImageJ (Figure 4d). The selection was used to isolate a cylindrical bone sample from the pre-experimental scan (Figure 4e). A fixed global threshold was applied to the reconstructions, creating a binary image where bone tissue could be distinguished from its surrounding. To determine the bone architecture, a batch process was executed in the ImageJ plugin BoneJ version 1.3.3 [44].

Statistics

To correlate the drilling depth to the water jet settings and the bone architectural properties, a multivariate linear regression analysis (ANOVA) with backward selection procedure was performed by using the nozzle diameter and the seven bone architecture properties as a predictor and the hole depth (L_{hole}) as a dependent factor. The influence of the nozzle diameter was considered to be quadratic given the effect on the mass flow rate (Eq. 2). Collinear predictors that could inflate the standard

errors were detected by including variance inflation factors (VIF) in the multivariate linear regression analysis. A VIF threshold of 10 was used for exclusion of the predictor that contributed least to the coefficient of determination (R^2) after removing each one individually. The multivariate linear regression analysis was repeated after each exclusion of the least significant predictor with a significance higher than 0.05. Additionally, the influence of each bone architectural property was analyzed individually. Therefore, multivariate regression analyses were performed with the individual bone architectural property and the nozzle diameter as sole predictors and the drilling depth as a dependent factor. This statistical analysis protocol was repeated to determine the influence of the nozzle diameter and the bone architectural properties on the hole diameter (D_{hole}). The effect of the nozzle diameter on the hole diameter was considered linear. The tissue layer that is most resilient to waterjets was determined by performing a multi linear regression analysis for each bone type (femur or bone) individually with the cartilage thickness, subchondral plate thickness and nozzle diameter as independent factors and L_{hole} as dependent factor. When significant, the results with the highest coefficient of determination (R^2) were presented as linear equations using the mean values of the regression coefficients. All statistical tests were performed in SPSS Statistics version 19 (IBM Corporation, Armonk, New York, USA) with a confidence interval of 95% and level of significance of 0.05.

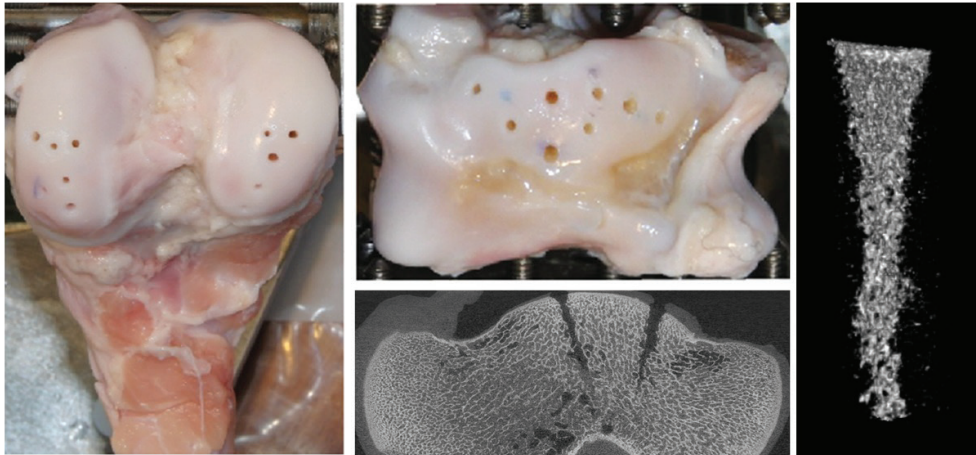


Figure 5. Left: Pig femur. Middle top: Pig talus. Middle bottom: μ CT scan of talus bone. Right: trabecular bone that was removed by the waterjet.

Results

The number of measurements used for the analyses were 83, 91 and 108 for the hole depth, hole diameter and layer thickness analyses respectively. Not all measurements on every hole could be performed: a number of holes that were machined with a nozzle of 0.5 and 0.6 mm crossed other holes inside the bone and were excluded from the study; some hole dimensions exceeded the area that was scanned in the pre- or post-experimental scan.

Regardless of the nozzle diameter or bone type that was used, all drilled holes had a circular cross-section at the drill site and conical in shape. Variations in hole diameter caused by the different waterjet diameters were distinguishable by eye (Figure 5). The multivariate regression analyses to predict the drilling depth resulted in exclusion of all predictors except the nozzle diameter and the BV/TV, resulting in a significant linear correlation described by:

$$L_{hole} = 34.3 \cdot D_{nozzle}^2 - 17.6 \cdot \frac{BV}{TV} + 10.7 \quad (R^2=0.90, p<0.001) \quad (3)$$

with both D_{nozzle} and L_{hole} in mm. Figure 6 gives a graphical depiction of the results. The average measured BV/TV of the femoral condyles was 0.37 (SD 0.07) and of the tali 0.59 (SD 0.13). The Tb.Th was found to be co-linear with the bone volume fraction and was excluded. The Conn.D, DA, Tb.Sp and plateness were also excluded after each iteration of the analysis due to their insignificant added value to the predictive model.

On an individual level, the plateness, Tb.Th, Tb.Sp, SMI and Conn.D, correlated significantly with L_{hole} when combined with D_{nozzle} as a predictive factor (Table 2). No significant correlation was found for the anisotropy on the drilling depth.

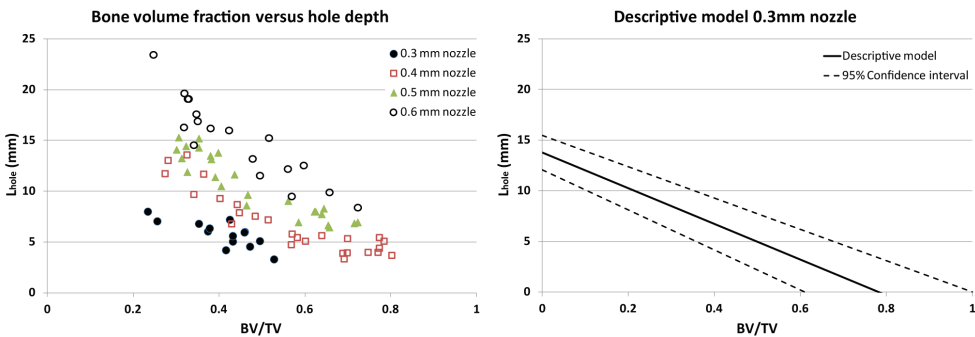


Figure 6. Left: A graphical representation of the bone volume fraction (BV/TV) plotted against the hole depth (L_{hole}). Right: The descriptive drilling depth model and its upper and lower bounds of the 95% confidence interval for a 0.3 mm waterjet nozzle.

The hole diameter (D_{hole} , mm) is best represented by D_{nozzle} and BV/TV as predictors:

$$D_{\text{hole}} = 3.1 \cdot D_{\text{nozzle}} - 0.45 \cdot \frac{BV}{TV} + 0.54 \quad (R^2 = 0.58, p=0.02) \quad (4)$$

The Tb.Th. was excluded due to co-linearity with the BV/TV. All other bone architectural properties were excluded in the multivariate regression analysis due to insignificance. On an individual level, only the Tb.Th. correlated significantly with D_{hole} when combined with D_{nozzle} as predictive factor (Table 2).

The average thickness of the cartilage layers was 0.69mm (SD 0.30) for the talus and 2.42 (SD 0.35) for the femur. The average subchondral plate thickness was 0.23mm (SD 0.05) and 0.35mm (SD 0.06) for the talus and femur, respectively. No significant correlation was found between the thicknesses of the cartilage or the subchondral bone and the drilling depth or diameter (Table 2).

Table 2. The results of the multivariate linear regression analyses performed individually for each predictor in combination with D_{nozzle} .

Bone Architecture Predictors	Hole depth (N=83)		Hole diameter (N=91)	
	R^2	Significance	R^2	Significance
D_{nozzle} + Bone Volume Fraction	0.90	< 0.001	0.58	0.02
D_{nozzle} + Plateness Middle-Longest	0.78	< 0.001		0.15
D_{nozzle} + Plateness Shortest-Longest	0.77	< 0.001		0.18
D_{nozzle} + Trabecular Thickness	0.84	< 0.001	0.58	0.04
D_{nozzle} + Structure Model Index	0.85	< 0.001		0.11
D_{nozzle} + Trabecular Spacing	0.76	< 0.001		0.12
D_{nozzle} + Connectivity Density	0.73	< 0.001		0.07
D_{nozzle} + Anisotropy		0.54		0.27

Discussion

The influence of waterjet diameter and bone architectural properties on the drilling depth and diameter was determined. An increase of 0.1 mm in nozzle diameter resulted in holes that are approximately 3 mm deeper (Equation 3) and 0.3 mm larger in diameter (Equation 4). Therefore, from a clinical point of view, changing the waterjet diameter can be mainly used to control the hole depth, because the hole diameter is less influenced. The BV/TV is the most influential bone architectural property in determining the bone's ability to withstand waterjets (Table 2). This can be explained by the known correlations of bone volume fraction and bone mechanical properties like the maximum tensile strength, the compressive strength and the modulus of elasticity [31, 45, 46]. These properties predominantly

determine bone's machinability with waterjets [14]. Additionally, an increase in bone volume fraction requires more bone tissue to be eroded by the waterjet to drill to the same depth.

The majority of prior studies on waterjet surgery have addressed cutting cortical bone with abrasive suspensions and fixed nozzle diameters [19-27], whereas the current study focuses on drilling with pure water in articular bone. Previous studies that did involve pure waterjets to machine bone resulted in average depths that ranged from 1 to 2 mm when cutting with waterjet diameters of 0.2 and 0.3 mm [20-22, 24]. In those studies, cortical bone tissue was used having BV/TV's of 0.90 or higher. These parameters cannot be used to estimate and compare the drilling depth by using Equation (3), as cutting differs substantially from waterjet drilling. Whilst cutting, the water flow is bended towards the kerf after its initial material impact, thereby further increasing the depth of the cut after its initial passing. For waterjet drilling, the incoming and outgoing jet interfere with each other, causing the impact pressure and kinetic energy to diminish [14, 15, 47-49]. As a result, waterjet drilling results in lower machining depths than waterjet cutting, which is beneficial for controlling the drilling depth and thus the clinical safety.

Limiting factors could have influenced the results. Any research involving the determination of bone architectural measurements with μ CT scans requires a segmentation step, which comprises the determination of a grey level above or below which the pixels indicate bone or background respectively. The process of determining this grey level (threshold) can influence the outcomes of the bone architectural measurements [50]. For this study, the threshold was determined manually and applied to all scan reconstructions (Figure 4e). Automatic algorithms to determine the threshold were not used as they frequently rely on distinct grey level peaks for bone and background tissue [51, 52], which was not the case for the scan reconstructions.

Not for all holes, the depth, diameter and bone architecture could be measured. However, the missing values are considered not to have affected the results given the strong and significant correlations that were found. The influence of the subchondral plate thickness had no effect on the drilling depth or diameter. The small variations in subchondral plate thickness between specimens are likely the cause of this. Larger variations in subchondral plate thickness are expected to have more influence the drill outcomes.

The presented descriptive models (Equations 3 and 4) were based on empirical data from waterjet diameters ranging from 0.3 to 0.6 mm. The accuracy of the models by extrapolation to smaller or larger waterjet diameters can therefore not be guaranteed. Within the tested range of waterjet diameters, the lower and upper bounds of the 95% confidence interval shows the drilling depth can vary from ± 1.7 mm for small nozzle diameters and low BV/TV's up to ± 4.8 mm for large nozzle diameters and high BV/TV's (Figure 6). The coefficient of determination for the

hole diameter is lower than for the drilling depth, but so are the potential variations that can occur due to the relative small influence of D_{nozzle} and BV/TV on the hole diameter. The accuracy of both models is sufficient for procedures such as drilling pilot holes for screw fixation of implants and debridement and drilling procedures for osteochondral defects [12, 28, 53].

The correlations that describe the hole depth and diameter (Equations 3 and 4) can be used to drill holes in articular bone with a predetermined depth by choosing the proper nozzle diameter. In order to do so, the BV/TV of the bone should be known preoperatively. Empirical data regarding the bone architecture of patient specific groups can provide an estimation of the BV/TV. The BV/TV of human tali and femora, that are frequently surgically treated, have BV/TVs of approximately 0.23 [32, 33, 54-56]. Using this value for BV/TV and assuming a needed drill depth of 2 mm to perform surgical debridement and drilling of osteochondral defects [12, 28], a nozzle diameter of 0.1 would suffice (Equation 3). For cortical bone with a BV/TV of 0.90 and higher, a 0.5 mm nozzle would be required. To obtain optimal accuracy, the local BV/TV has to be known, which can be estimated using Dual-energy X-ray Absorptiometry or determined from ordinary CT scans, micro-Magnetic Resonance Imaging and High-Resolution Peripheral Quantitative Computed Tomography [52, 57-59]. Although these methods for clinically assessing the BV/TV have been proven, their availability is still limited and they are not powerful enough to provide information on the local bone architecture of every bone. However, fast developments of in-vivo imaging techniques might allow local bone structural measurements in the near future [60-62].

The results of this study contribute to the safe application of waterjet technology in orthopedic surgery by providing control over the drilling depth, thereby preventing unwanted tissue damage. Given the great potential of a compliant waterjet drilling instrument for arthroscopic surgery in narrow human joint spaces, future developments will focus on miniaturization of the waterjet nozzle.

Conclusion

The depth of the hole as a result of waterjet drilling in bone is correlated to the waterjet diameter and the local BV/TV. For pure waterjet drilling of cortical bone, a nozzle of 0.5 mm is recommended to ensure penetration, whereas for articular bone, a nozzle diameter of 0.2 mm suffices. The predictive equations presented provide fundamental insight in water jet drilling of bone and can be used for the development of orthopedic surgical instruments based on waterjet technology.

Acknowledgements

This research is supported by the Marti-Keuning Eckhart Stichting and the Dutch Technology Foundation STW (grant number 10851), which is part of the Netherlands Organisation for Scientific Research (NWO), and which is partly funded by Ministry of Economic Affairs. The sponsor had no involvement in the study design, analysis or interpretation of the data. We are grateful to Myrth Kwast and Chris Wierikx for their help in preparing and performing the experiment. We would like to thank dr. ir. B. van Rietbergen from the Eindhoven University of Technology and drs. I.N. Sierevelt from the Academic Medical Center for their help in the experiment design and statistical analyses.

References

1. Eriksson, A.R., T. Albrektsson, and B. Albrektsson, Heat caused by drilling cortical bone. Temperature measured in vivo in patients and animals. *Acta Orthopaedica Scandinavica*, 1984. 55(6): p. 629-31.
2. Matthews, L.S. and C. Hirsch, Temperatures measured in human cortical bone when drilling. *Journal of Bone and Joint Surgery-American Volume*, 1972. 54(2): p. 297-308.
3. Eriksson, R.A. and T. Albrektsson, The effect of heat on bone regeneration: an experimental study in the rabbit using the bone growth chamber. *J Oral Maxillofac Surg*, 1984. 42(11): p. 705-11.
4. Eriksson, R.A., T. Albrektsson, and B. Magnusson, Assessment of bone viability after heat trauma. A histological, histochemical and vital microscopic study in the rabbit. *Scand J Plast Reconstr Surg*, 1984. 18(3): p. 261-8.
5. Iyer, S., C. Weiss, and A. Mehta, Effects of drill speed on heat production and the rate and quality of bone formation in dental implant osteotomies. Part II: Relationship between drill speed and healing. *Int J Prosthodont*, 1997. 10(6): p. 536-40.
6. Hillery, M.T. and I. Shuaib, Temperature effects in the drilling of human and bovine bone. *Journal of materials processing technology*, 1999. 93: p. 302-308.
7. Udiljak, T., D. Ciglar, and S. Skoric, Investigation into bone drilling and thermal bone necrosis. *Advance in Production Engineering & Management*, 2007. 3: p. 103-112.
8. Moritz, A.R. and F.C. Henriques, Studies of Thermal Injury: II. The Relative Importance of Time and Surface Temperature in the Causation of Cutaneous Burns. *Am J Pathol*, 1947. 23(5): p. 695-720.
9. Lundskog, J., Heat and bone tissue. An experimental investigation of the thermal properties of bone and threshold levels for thermal injury. *Scand J Plast Reconstr Surg*, 1972. 9: p. 1-80.
10. Eriksson, A.R. and T. Albrektsson, Temperature threshold levels for heat-induced bone tissue injury: a vital-microscopic study in the rabbit. *J Prosthet Dent*, 1983. 50(1): p. 101-7.
11. Schmolke, S., et al., Temperature measurements during abrasive water jet osteotomy. *Biomedizinische Technik*, 2004. 49(1-2): p. 18-21.
12. Steadman, J.R., W.G. Rodkey, and J.J. Rodrigo, Microfracture: surgical technique and rehabilitation to treat chondral defects. *Clinical Orthopaedics and Related Research*, 2001. 391: p. S362.
13. van Bergen, C.J., P.A. de Leeuw, and C.N. van Dijk, Potential pitfall in the microfracturing technique during the arthroscopic treatment of an osteochondral lesion. *Knee Surg Sports Traumatol Arthrosc*, 2009. 17(2): p. 184-7.
14. Tikhomirov, R.A., et al., High-pressure jetcutting. 1992, New York: ASME Press. 197.
15. Summers, D., *Waterjetting Technology*, 1995. 1995, London: E & FN Spon. 882.
16. Akkurt, A., The effect of material type and plate thickness on drilling time of abrasive water jet drilling process. *Materials & Design*, 2009. 30(3): p. 810-815.
17. Hashish, M., Deep hole drilling in metals using abrasive-waterjets. 13th International Conference on Jetting Technology, ed. C. Gee. 1996, Edmunds: Mechanical Engineering Publ. 691-707.
18. Liu, H.T., Hole drilling with abrasive fluidjets. *The International Journal of Advanced Manufacturing Technology*, 2007. 32(9): p. 942-957.
19. Bach, F.-W., et al. Investigation of the AWIJ-Drilling Process in Cortical Bone. in *Proceedings of the 2007 American WJTA Conference and Expo*. 2007. Houston, USA.
20. Honl, M., et al., The use of water-jetting technology in prostheses revision surgery - First results of parameter studies on bone and bone Cement. *Journal of Biomedical Materials Research*, 2000. 53(6): p. 781-790.
21. Honl, M., et al., The water jet as a new tool for endoprosthesis revision surgery - An in vitro study on human bone and bone cement. *Bio-Medical Materials and Engineering*, 2003. 13(4): p. 317-325.
22. Honl, M., et al., Water jet cutting of bone and bone cement. A study of the possibilities and limitations of a new technique. *Biomedizinische Technik*, 2000. 45(9): p. 222-227.
23. Schwieger, K., et al., Abrasive water jet cutting as a new procedure for cutting cancellous bone - In vitro testing in comparison with the oscillating saw. *Journal of Biomedical Materials Research Part B-Applied Biomaterials*, 2004. 71B(2): p. 223-228.
24. Honl, M., et al., The pulsed water jet for selective removal of bone cement during revision arthroplasty. *Biomedizinische Technik*, 2003. 48(10): p. 275-280.
25. Hloch, S., J. Valicek, and D. Kozak, Preliminary Results of Experimental Cutting of Porcine Bones by Abrasive Waterjet. *Tehnicki Vjesnik-Technical Gazette*, 2011. 18(3): p. 467-470.
26. Kuhlmann, C., et al., Evaluation of potential risks of abrasive water jet osteotomy in-vivo. *Biomedizinische Technik. Biomedical Engineering*, 2005. 50(10): p. 337.
27. Hreha, P., et al., Water Jet Technology Used in Medicine. *Tehnicki Vjesnik-Technical Gazette*, 2010. 17(2): p. 237-240.

28. Mithoefer, K., et al., Chondral resurfacing of articular cartilage defects in the knee with the microfracture technique. Surgical technique. *Journal of Bone and Joint Surgery-American Volume*, 2006. 88 Suppl 1 Pt 2: p. 294-304.
29. Yuehuei, H.A. and A.D. Robert, Mechanical testing of bone and the bone-implant interface. 1999, CRC Press. p. 648.
30. Petit, M.A., et al., Femoral bone structural geometry adapts to mechanical loading and is influenced by sex steroids: The Penn State Young Women's Health Study. *Bone*, 2004. 35(3): p. 750-759.
31. Day, J.S., Bone Quality: The Mechanical Effects of Microarchitecture and matrix properties. 2005, Optima Grafische Publicatie: Rotterdam.
32. Ulrich, D., et al., The ability of three-dimensional structural indices to reflect mechanical aspects of trabecular bone. *Bone*, 1999. 25(1): p. 55-60.
33. Teo, J.C.M., et al., Correlation of cancellous bone microarchitectural parameters from microCT to CT number and bone mechanical properties. *Materials Science and Engineering: C*, 2007. 27(2): p. 333-339.
34. Uchiyama, T., et al., Three-dimensional microstructural analysis of human trabecular bone in relation to its mechanical properties. *Bone*, 1999. 25(4): p. 487-491.
35. Helgason, B., et al., Mathematical relationships between bone density and mechanical properties: a literature review. *Clin Biomech (Bristol, Avon)*, 2008. 23(2): p. 135-46.
36. Miller, E. and D. Ullrey, The pig as a model for human nutrition. *Annual review of nutrition*, 1987. 7(1): p. 361-382.
37. Tanck, E., et al., Increase in bone volume fraction precedes architectural adaptation in growing bone. *Bone*, 2001. 28(6): p. 650-654.
38. Teo, J., et al., Relationship between CT intensity, micro-architecture and mechanical properties of porcine vertebral cancellous bone. *Clinical Biomechanics*, 2006. 21(3): p. 235-244.
39. Abràmoff, M.D., P.J. Magalhães, and S.J. Ram, Image processing with ImageJ. *Biophotonics international*, 2004. 11(7): p. 36-42.
40. Schneider, C.A., W.S. Rasband, and K.W. Eliceiri, NIH Image to ImageJ: 25 years of image analysis. *Nature Methods*, 2012. 9(7): p. 671-675.
41. Parker, J.A. Stack Alignment Align3 TP Plugin. [Software] 2010 2012/12/12; 2012/12/12:[Available from: <http://www.med.harvard.edu/jpnm/ij/plugins/Align3TP.html>].
42. Meijering, E.H., W.J. Niessen, and M.A. Viergever, Quantitative evaluation of convolution-based methods for medical image interpolation. *Med Image Anal*, 2001. 5(2): p. 111-26.
43. Harrigan, T.P., et al., Limitations of the continuum assumption in cancellous bone. *Journal of Biomechanics*, 1988. 21(4): p. 269-275.
44. Doube, M., et al., BoneJ: Free and extensible bone image analysis in ImageJ. *Bone*, 2010. 47(6): p. 1076-1079.
45. Cory, E., et al., Compressive axial mechanical properties of rat bone as functions of bone volume fraction, apparent density and micro-ct based mineral density. *J Biomech*, 2010. 43(5): p. 953-60.
46. Nazarian, A., et al., Tensile properties of rat femoral bone as functions of bone volume fraction, apparent density and volumetric bone mineral density. *J Biomech*, 2011. 44(13): p. 2482-8.
47. Orbanic, H. and M. Junkar, An experimental study of drilling small and deep blind holes with an abrasive water jet. *Proceedings of the Institution of Mechanical Engineers Part B-Journal of Engineering Manufacture*, 2004. 218(5): p. 503-508.
48. Ohlsson, L., et al., Optimisation of the piercing or drilling mechanism of abrasive water jets. *Fluid mechanics and its applications*, 1992. 13: p. 359-359.
49. Leach, S. and G. Walker, The application of high speed liquid jets to cutting. *Philosophical Transactions of the Royal Society of London Series A, Mathematical and Physical Sciences*, 1966. 260(1110): p. 295-310.
50. Ding, M., A. Odgaard, and I. Hvid, Accuracy of cancellous bone volume fraction measured by micro-CT scanning. *J Biomech*, 1999. 32(3): p. 323-6.
51. Sezgin, M., Survey over image thresholding techniques and quantitative performance evaluation. *Journal of Electronic imaging*, 2004. 13(1): p. 146-168.
52. Waarsing, J.H., Exploring bone dynamics using in-vivo micro-CT imaging. 2006: Erasmus University Rotterdam.
53. Stannard, J. and A. Schmidt, Surgical treatment of orthopaedic trauma. 2007: TNY.
54. Hildebrand, T., et al., Direct three-dimensional morphometric analysis of human cancellous bone: microstructural data from spine, femur, iliac crest, and calcaneus. *J Bone Miner Res*, 1999. 14(7): p. 1167-74.
55. Kim, H.J., et al., Micro-Structural Profiles of Trabecular Bone at the Ankle Joint. *Journal of Korean Foot and Ankle Society*, 2004. 8(2): p. 157-160.
56. Bevil, G., et al., Influence of bone volume fraction and architecture on computed large-deformation failure

- mechanisms in human trabecular bone. *Bone*, 2006. 39(6): p. 1218-1225.
57. Kuhn, J., et al., Evaluation of a microcomputed tomography system to study trabecular bone structure. *Journal of orthopaedic research*, 2005. 8(6): p. 833-842.
 58. MacNeil, J.A. and S.K. Boyd, Accuracy of high-resolution peripheral quantitative computed tomography for measurement of bone quality. *Medical Engineering & Physics*, 2007. 29(10): p. 1096.
 59. Gomberg, B.R., et al., Reproducibility and error sources of mu-MRI-based trabecular bone structural parameters of the distal radius and tibia. *Bone*, 2004. 35(1): p. 266-276.
 60. Mulder, L., et al., Determination of vertebral and femoral trabecular morphology and stiffness using a flat-panel C-arm-based CT approach. *Bone*, 2012. 50(1): p. 200-208.
 61. Cheung, A.C., et al., Reproducibility of trabecular structure analysis using flat-panel volume computed tomography. *Skeletal Radiology*, 2009. 38(10): p. 1003-1008.
 62. Gupta, R., et al., Flat-Panel Volume CT: Fundamental Principles, Technology, and Applications. *Radiographics*, 2008. 28(7): p. 2009-2022.

How do jet time, pressure and bone volume fraction influence the drilling depth when water jet drilling in porcine bone?

Steven den Dunnen, Jenny Dankelman, Gino M.M.J. Kerkhoffs,
Gabrielle J.M. Tuijthof

“How do jet time, pressure and bone volume fraction influence the drilling depth when water jet drilling in porcine bone?”

Journal of the Mechanical Behavior of Biomedical materials, vol. 62, p 495-503, 2016

Using water jets for orthopedic procedures that require bone drilling can be beneficial due to the absence of thermal damage and the always sharp cut. Previously, the influence of the water jet diameter and bone architectural properties on the drilling depth have been determined. To develop water jet instruments that can safely drill in orthopedic surgery, the impact of the two remaining primary factors were determined: the jet time (t_{jet} [s]) and pressure (P [MPa]). To this end, 84 holes were drilled in porcine tali and femora with water jets using \varnothing 0.4 mm nozzle. t_{jet} was varied between 1, 3 and 5 seconds and P between 50 and 70 MPa. Drilling depths L_{hole} (mm), diameters D_{hole} (mm) and the volume of mineralized bone per unit volume (BV/TV) were determined with microCT scans.

A non-linear regression analysis resulted in the predictive equation:

$$L_{\text{hole}} = 0.22 * t_{\text{jet}}^{0.18} * (1.2 - \text{BV/TV}) * (P - 29) \quad (R^2=0.904).$$

The established relation between the machine settings and drilling depth allows surgeons to adjust jet time and pressure for the patient's BV/TV to drill holes at a predetermined depth. For developers, the relation allows design decisions to be made that influence the dimensions, flexibility and accuracy of water jet instruments. For a pressure of 50 MPa, the potential hole depth spread indicated by the 95% confidence interval is < 1.6 mm for all tested jet times. This maximum variance is smaller than the accuracy required for bone debridement treatments (2-4 mm deep), which confirms that water jet drilling can be applied in orthopedic surgery to drill holes in bone with controlled depth.

Introduction

Using water jets for cutting and drilling bone in orthopedic surgery can be beneficial due to the absence of thermal damage in comparison to instruments that rely on mechanical machining, such as drill bits or oscillating saws [1]. Furthermore, application of water jet technology allows flexible tubing to be used to transport the water. This enables the development of steerable or compliant instruments for arthroscopic procedures to maneuver through complex intra-articular joint spaces in the human body that cannot be reached with rigid instruments. Finally, a water jet never gets blunt, thereby providing a constant cut or hole in the bone over time. Potential uses in orthopedic surgery that can benefit from water jet technology are debridement and drilling of osteochondral defects [2, 3], prostheses (re)fixations [4-6] and drilling pilot holes for screw fixations [7]. The focus in this study is on bone debridement and drilling of osteochondral defects (microfracturing), where holes between 2 and 4 mm deep are drilled in articular bone [8, 9].

To ensure clinical safety, control over the drilling depth is a key factor, because exceeding a predetermined depth could lead to unwanted damage to surrounding healthy tissue. To this end, the influence of the primary water jet settings on the machining capacity should be known, since this allows the creation of an inherently safe system that can guarantee a certain drilling depth. So far, researchers have unveiled the effect of pressure [5, 6, 10-12], impact angle [6], pulse-time[11], jet time [10], suspension [6, 13] and abrasive-feed rate [10] for cutting in bone. In these studies, the structural properties of the bone tissue have not been addressed, although they are highly correlated to mechanical properties and thus the machinability with water jets. Therefore, the outcomes of these studies can only be applied for the specific specimens that were tested. A study that included the structural properties of the bone tissue showed that the volume of mineralized bone per unit volume BV/TV and the squared nozzle diameter highly correlate to the drilling depth ($R^2=0.90$, $p<0.001$) [14]. During surgery, controlling the drilling depth by altering the nozzle diameter would require an instrument change, which compromises surgical workflow. Other machine settings, such as the pressure and jet time, can be adjusted externally at the pump, which is more practical. Subsequently, for the development of a clinical water jet drilling instrument that is inherently safe, a quantification of the influence is required of the primary factors jet time t_{jet} and pressure P . Therefore, the goal of this study was to determine a mathematical description that can be used to predict the drilling depth based on the pressure, jet time and BV/TV, which makes this equation suitable for any bone type since the primary bone structural property is accounted for.

Materials and methods

Theoretical overview and experiment considerations

A theoretical overview of waterjet settings is introduced to define the expected correlations and to determine the starting conditions of this study. The machining capacity of a water jet is primarily determined by its velocity v_{liquid} (m/s) and the total volume of water V_{total} (m³) [13, 14], which can be expressed by:

$$v_{liquid} = \sqrt{\frac{2P}{\rho}} \quad (1)$$

$$V_{total} = \frac{\pi}{4} \cdot d^2 \cdot \sqrt{\frac{2P}{\rho}} \cdot t_{jet} \quad (2)$$

in which P is the pressure (N/m²), ρ is the density of the liquid (kg/m³), t_{jet} (s) is the waterjet time and d (m) is the nozzle diameter.

The influence of the squared diameter on the drilling depth has already been established [14]. Analysis of the other parameters gives that ρ can be considered constant leaving P and t_{jet} as the machine settings that need to be investigated for their influence on the drilling depth in combination with the bone structural properties. For homogeneous bone or industrial materials, the influence of P on the cutting or drilling depth is linear up to pressures of 120 MPa [5, 15-17]. Therefore, two distinct pressures were chosen for adequate determination of the magnitude of linearity. To ensure that holes are actually drilled, 50 MPa was chosen as the lowest pressure, because the minimum pressure for penetrating bone tissue with pure waterjets ranges between 30 and 45 MPa [5, 12, 15]. Our previous research showed that a pressure of 70 MPa with a nozzle of 0.4 mm and a jet time of 5 seconds results in drilling depths of approximately 8 mm deep [18]. This depth is sufficient for bone debridement treatments where holes less than 4 mm deep are typically made [3, 8]. Taking into account that jet times are selected shorter than 5 seconds, 70 MPa was set as the second pressure.

The drilling depth is not proportional to the jet time [10, 17, 19, 20]. The increase in drilling depth is maximum after the jet-initiation, but diminishes as the jet time prolongs, since the interference of the water jet and the water already present in the hole becomes larger at an increased depth [17, 21]. Research on the correlation between jet time and drilling depth when drilling with pure waterjets is scarce. Overviewing research on pure waterjet cutting and abrasive waterjet drilling (drilling enhanced by solid particles) in which the effect of jet time is investigated on the kerf depth (depth of the cut), it is adopted that the relation between jet time and drilling depth can be described best with a power function [17, 22] with an expected

exponent between 0.4 and 0.95 [10, 16, 17, 20]. To verify the high impact of the jet time on the drilling depth at the start of the drilling process and to determine the power of t_{jet} , jet times of 1, 3 and 5 seconds were tested.

For a general equation that describes the drilling depth L_{hole} (mm) in bone for a given t_{jet} and P , the mechanical properties of the tissue need to be incorporated in the form of the bone volume fraction (BV/TV) [13]. An increase in BV/TV causes the tensile strength and Young's modulus to increase linearly [23, 24]. These mechanical properties are of primary influence in resisting the destructive power of a waterjet [25]. The correlation between the drilling depth and the mechanical properties of the material is inversely proportional [25]. Hence, the value of BV/TV is assumed to affect the drilling depth inversely proportional on a linear basis for both jet time and pressure. Finally, a threshold value needs to be set in the equation that indicates the minimum power for the water jet to drill in bone. In previous studies, the minimum values of pressure, jet velocity, energy density or penetration force have been considered to indicate the threshold for various materials [26-32]. Since the pressure can easily be adapted in a clinical setting, P is used to set a threshold. Integrating the above theoretical considerations, a general expression of the equation describing the drilling depth L_{hole} (mm) for a given P , t and BV/TV can be formulated as:

$$L_{hole} = A \cdot t_{jet}^B \cdot \left(C - \frac{BV}{TV}\right) \cdot (P - D) \quad (3)$$

Limits of the values of parameters B to D can be set with data from previous research. The power function's exponent (B) of the influence of the jet time will be less than 1 due to its decreasing influence over time [10, 16, 17, 20]. C must be larger than 1, since water jets can penetrate even the highest density bone which has a BV/TV value of 1 [5, 12, 14, 15]. D will be less than 45 MPa, referring to the highest minimum pressure that is required to penetrate bone tissue [5, 12, 15].

Waterjet set-up and specimens

The waterjet experiments were performed with a custom made waterjet machine [14, 18] that allowed water pressures to be generated up to 72MPa within 0.3 seconds with a maximum variation of ± 0.2 MPa (Figure 1). Pressures were monitored at the nozzle with a KLPT-WH pressure transmitter (Koppen & Lethem, Newark, United Kingdom).

Four fresh porcine tali and four femora were obtained from animal experiments and frozen directly after harvesting (Figure 1). The specimens were thawed to room temperature 90 minutes prior to the experiment using a 0.9% saline solution. The water jet drilling procedure was identical to previous experiments [14, 33]: holes were drilled with a sapphire nozzle of 0.4 mm perpendicular to the tibial surface of the talus and femoral condyles with a stand-off distance of 8 mm (Figure 1a). Tap water

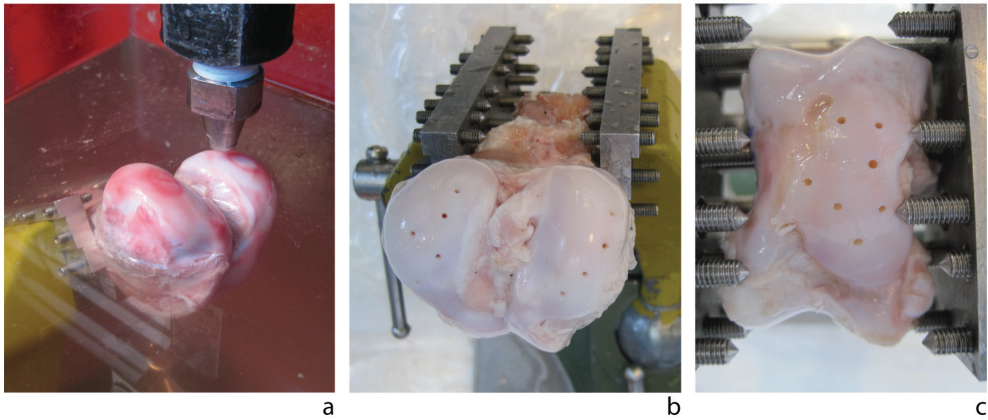


Figure 1. (a) The nozzle is aligned to the bone to ensure correct positioning and stand-off distance using a 0.2 MPa jet. After alignment the bone and nozzle are submerged. (b) Femur bone after water jet drilling. (c) Talus bone after water jet drilling.

Table 1. Summary of the number of holes that were drilled for different values of pressure and jet time.

Jet time	Tali (n=4)		Femora (n=4)	
	50 MPa	70 MPa	50 MPa	70 MPa
1 s	6	6	8	8
3 s	6	6	8	8
5 s	6	6	8	8

was used as a suspension for the jet. The experiment was performed underwater to mimic arthroscopic surgery. Pressure of 50 and 70 MPa and jet times of 1, 3 and 5 seconds were tested. The size of the specimens allowed nine holes to be machined in a talus and twelve in a femur. Consequently, each machine setting was tested 14 times (Table 1).

Measurements

The measurement procedure for determining the drilling depth, hole diameter and BV/TV was identical to previous studies [14, 33]. Pre- and post-experimental Micro-Computed Tomography (μ CT) scans were made of each specimen using a Scanco microCT 80 scanner (Scanco Medical AG, Brüttisellen, Switzerland) with a spatial resolution and slice thickness of 37 micrometer. The drilling depth and diameter were measured in the post-experimental μ CT scan with ImageJ version 1.46m [34, 35] and the Stack Alignment plugin [36]. Each measurement was performed by three individuals and averaged. The local BV/TV of the drilling site was determined as follows: the post-experimental μ CT scan was registered to the pre-experimental scan

with Amira version 5.3.3 (Visualization Sciences Group, Burlington, Miami, USA) and the ImageJ plugin TransformJ Affine version 2.8.0 [37]. A cylindrical region of interest (ROI) at a drilling site with a height and diameter equal to the specific drilling depth and diameter was copied from the post-experimental scan to the pre-experimental scan using the ROI Manager in ImageJ. A minimum of 2 mm in diameter was kept to ensure a valid bone structure measurement [38]. The cylindrical region of interest was used to isolate the bone structure in the pre-experimental scan. A fixed threshold was applied to the reconstruction to create a binary image, which was processed in the ImageJ plugin BoneJ version 1.3.3 [39] to determine the BV/TV. A further elaboration how the BV/TV was determined can be found in [14].

Statistics

To correlate the drilling depth to the predictors P , t_{jet} and BV/TV, a non-linear regression analysis was performed using IBM SPSS Statistics 22.0 for Windows (Armonk, NY: IBM Corp.). Equation (3) was used for determining parameters A, B, C and D. Compared to a linear model, a non-linear model can take many different unstandardized forms. As a result, the consistency of the model cannot be expressed by a p-value. Additionally, the coefficient of determination (R^2) is also considered to be inadequate to assess the performance of a non-linear predictive model [40], because the variance of the regression model and the error variance do not add up to the total variance. Instead, the 95% confidence intervals were determined to provide insight in the potential spread in drilling depth for the given predictors and thereby to indicate the significance and accuracy of the model. A difference between the 5% and 95% confidence interval of less than 2 mm is considered acceptable to ensure a safe drilling depth for bone debridement treatments, because no clinically significant difference in cartilage healing was found for this variance [2, 8, 41]. To find the primary predictors that affect the hole diameter and to which extent, a multivariate linear regression analysis with backward selection procedure was performed. BV/TV, t_{jet} , and P were used as starting parameters.

Results

The number of measurements used for the statistical analyses were 71. 11 holes were excluded post-experimentally due to non-perpendicular alignment of the jet to the bone (9 holes) or crossing holes inside the bone (2 holes). Two holes were excluded due to an engaging safety system of the pump which prevented proper execution of the full drilling cycle. All tested machine settings resulted in the round-shaped holes

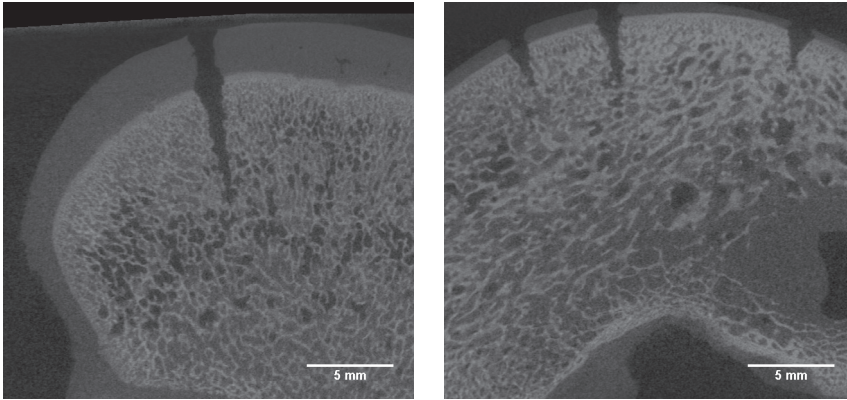


Figure 2. MicroCT images of the holes created by a water jet in a femur (left) and talus (right). Bright white represents bone tissue. The outer layers of the bone are more dense than the inner layers.

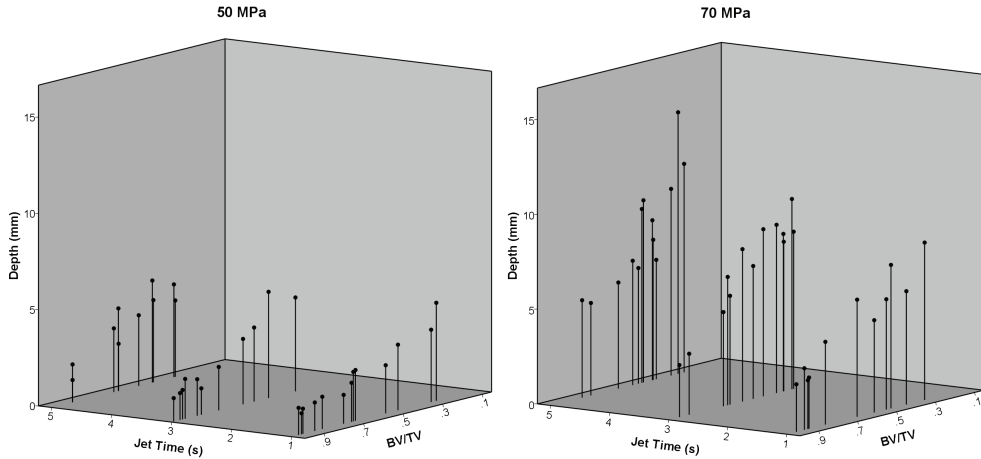


Figure 3. The drilling depths plotted against the t_{jet} and BV/TV at 50 MPa (left) and 70 MPa (right).

Model	Descriptive equation	Example outcomes for different predictors*			
		$T_{jet}=1; P=50; BV/TV=0.5$	$T_{jet}=5; P=50; BV/TV=0.5$	$T_{jet}=1; P=70; BV/TV=0.5$	$T_{jet}=5; P=70; BV/TV=0.5$
5% confidence interval model	$L_{hole} = 0.174 \cdot T_{jet}^{0.114} \cdot (1.13 - \frac{BV}{TV}) \cdot (P_{spr} - 24.2)$	2.8 mm	3.4 mm	5.0 mm	6.0 mm
Predictive model	$L_{hole} = 0.217 \cdot T_{jet}^{0.180} \cdot (1.21 - \frac{BV}{TV}) \cdot (P_{spr} - 29.0)$	3.2 mm	4.3 mm	6.3 mm	8.5 mm
95% confidence interval model	$L_{hole} = 0.260 \cdot T_{jet}^{0.247} \cdot (1.30 - \frac{BV}{TV}) \cdot (P_{spr} - 33.8)$	3.3 mm	5.0 mm	7.5 mm	11.0 mm
Potential spread	95% confidence interval – 5% confidence interval	0.5 mm	1.6 mm	2.5 mm	5.0 mm

*These columns provide the depth values for the extremes in jet time (1 and 5 seconds) and pressure (50 and 70 MPa) that were tested for a given bone volume fraction (BV/TV).

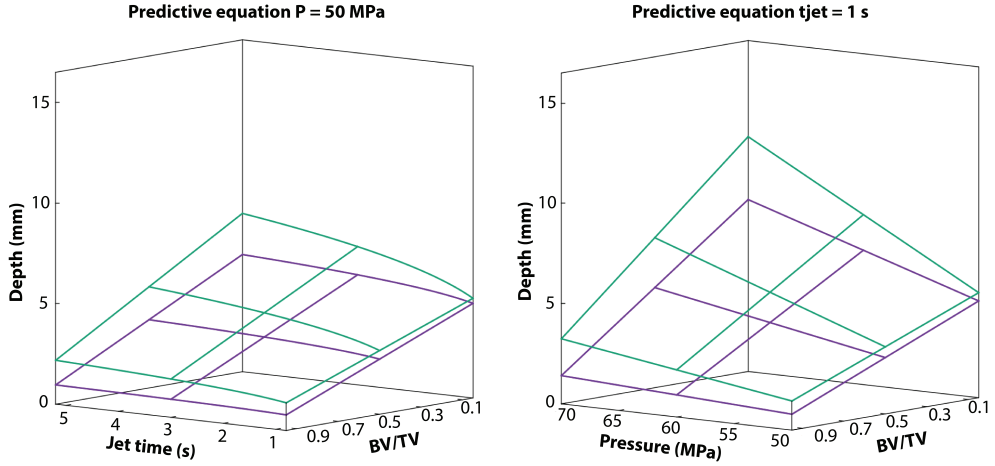


Figure 4. The 5% (purple) and 95% (green) confidence intervals (CI) for $P = 50$ MPa (left) and $t_{jet} = 1$ s (right) and. The distance between the CI surfaces in the graph represent the potential spread that can occur. At a pressure of 50 MPa and a jet time of 1 second, the potential spread is less than 0.5 mm for any BV/TV. An increase in jet time (left) and pressure (right) will result in a larger potential spread.

at the impact site (Figures 1b, 1c) and a concave cavity in the bone (Figure 2).

Fig. 3 provides the measured drilling depths as function of t_{jet} , BV/TV and P . The non-linear regression analysis to predict L_{hole} with predictors t_{jet} , BV/TV and P resulted in the following descriptive equation:

$$L_{hole} = 0.217 \cdot t_{jet}^{0.180} \cdot \left(1.21 - \frac{BV}{TV}\right) \cdot (P_{MPa} - 29.0) \quad (R^2 = 0.904) \quad (4)$$

with L_{hole} in mm, t_{jet} in seconds and P_{MPa} in MPa. Table 2 shows the small difference between the 5% and 95% confidence intervals of the predictive model, especially when using a pressure of 50 MPa. The small difference in outcomes indicates a strong consistency of the predictive model. Equation (4) and the 95% confidence intervals are visualized in Figure 4. The average measured BV/TV of the tali and femora were 0.65 (SD 0.21) and 0.60 (SD 0.21) respectively. The major part of the drilling process takes place in the first fractions of a second. After that, the depth only increases with tenths of millimeters per added second of jet time. For the pressure to have an impact on the drilling depth, a minimum threshold needs to be set of approximately 29 MPa. After that, an increase of 10 MPa results in a depth increase between 1.5 and 2 mm. The BV/TV is inversely proportional on a linear basis to the drilling depth. For each 0.1 increase, the depth decreases approximately 0.4 mm at 50 MPa and 0.9 mm at 70 MPa when jetting for 1 second.

The multi-variate linear regression analysis with backward selecting procedure to predict the hole diameter (D_{hole}) resulted in the exclusion of the BV/TV predictor

due to insignificance, leading to the following equation:

$$D_{hole} = 0.010 \cdot P_{MPa} + 0.064 \cdot t_{jet} + 0.61 \quad (p < 0.001, R^2 = 0.36) \quad (5)$$

The mean diameter was 1.4 mm (SD 0.26 mm). Equation (5) indicates that increasing the pressure by 10 MPa will result in a 0.1 mm wider hole. Per added second of jet time, the diameter increases 0.06 mm.

Discussion

Outcomes

The influence of the jet time, pressure and the bone volume fraction on the drilling depth were determined and provided in a predictive mathematical description (Equation (4)). Both t_{jet} and P_{MPa} can be used to control the drilling depth provided the bone volume fraction is known.

Equation (4) shows a difference between the 5% and 95% confidence intervals of maximally 1.6 mm at 50 MPa and jet times between 1 and 5 seconds (Table 2). This is below the clinically relevant set threshold of 2 mm [8, 41]. This result indicates that water jet drilling a safe technology for bone debridement treatments regarding depth control. The potential spread increases with circa 1.0 mm per 10 MPa of added pressure. Per added second, the spread rises roughly 0.3 mm at 50 MPa and 0.6 mm at 70 MPa.

Interpretation and verification results

The minimum pressure of approximately 29 MPa that needs to be exceeded before any water jet drilling takes place (Equation (4)) is in accordance with previous research, where values between 30 and 45 MPa were found [5, 6, 12]. The relative large range of minimum penetration pressures that was found in previous research is caused by variations in bone type (cortical or trabecular), animal, impact angle, nozzle diameter and machining method (drilling or cutting). Additionally, in previous research the definition of penetration was not always defined or bone tissue was examined with insufficient accurate equipment. This may have led to overlooking shallow (< 0.5mm) cutting or drilling depths in determining the pressure threshold. The strength of the threshold found in this study is that it is valid regardless any bone type, since the BV/TV is included in the predictive equation. For example, a 30 MPa water jet directed at high density cortical bone (BV/TV of 0.9) can penetrate the bone tissue, but will result in a shallow drilling depth between 0 and 0.3 mm (95% confidence interval).

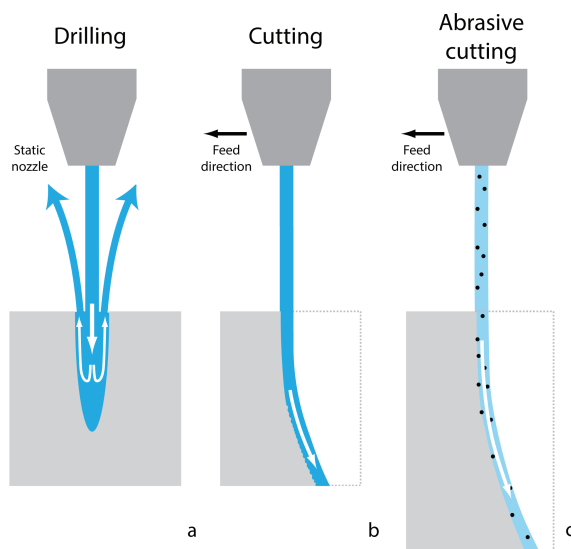


Figure 5. Illustration of the difference between pure water jet drilling, cutting and abrasive cutting (cross sections). (a) For pure water jet drilling, the incoming and outgoing flow interfere, causing the incoming jet to be impaired, which results in a shallower depth. (b) For pure water jet cutting, the water jet passes through the object without interference of back splashing water, which results in a deeper cut than for pure water jet drilling. (c) For abrasive water jet cutting, the water is primarily used to transport the hard solid particles with a high velocity towards the material. The solid particles increase the machining capacity due to an increased energy density that impacts the material.

The exponent (B) of the jet time is 0.18 (Equation (4)), which is considerably lower than the 0.45-0.95 range found in literature [10, 16, 17, 20]. The reason for this difference is to be found in the different types of water jet machining. Previous research performed pure water jet cutting or abrasive drilling. In this study, pure water jet drilling was applied (Figure 5). Water jet cutting or abrasive drilling increase the potential penetration depth of a water jet, which increases the influence of t_{jet} on the depth. When water jet drilling, the water of the incoming water jet has to come out through the same hole it created, causing turbulence and interference between the incoming and outgoing flow (Figure 5) [17, 21]. Therefore, the incoming water jet when water jet drilling will be less powerful than for water jet cutting, because when cutting the surplus water exits at the other side of the material without causing interference. For abrasive water jet drilling, solid particles are added to the water jet. The solid particles have a higher density than pure water, which increases the energy that erodes the material. Hence, the potential drilling depth is increased, thereby extending the influence of the jet time and thus increasing the value of exponent B.

The inversely proportional linear relation between the BV/TV and the drilling depth is in agreement with the applied theory. A higher BV/TV increases the tensile

strength and Young's modulus, resulting in a more difficult to machine material for water jets. This relation is linear [25]. Parameter C in Equation (3) has a fitted value of 1.2, which confirms that even the most dense bone having a BV/TV of almost 1 can be drilled. This is in accordance with our findings and those of others [5, 6, 12]. Parameter C also indicates the maximum differences in drilling depth that can be caused by a varying BV/TV along the drilling direction. Hypothetically, the depths can differ up to a factor 6 for the extreme BV/TV's of 0 and 1. In this study, a maximum spread of 0.4 was found in BV/TV for a given drilling depth for both talus and femoral bone. This spread in BV/TV was pursued to be maximal by drilling holes on the entire articular surfaces, including close to the edges. It is expected that in a clinical setting, local bone variances within one specimen is even smaller.

The average BV/TV of tali and femoral bone were 0.65 and 0.60 respectively, which is higher than 0.59 and 0.37 found in a previous study performed on similar bone [14]. The reason for the discrepancy is that the machine settings of a previous study created deeper holes. Bone physiology dictates that the density at the center of (articular) bone tissue is lower than the outsides (Figure 3). Hence, for greater holes depths, the average BV/TV is less than for shallow depths for the same drilling location. In this study, talus bone decreased approximately 0.07 BV/TV per added mm of depth. For femoral bone, this was 0.02. Therefore, the relative shallow holes caused by the applied machine settings in this study resulted in a higher average BV/TV.

Model performance

The accuracy and significance of predictive Equation (4) is more than adequate to ensure medical safety for bone debridement treatments regarding drilling depth control. An increase in both the jet time and the pressure results in a larger potential spread in depth (Figure 4).

The 5% and 95% boundaries for a given set of parameters (Table 2, Figure 4) show a maximum potential spread of approximately 0.5 mm for a 1 second jet time, and up to 1.6 mm for a 5 second jet time when water jet drilling at 50 MPa. For bone debridement treatments, where holes between 2 and 4 mm deep are made in the bone tissue [2, 3], a difference in depth of 2 mm does not affect the healing of the tissue [2, 8, 41]. This 2 mm accuracy is provided when jet times between 1 and 5 seconds are used with a pressure of 50 MPa. This potential spread in drilling depth is also acceptable when drilling pilot holes for screw-plate fixations. However, the use of a jet time of 5 seconds in combination with a pressure of 70 MPa is not recommend for drilling blind holes in orthopedics surgery, because the maximum variance can increase to 5 mm, which is more than two times higher than the set threshold of 2 mm.

The performance of Equation (5) in predicting the hole diameter is poor

considering the relative spread that can occur in relation with the average diameter, hence the low R^2 of 0.36. However, in view of the absolute values, the maximum spread that was found for a given machine setting is 0.6 mm. From a clinical point of view, this is not an issue and will not significantly influence the healing capacity after a bone debridement treatment [41].

Limiting factors

Limiting factors could have influenced the results. Processing (micro)CT scans to assess bone architectural properties always requires a “thresholding” step, to determine what grey level and lighter tints are considered bone tissue and what is not. For this study, the threshold level was determined manually and applied to all segmentations. The threshold can significantly influence BV/TV measurements [42]. However, since the same threshold was applied to all segmentations the relative influence of the BV/TV is accounted for. One to one comparison of bone architectural properties (such as BV/TV) to other studies is expected to give an offset.

Equations (4) and (5) are valid for their tested range of machine settings and the bone structural properties of the bone specimens. Regardless the strong performance of drilling depth prediction of this descriptive model, extrapolating the results outside the tested range can lead to invalid assumptions.

Perspective

This study shows that water jet drilling has the potential to become a safe drilling method in orthopedic surgery with respect to control over the drilling depth. The machine settings that are to be used to achieve a specific drilling depth for an individual bone can be deduced from the mathematical equation, as well as its potential expected variance. In this study, an overall variation in BV/TV of 0.4 was found per bone type for a given depth, but per individual bone specimen the spread in BV/TV was approximately 0.2. If this latter value is assumed reasonable when performing a bone debridement treatment (e.g. BV/TV varies between 0.5-0.7), this would result in a predicted drilling depth between 1.9 (5% confidence interval BV/TV 0.7) and 3.3 mm (95% confidence interval BV/TV 0.5) using a jet time of 1 sec and a pressure of 50 MPa. This expected variation is very well acceptable for this type of treatment. As indicated in our examples of application of the mathematical equation, it is crucial that the bone's BV/TV is required preoperatively. Imaging techniques such as regular Computer Tomography, Dual-energy X-Ray Absorptiometry, micro-Magnetic Resonance Imaging and High Resolution Peripheral Quantitative Computer Tomography can be used to quantify the BV/TV [43-46]. However, these imaging devices are not widely available in hospitals, not routinely used as part of diagnostic protocols and are not always sufficiently powerful to determine the local BV/TV

of the predetermined surgical spot. Also, the experimental water jet setup used in this study cannot be used in the operating room. Therefore, Equations (4) and (5) are primarily suitable for developers of water jets instruments who can choose the machine settings within the limitations of their design.

Some considerations regarding design optimizations are discussed. To reach a certain drilling depth, a high pressure combined with a short jet time, or a lower pressure combined with a longer jet time can be chosen. Using a high pressure complicates the design of the pump and tubing, but minimizes the total volume of water that is required which can be beneficial to the patients' safety due to the reduced exposure to xenobiotic substances. Using a long jet time requires a pump that can maintain a steady pressure for a longer period of time, but enables a better control over the drilling depth, since the jet time affects the depth only marginally after the first second.

Conclusion

The depth of a hole when water jet drilling in bone is correlated to the water pressure, jet time and the local bone volume fraction of the bone. The most accurate results in drilling depth (variation < 1.6 mm) can be achieved by applying a nozzle of Ø 0.4 mm, a pressure of 50 MPa and jet times between 1 and 5 seconds. This predictive mathematical model indicates that control over the drilling depth allows the safe application of water jet drilling in human bone.

Acknowledgements

This research is supported by the Marti-KeuningEckhart Stichting and the Dutch Technology Foundation STW (Grant number 10851), which is part of the Netherlands Organisation for Scientific Research (NWO), and which is partly funded by Ministry of Economic Affairs. The sponsor had no involvement in the study design, analysis or interpretation of the data. We are grateful to Mark Koster and Michiel van Breugel for their help in preparing and performing the experiment.

References

1. Schwieger, K., et al., Abrasive water jet cutting as a new procedure for cutting cancellous bone--in vitro testing in comparison with the oscillating saw. *J Biomed Mater Res B Appl Biomater*, 2004. 71(2): p. 223-8.
2. Steadman, J.R., W.G. Rodkey, and J.J. Rodrigo, Microfracture: surgical technique and rehabilitation to treat chondral defects. *Clinical Orthopaedics and Related Research*, 2001. 391: p. S362.
3. Steadman, J.R., et al., Outcomes of microfracture for traumatic chondral defects of the knee: average 11-year follow-up. *Arthroscopy*, 2003. 19(5): p. 477-84.
4. Kraaij, G., et al., Waterjet cutting of periprosthetic interface tissue in loosened hip prostheses: An in vitro feasibility study. *Medical engineering & physics*, 2015. 37(2): p. 245-250.
5. Honl, M., et al., The use of water-jetting technology in prostheses revision surgery - First results of parameter studies on bone and bone Cement. *Journal of Biomedical Materials Research*, 2000. 53(6): p. 781-790.
6. Honl, M., et al., The water jet as a new tool for endoprosthesis revision surgery - An in vitro study on human bone and bone cement. *Bio-Medical Materials and Engineering*, 2003. 13(4): p. 317-325.
7. Bronzino, J.D., *The biomedical engineering handbook*. 2nd ed. The electrical engineering handbook series. 2000, Boca Raton, FL: CRC Press.
8. Kok, A.C., et al., Is Technique Performance a Prognostic Factor in Bone Marrow Stimulation of the Talus? *Journal of Foot & Ankle Surgery*, 2012. 51(6): p. 777-782.
9. Becher, C., et al., Microfracture for chondral defects of the talus: maintenance of early results at midterm follow-up. *Knee Surgery, Sports Traumatology, Arthroscopy*, 2010. 18(5): p. 656-663.
10. Bach, F.-W., et al., Investigation of the AWIJ-Drilling Process in Cortical Bone. in *Proceedings of the 2007 American WJTA Conference and Expo*. 2007, Houston, USA.
11. Honl, M., et al., The pulsed water jet for selective removal of bone cement during revision arthroplasty. *Biomedizinische Technik*, 2003. 48(10): p. 275-280.
12. den Dunnen, S., et al., Pure waterjet drilling of articular bone: an in vitro feasibility study. *Journal of Mechanical Engineering - Strojinski vestnik*, 2013. 59(7-8): p. 425-432.
13. Hloch, S., J. Valicek, and D. Kozak, Preliminary Results of Experimental Cutting of Porcine Bones by Abrasive Waterjet. *Tehnicki Vjesnik-Technical Gazette*, 2011. 18(3): p. 467-470.
14. den Dunnen, S., et al., Waterjet drilling in porcine bone: The effect of the nozzle diameter and bone architecture on the hole dimensions. *Journal of the Mechanical Behavior of Biomedical Materials*, 2013(0).
15. Honl, M., et al., Water jet cutting of bone and bone cement. A study of the possibilities and limitations of a new technique. *Biomedizinische Technik*, 2000. 45(9): p. 222-227.
16. Mohamed, M.A.K., *Waterjet cutting up to 900 MPa*. 2004, Universitat Hannover. p. 122.
17. Orbanic, H. and M. Junkar, An experimental study of drilling small and deep blind holes with an abrasive water jet. *Proceedings of the Institution of Mechanical Engineers Part B-Journal of Engineering Manufacture*, 2004. 218(5): p. 503-508.
18. den Dunnen, S., et al., Waterjet Drilling in Porcine Femur Bone: the Effect of Nozzle Diameter on Hole Geometry. in *BioMed*. 2013, Innsbruck.
19. Akkurt, A., The effect of material type and plate thickness on drilling time of abrasive water jet drilling process. *Materials & Design*, 2009. 30(3): p. 810-815.
20. Pandey, N.P., Vijay; Katiyar, Jitendra Kr., Investigation of drilling time v/s material thickness using abrasive waterjet machining. *International Journal of Advances in Engineering & Technology*, 2012. 4(1): p. 672-678.
21. Ohlsson, L., et al., Optimisation of the piercing or drilling mechanism of abrasive water jets. *Fluid mechanics and its applications*, 1992. 13: p. 359-359.
22. Ohlsson, L., et al., Optimisation of the Piercing or Drilling Mechanism of Abrasive Water Jets, in *Jet Cutting Technology*, A. Lichtarowicz, Editor. 1992, Springer Netherlands. p. 359-370.
23. Ulrich, D., et al., The ability of three-dimensional structural indices to reflect mechanical aspects of trabecular bone. *Bone*, 1999. 25(1): p. 55-60.
24. Teo, J.C.M., et al., Correlation of cancellous bone microarchitectural parameters from microCT to CT number and bone mechanical properties. *Materials Science and Engineering: C*, 2007. 27(2): p. 333-339.
25. Tikhomirov, R.A., et al., *High-pressure jetcutting*. 1992, New York: ASME Press. 197.
26. Paul, S., et al., Analytical and experimental modelling of the abrasive water jet cutting of ductile materials. *Journal of materials processing technology*, 1998. 73(1-3): p. 189-199.
27. Bitter, J., A study of erosion phenomena part I. *Wear*, 1963. 6(1): p. 5-21.
28. Bitter, J., A study of erosion phenomena: Part II. *Wear*, 1963. 6(3): p. 169-190.

29. Hashish, M., A Model for Abrasive-Waterjet (Awj) Machining. *Journal of Engineering Materials and Technology-Transactions of the Asme*, 1989. 111(2): p. 154-162.
30. Chillman, A., M. Hashish, and M. Ramulu, Energy Based Modeling of Ultra High-Pressure Waterjet Surface Preparation Processes. *Journal of Pressure Vessel Technology-Transactions of the Asme*, 2011. 133(6).
31. Hoogstrate, A., Towards high-definition abrasive waterjet cutting. TU Delft, 2000.
32. Liu, H.T., Hole drilling with abrasive fluidjets. *The International Journal of Advanced Manufacturing Technology*, 2007. 32(9): p. 942-957.
33. Den Dunnen, S. and G.J.M. Tuijthof The influence of water jet diameter and bone structural properties on the efficiency of pure water jet drilling in porcine bone. article, 2014.
34. Abràmoff, M.D., P.J. Magalhães, and S.J. Ram, Image processing with ImageJ. *Biophotonics international*, 2004. 11(7): p. 36-42.
35. Schneider, C.A., W.S. Rasband, and K.W. Eliceiri, NIH Image to ImageJ: 25 years of image analysis. *Nature Methods*, 2012. 9(7): p. 671-675.
36. Parker, J.A. Stack Alignment Align3 TP Plugin. [Software] 2010 2012/12/12; 2012/12/12:[Available from: <http://www.med.harvard.edu/jpnm/ij/plugins/Align3TP.html>].
37. Meijering, E.H., W.J. Niessen, and M.A. Viergever, Quantitative evaluation of convolution-based methods for medical image interpolation. *Med Image Anal*, 2001. 5(2): p. 111-26.
38. Harrigan, T.P., et al., Limitations of the continuum assumption in cancellous bone. *Journal of Biomechanics*, 1988. 21(4): p. 269-275.
39. Doube, M., et al., BoneJ: Free and extensible bone image analysis in ImageJ. *Bone*, 2010. 47(6): p. 1076-1079.
40. Spiess, A.-N. and N. Neumeyer, An evaluation of R^2 as an inadequate measure for nonlinear models in pharmacological and biochemical research: a Monte Carlo approach. *BMC pharmacology*, 2010. 10(1): p. 6.
41. Kok, A.C., et al., No Effect of Hole Geometry in Microfracture for Talar Osteochondral Defects. *Clinical Orthopaedics and Related Research*, 2013. 471(11): p. 3653-3662.
42. Ding, M., A. Odgaard, and I. Hvid, Accuracy of cancellous bone volume fraction measured by micro-CT scanning. *J Biomech*, 1999. 32(3): p. 323-6.
43. Gomberg, B.R., et al., Reproducibility and error sources of mu-MRI-based trabecular bone structural parameters of the distal radius and tibia. *Bone*, 2004. 35(1): p. 266-276.
44. Kuhn, J., et al., Evaluation of a microcomputed tomography system to study trabecular bone structure. *Journal of orthopaedic research*, 2005. 8(6): p. 833-842.
45. MacNeil, J.A. and S.K. Boyd, Accuracy of high-resolution peripheral quantitative computed tomography for measurement of bone quality. *Medical Engineering & Physics*, 2007. 29(10): p. 1096.
46. Waarsing, J.H., Exploring bone dynamics using in-vivo micro-CT imaging. 2006: Erasmus University Rotterdam.

The influence of water jet diameter and bone structural properties on the efficiency of pure water jet drilling in porcine bone

Steven den Dunnen, Gabrielle J.M. Tuijthof

“The influence of water jet diameter and bone structural properties on the efficiency of pure water jet drilling in porcine bone ”

Mechanical Sciences, vol. 5, p53-58, 2014

Using water jets in orthopedic surgery to drill holes in bones can be beneficial due to the absence of thermal damage and the always sharp cut. To minimize operating time and the volume of water that is used, the efficiency (volume of removed bone per added volume of water) of the water jet should be maximized. The goal was to study the effect of the open trabecular bone structure on the efficiency for different water jet diameters. 86 holes were drilled in porcine tali and femora submerged in water with nozzles of 0.3, 0.4, 0.5 and 0.6 mm at 70 MPa during 5 seconds and a standoff distance of 8mm. MicroCT scans were made to measure the removed bone volume and the bone structural properties Trabecular Spacing (Tb.Sp.), Trabecular Thickness (Tb.Th.) and Bone Volume Fraction (BV/TV). Pearson's correlation tests ($p < 0.05$, 95% confidence interval) were performed for each water jet diameter using the bone structural property as an independent factor and the efficiency as a dependent factor. No significant differences were found between the nozzle diameters in the material removal rates per added volume of water. The efficiency decreased for an increase in Tb.Th. and BV/TV for nozzles of 0.3, 0.4 and 0.5 mm. The 0.6 mm nozzle showed less influence of the Tb.Th. and BV/TV. The Tb.Sp. has no influence on the efficiency of a water jet.

The total volume of added water combined with the Tb.Th. or BV/TV is a leading measure for the volume of bone material that is removed, which provides freedom in the development of water jet instruments as the nozzle diameter, pressure and jet time can be chosen in accordance to the maximum operating time requirements or dimensional limitations of a design.

Introduction

Water jet technology can provide a valuable contribution for drilling of bone in orthopedic surgery due to its potential advantages over existing bone cutting or drilling instruments. Conventional drill bits used for bone drilling increase the temperature of the surrounding bone tissue [1, 2], which can lead to unwanted cell damage or cell death, causing poor bone healing [3-5]. Using water jets to machine bone barely increases the temperature of the surrounding tissue [6], causing no thermal damage to the cells. Besides the thermal advantage, the cut of a water jet is always sharp and clean due to the absence of contact between the tissue and the water jet instrument.

The water volume flow during surgery should be minimized to allow the irrigation system to remove the superfluous water when water jetting. Commercially available irrigation systems such as the HydroFlex AD (Daval, Warwick, RI, USA) are able to pump out up to 2500 ml/min. This is equivalent to the flow rate of a nozzle diameter of 0.37 mm at 70 MPa. When the volume flow of the water jet instrument exceeds the maximum capacity of the irrigation pump, only a small amount of water can be temporarily stored in the tight spaces of the intra-articular joint before an uncontrolled outflow occurs and superfluous extravasation into the surrounding capsule takes place. To decrease the volume flow of a water jet, intermittent water jetting can be performed or a smaller water jet diameter can be chosen. The latter can influence the efficiency of the water jet, which is the removed volume of (bone) material per added volume of water. Efficiency can be influenced as follows. Bone

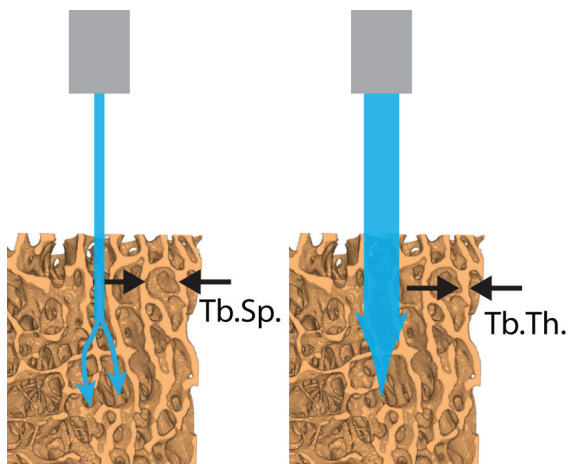


Figure 1. The potential cause for a change in efficiency of a water jets with a smaller diameter than the Tb.Th. or Tb.Sp.. The water takes the path of the least resistance in the spacing between the trabeculae without breaking the struts.

consists of a characteristic open structure of trabeculae with a certain thickness (Tb. Th.), spacing (Tb.Sp.) and density (BV/TV) [7] (Fig. 1). Water jets having a smaller diameter than the Tb.Sp. can pass through the cavities of the bone without removing the bone itself, and trabecular struts with a larger Tb.Th. than the water jet diameter might not break (Fig. 1). These aspects can result in a decreased efficiency for water jet diameters with a smaller diameter than the Tb.Sp. or Tb.Th.. In that case, increased jet times and as a result larger water volumes are required to remove the same quantity of bone tissue. For application in surgery, this would imply an increased operating time or an increased total volume of added water.

This study investigates the efficiency of water jets with various diameters for drilling in bone tissue by comparing the bone tissue removal rates per added volume of water. To investigate whether the bone tissue structure affects the efficiency, the BV/TV, Tb.Th. en Tb.Sp. are analyzed. The results of this study can be used for future design of orthopedic water jets instruments by providing the optimal water jet diameter for minimizing the total volume of added water or operating time.

Materials and methods

The volume of water and its velocity provide a good indication of the effectiveness of a water jet when machining homogeneous materials [8]. The velocity of a water jet v_{liquid} (m/s) can be determined by a simplification of Bernoulli's equation:

$$v_{liquid} = \sqrt{\frac{2P}{\rho}} \quad (1)$$

in which P is the water pressure (N/m²) and ρ is the fluid density (kg/m³). The volume of water V_{water} (m³) can be determined by Equation (2):

$$V_{water} = \frac{1}{4} \pi \cdot D^2 \cdot v_{liquid} \cdot t \quad (2)$$

in which D (m) is the water jet diameter and t (s) is the jet time.

Using a traditional dimensionless energy equation to describe the efficiency has limited value, since a percentage cannot be used for determining the water jet machine settings to remove a predetermined volume of bone. Instead, the measure to describe the efficiency is defined as the volume of removed bone tissue per added volume of water VRR (mm³/l) in accordance to:

$$VRR = \frac{V_{rembonetissue}}{1000 \cdot V_{water}} = \frac{V_{rembonetissue}}{250 \cdot \pi \cdot D^2 \cdot \sqrt{\frac{2P}{\rho}} \cdot t} \quad (3)$$

in which $V_{rembonetissue}$ (mm^3) is the volume of removed bone tissue. Using the VRR shows how much water is required to machine a certain volume of bone tissue, allowing Eq. (1) and (2) to be used for determining P, D and t.

To investigate the influence of the trabecular structures on the water jet efficiency of various water jet diameters, nozzle diameters were chosen that were smaller than, larger than or equal to the mean Tb.Th.(0.5mm) and Tb.Sp. (0.3mm) found in porcine bone specimens [9]. This resulted in the following nozzle diameters that were tested: 0.3, 0.4, 0.5 and 0.6 mm. The experiment layout is summarized in Table (1).

Water jet drilling of bony tissue was performed with a custom-made setup that used a MTS model 311.21 tensile tester (HTS, Eden Prairie, Minnesota, United States of America) to compress a water filled cylinder (Holmatro HAC30S15, Glen Burnie, Maryland, USA) with a force of 295 kN, resulting in a water pressure of 70 MPa at the nozzle [9]. Via a hose the cylinder was connected to a holder that allowed nozzles with various diameters to be connected.

Ten fresh porcine tali and ten femoral condyles (3-4 months, approximately 40 kg) obtained from an animal experiment were used. The distance between the specimen and the nozzle (stand-off distance) was 8 mm and the jet time 5 seconds. During the experiment, both the nozzle and the specimen were situated underwater to mimic arthroscopic surgery. 86 holes were drilled in a random order of sequence perpendicularly in the articular surface of the tali and femora: 13, 26, 26 and 22 holes with nozzle diameters of 0.3, 0.4, 0.5 and 0.6 mm, respectively.

Pre- and post-experimental microCT scans of each bone specimen were used to measure the BV/TV, Tb.Th., Tb.Sp. and Vbonetissue by using a Scanco microCT80 scanner (Scanco Medical AG, Brüttisellen, Switzerland) at a spatial resolution of 37 micron. The scans were registered using Amira version 5.3.3 (Visualization Sciences Group, Burlington, Miami, USA). Regions of interest of each drilled hole were identified in the post-experimental scan and copied to the pre-experimental scan using ImageJ version 1.46m. Segmentations were made from the regions of interest. After applying a global threshold to the segmentations, the mean BV/TV, Tb.Th.,

Table 1. The experiment variables and factors.

	Nozzle diameter	0.3, 0.4, 0.5, 0.6 mm
Independent variable	Bone structural properties	BV/TV, Tb.Th., Tb.Sp.
Dependent variable	Water jet efficiency	VRR

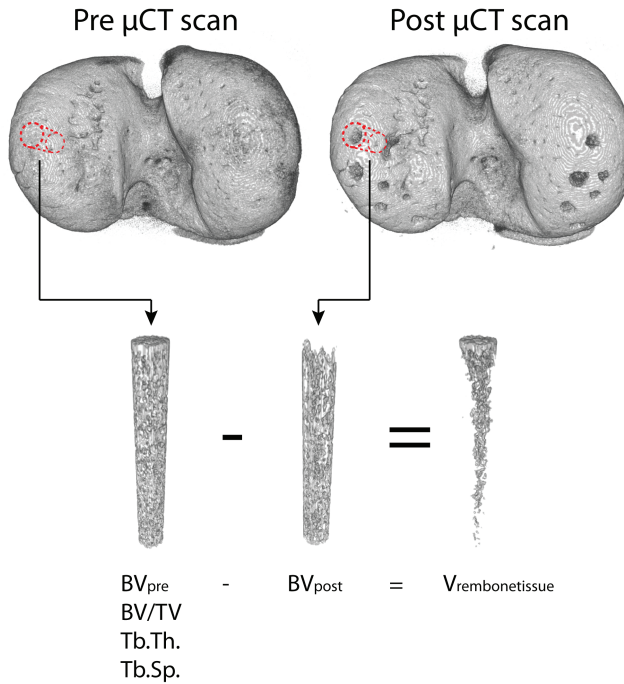


Figure 2. Method of measuring the bone structural properties and bone volumes.

Tb.Sp. and the total bone volume of the segmentation (BV_{pre}) were determined in the pre-experimental scan. In the segmentation of the post-scan, the total bone volume was measured (BV_{post}). $V_{rembonetissue}$ was determined by subtracting BV_{post} from BV_{pre} (Fig. (2)).

To determine whether there is a difference in efficiency between the nozzles, Pearson's correlation tests are performed for each water jet diameter using the bone structural property as an independent factor and the VRR as a dependent factor. If no difference in efficiency is found, the same test is used to create a model that predicts the removed bone tissue for a given bone structural property. The tests were performed in IBM SPSS Statistics version 20 (Armok, New York, USA) with a confidence interval of 95% ($\alpha = 0.05$).

This study is a continuation of a published experiment that determined a correlation between the drilling depth, nozzle diameter and bone structural properties [9] and has therefore overlap regarding the actual performed experiment. The data presented in this article is new.

Results

All water jet diameters resulted in holes in bone tissue (Fig. 3). Significant predictive models were determined to calculate the VRR for each nozzle diameter when using the BV/TV or Tb.Th. as a dependent factor (Table 2 and Fig. 4). The area covered by the 95% confidence interval overlapped for all nozzles. For the 0.6 mm nozzle model, the significance and R^2 was lower and the slope less steep than for the other three nozzle diameters (Table 2). No significant models were found using the Tb.Sp. as a predictor.

A linear regression analysis with the BV/TV, Tb.Th. or Tb.Sp. combined with the added volume of water as predictors showed the following three significant models to calculate the removed bone tissue:

$$V_{\text{rembone tissue}} = 18.4 \cdot V_{\text{water}} - 8.4 \cdot \frac{BV}{TV} + 3.3 \quad (p < 0.001, R^2 = 0.78) \quad (4)$$

$$V_{\text{rembone tissue}} = 20.4 \cdot V_{\text{water}} - 20.4 \cdot Tb.Th. + 2.6 \quad (p = 0.001, R^2 = 0.77) \quad (5)$$

$$V_{\text{rembone tissue}} = 16.5 \cdot V_{\text{water}} + 16.6 \cdot Tb.Sp. - 4.4 \quad (p < 0.001, R^2 = 0.70) \quad (6)$$



Figure 3. Drilled holes in porcine femora using water jets with various nozzle diameters.

Nozzle	BV/TV		Tb.Th.		Tb.Sp.
	R^2	p	R^2	p	p
0.3 mm	0.47	0.01	0.51	0.01	0.78
0.4 mm	0.64	<0.001	0.55	<0.001	0.35
0.5 mm	0.57	<0.001	0.55	<0.001	0.80
0.6 mm	0.17	0.05	0.19	0.04	0.45
All nozzles	0.47	<0.001	0.36	<0.001	0.64

R^2 : coefficient of determination. p : significance of the regression analysis.

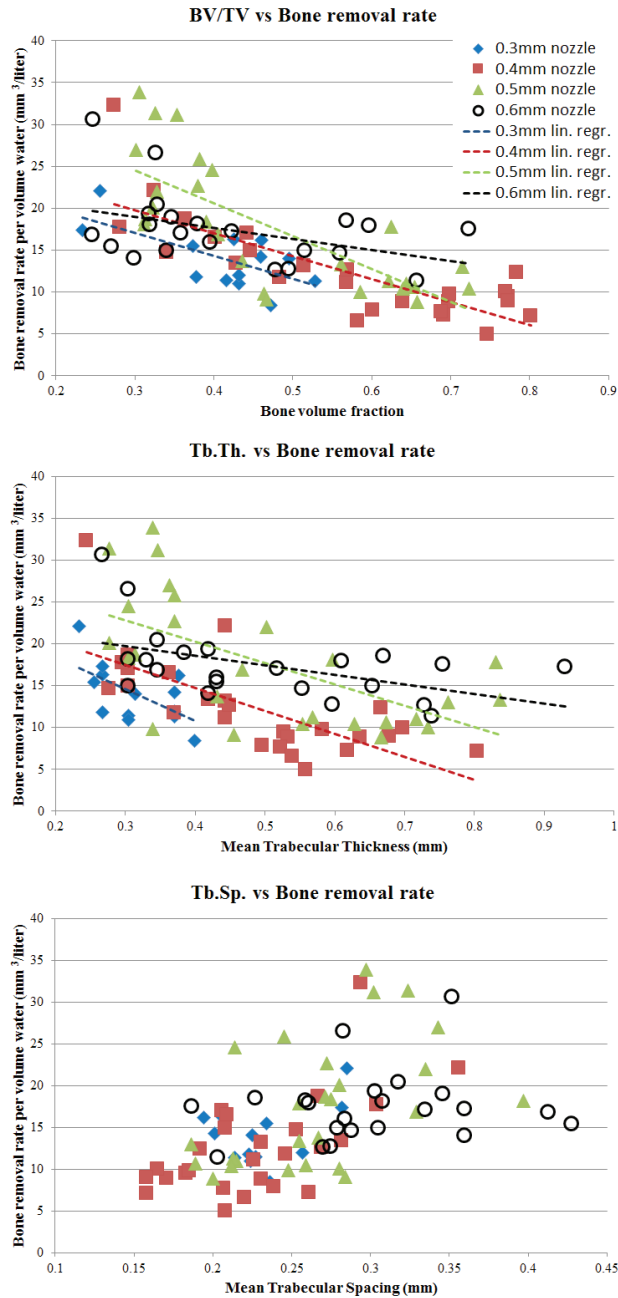


Figure 4. The influence of the nozzle diameter, BV/TV, Tb.Th. and Tb.Sp. on the VRR. The dashed lines represent the outcomes of linear regression analyses for the individual nozzle diameters. The overlap in VRR and regression trend lines indicate an absence of influence of the nozzle diameter on the VRR. No trend lines were depicted in the Tb.Sp. graph due to the lack of significance of the regression analysis for the individual nozzle diameters (Table 2).

Discussion

No evidence was found that the nozzle diameter affects the efficiency when water jet drilling in bone tissue. The individual measurements as well as the predictive models overlap for all nozzle diameters (Fig. 4). Hence, the VRR and thus the efficiency is not influenced by the nozzle diameter. Consequently, the total volume of added water appears to be a leading factor for the drilling capacity. For nozzles smaller than 0.6 mm, a clear decline in VRR is present for an increase in BV/TV or Tb.Th. An explanation for this trend can be that the BV/TV and the Tb.Th. determine to a large extent the mechanical properties of the bone [10]. A higher BV/TV or Tb.Th. results in an increased maximum tensile strength, compressive strength and modulus of elasticity of the tissue [11, 12]. The increased strength has a negative effect on the machinability of bone with pure water jets [13]. Thus, it is not the efficiency of the water jet that changes, but the mechanical properties of the material that is drilled in, which makes the removal of the bone more difficult.

Regardless the overlap, the 0.6 mm nozzle seems to be less affected by the Tb.Th. and BV/TV than the other nozzles. An explanation of this can be that the width of the water jet exceeds the average width of a trabecular strut, which was 0.48 mm in the experiment. This causes the water jet to fully enclose the strut in its devastating stream of water, washing it away entirely instead of nibbling bone material away at the sides of the strut, which is the case for smaller nozzle diameters.

The experiment supports previous research [8, 13, 14] that the velocity (Eq. (1)) and the volume of water (Eq. (2)) that is directed towards an object is leading for the total volume of material removal. By keeping V_{water} constant, D , t and P can be chosen arbitrarily to remove a certain volume of material. However, the results cannot be extrapolated for all machine settings. Especially extreme low or high settings of D , t and P the model will be inaccurate. Eq. (2) suggests a linear influence of jet time (t) on the material removal. Previous studies showed that the drilling depth increase is maximum after initiating the water jet [15-19], and, after the first few tenths of a second, increases almost linearly until a maximum depth is reached. The linear phase is therefore limited to a specific range of t . The same holds for P and D in their respective ranges. For P , a minimal threshold needs to be met before bone material is removed, which lies between 30 and 45 MPa depending on the bone tissue and D [20-22]. The pressure range in which the pressure can be considered to have a linear influence is up to 120 MPa [17, 23]. Thus, the volume of and velocity of the water is a good measure for the total volume of material removal, but only when no extreme values for D , t and P are used to achieve this volume and velocity of the water.

Limiting factors could have influenced the results. In the experiment, the VRR was used to normalize for the differences in V_{water} that is caused by differences in nozzle diameter. Keeping V_{water} constant by adjusting t (Eq. (2)) might have resulted

in different outcomes, as no compensation per unit volume of water would have been required. A drawback of adjusting t would have been the increased influence of the attack time, which is the time required to build up the water pressure. In this experiment, the attack time was 0.3 s, which consistently increased the jet time by 6% for all holes that were drilled. When various jet times would have been used, the influence of the attack time would not have been constant. Therefore, the results were normalized using the VRR instead of adjusting t .

The predictive models (Eq. 4, 5 and 6) can be used for procedures where a predetermined volume of bone material needs to be removed, such as osteotomies and bone tumor removal. For these procedures, using the BV/TV to predict the volume of removed material (Eq. 4) is favorable since the BT/TV can be measured in conventional CT scanners that are available in hospitals. Additionally, the BV/TV model provides the highest accuracy of the three equations. Using Eq. (1) and (2), P and D can be determined for a given t . For time critical surgery, a low t can be chosen. For delicate procedures that require increased precision, a high t can be used, causing P and D to be lower providing the surgeon more control by the slow bone removal process.

Conclusion

For the development of surgical instruments for bone surgery that rely on water jet technology, a water jet diameter can be chosen in accordance to the specific requirements of the surgical procedure without affecting the total volume of water that is required to remove the specific volume of bone tissue. If an irrigation system is required for the removal of superfluous water, a smaller nozzle is advised to stay within the limits of the maximum capacity of the pump. For 70 MPa, this would mean a nozzle diameter smaller than 0.37 mm. For developments in minimally invasive surgery where the space in a joint is limited, the instrument should be equipped with a small nozzle, which allows thinner tubing but leads to an increased jet time. For time critical surgery, a larger nozzle is advised.

The total volume of added water combined with the Tb.Th., BV/TV or Tb.Sp. is a leading measure for the volume of bone material that is removed, which can be described by linear models described in this paper. The models can be used to determine the water jet machine settings for procedures where a predetermined volume of bone material needs to be removed, such as osteotomies and bone tumor removal.

References

1. Eriksson, A.R., T. Albrektsson, and B. Albrektsson, Heat caused by drilling cortical bone. Temperature measured in vivo in patients and animals. *Acta Orthopaedica Scandinavica*, 1984. 55(6): p. 629-31.
2. Matthews, L.S. and C. Hirsch, Temperatures measured in human cortical bone when drilling. *Journal of Bone and Joint Surgery-American Volume*, 1972. 54(2): p. 297-308.
3. Eriksson, R.A. and T. Albrektsson, The effect of heat on bone regeneration: an experimental study in the rabbit using the bone growth chamber. *J Oral Maxillofac Surg*, 1984. 42(11): p. 705-11.
4. Eriksson, R.A., T. Albrektsson, and B. Magnusson, Assessment of bone viability after heat trauma. A histological, histochemical and vital microscopic study in the rabbit. *Scand J Plast Reconstr Surg*, 1984. 18(3): p. 261-8.
5. Iyer, S., C. Weiss, and A. Mehta, Effects of drill speed on heat production and the rate and quality of bone formation in dental implant osteotomies. Part II: Relationship between drill speed and healing. *Int J Prosthodont*, 1997. 10(6): p. 536-40.
6. Schmolke, S., et al., Temperature measurements during abrasive water jet osteotomy. *Biomedizinische Technik*, 2004. 49(1-2): p. 18-21.
7. Hildebrand, T., et al., Direct three-dimensional morphometric analysis of human cancellous bone: microstructural data from spine, femur, iliac crest, and calcaneus. *J Bone Miner Res*, 1999. 14(7): p. 1167-74.
8. Summers, D., *Waterjetting technology*. first ed. 1995: Taylor & Francis.
9. den Dunnen, S., et al., Waterjet drilling in porcine bone: The effect of the nozzle diameter and bone architecture on the hole dimensions. *Journal of the Mechanical Behavior of Biomedical Materials*, 2013(0).
10. Day, J.S., *Bone Quality: The Mechanical Effects of Microarchitecture and matrix properties*. 2005, Optima Grafische Publicatie: Rotterdam.
11. Cory, E., et al., Compressive axial mechanical properties of rat bone as functions of bone volume fraction, apparent density and micro-ct based mineral density. *J Biomech*, 2010. 43(5): p. 953-60.
12. Nazarian, A., et al., Tensile properties of rat femoral bone as functions of bone volume fraction, apparent density and volumetric bone mineral density. *J Biomech*, 2011. 44(13): p. 2482-8.
13. Tikhomirov, R.A., et al., *High-pressure jetcutting*. 1992, New York: ASME Press. 197.
14. Hashish, M. and M.P. Duplessis, Theoretical and Experimental Investigation of Continuous Jet Penetration of Solids. *Journal of Engineering for Industry-Transactions of the Asme*, 1978. 100(1): p. 88-94.
15. Akkurt, A., The effect of material type and plate thickness on drilling time of abrasive water jet drilling process. *Materials & Design*, 2009. 30(3): p. 810-815.
16. Bach, F.-W., et al. Investigation of the AWIJ-Drilling Process in Cortical Bone. in *Proceedings of the 2007 American WJTA Conference and Expo*. 2007. Houston, USA.
17. Orbanic, H. and M. Junkar, An experimental study of drilling small and deep blind holes with an abrasive water jet. *Proceedings of the Institution of Mechanical Engineers Part B-Journal of Engineering Manufacture*, 2004. 218(5): p. 503-508.
18. Pandey, R.K. and S. Panda, Drilling of bone: A comprehensive review. *Journal of Clinical Orthopaedics and Trauma*, 2013.
19. Matthujak, A., et al., Characteristics of impact-driven high-speed liquid jets in water. *Shock Waves*, 2013. 23(2): p. 105-114.
20. Honl, M., et al., The use of water-jetting technology in prostheses revision surgery - First results of parameter studies on bone and bone Cement. *Journal of Biomedical Materials Research*, 2000. 53(6): p. 781-790.
21. Honl, M., et al., Water jet cutting of bone and bone cement. A study of the possibilities and limitations of a new technique. *Biomedizinische Technik*, 2000. 45(9): p. 222-227.
22. en Dunnen, S., et al., Pure waterjet drilling of articular bone: an in vitro feasibility study. *Journal of Mechanical Engineering - Strojnicki vestnik*, 2013. 59(7-8): p. 425-432.
23. Mohamed, M.A.K., *Waterjet cutting up to 900 MPa*. 2004, Universitat Hannover. p. 122.

Chapter 5

Depth control for water jet drilling in bone tissue

Sections:

Colliding jets provide depth control for water jetting in bone tissue

Colliding jets provide depth control for water jetting in bone tissue

Steven den Dunnen, Jenny Dankelman, Gino M.M.J. Kerkhoffs,
Gabrielle J.M. Tuijthof

“Colliding jets provide depth control for water jetting in bone tissue”
Journal of the Mechanical Behavior of Biomedical Materials, vol. 72, p. 219-228, 2017

In orthopaedic surgery, water jet drilling provides several advantages over classic drilling with rigid drilling bits, such as the always sharp cut, absence of thermal damage and increased manoeuvrability. Previous research showed that the heterogeneity of bone tissue can cause variation in drilling depth whilst water jet drilling.

To improve control over the drilling depth, a new method is tested consisting of two water jets that collide directly below the bone surface. The expected working principle is that after collision the jets will disintegrate, with the result of eliminating the destructive power of the coherent jets and leaving the bone tissue underneath the focal point intact. To assess the working principle of colliding water jets (CWJ), the influence of inhomogeneity of the bone tissue on the variation of the drilling depth and the impact of jet time (t_{wj}) on the drilling depth were compared to a single water jet (SWJ) with a similar power.

98 holes were drilled in 14 submerged porcine tali with two conditions CWJ (impact angle of 30 and 90 degrees) and SWJ. The water pressure was 70 MPa for all conditions. The water jet diameter was 0.3 mm for CWJ and 0.4 mm for SWJ. t_{wj} was set at 1, 3, 5 and 8 seconds. Drilling depth and hole diameter were measured using microCT scans. A non-parametric Levene's test was performed to assess a significant difference in variance between conditions SWJ and CWJ. A regression analysis was used to determine differences in influence of t_{wj} on the drilling depth. Hole diameter differences were assessed using a one way Anova. A significance level of $p < 0.05$ was set.

Condition CWJ significantly decreases the drilling depth variance caused by the heterogeneity of the bone when compared to SWJ. The mean depth for CWJ was 0.9 mm (SD 0.3 mm) versus 4.8 mm (SD 2.0) for SWJ. t_{wj} affects the drilling depth less for condition CWJ ($p < 0.01$, $R^2=0.30$) than for SWJ ($p < 0.01$, $R^2=0.46$). The impact

angle (30 or 90 degrees) of the CWJ does not influence the drilling depth nor the variation in depth. The diameters of the resulting holes in the direction of the jets is significantly larger for CWJ at 90 degrees than for 30 degrees or a single jet.

This study shows that CWJ provides accurate depth control when water jet drilling in an inhomogeneous material such as bone. The maximum variance measured by using the 95% confidence interval is 0.6 mm opposed to 5.4 mm for SWJ. This variance is smaller than the accuracy required for bone debridement treatments (2-4 mm deep) or drilling pilot holes. This confirms that the use of CWJ is an inherently safe method that can be used to accurately drill in bones.

Introduction

Water jet technology has increasingly gained popularity in surgical treatments [1-4]. Advantages over conventional rigid mechanical instruments are the lack of thermal damage [5, 6] and the always sharp cut. Additionally, it allows the design of instruments with increased manoeuvrability, since the water can be provided by a flexible tube [7]. Current commercial products are primarily used to treat soft tissue [1, 4, 5]. Recent developments do show that water jet technology can provide similar advantages for cutting or drilling through bone tissue [8-11]. This study focusses on water jet drilling for orthopaedic treatments such as drilling pilot holes for screw fixations and bone debridement treatments [12-14].

A challenge for orthopaedic water jet surgery lies in controlling the drilling depth, which is of utmost importance to prevent unintentional damage of healthy tissue during the procedure. The natural inhomogeneity of bone tissue causes local variances in its density, which affect the local mechanical properties. As a result, different hole depths are created when water jet drilling with identical machine settings [8, 9, 15]. Though the correlation between the bone density and drilling depth has been thoroughly investigated and can be compensated for to achieve a pre-set hole depth [9, 15], acquiring the local bone density in a clinical setting can still be difficult due to the absence of proper imaging protocols and prolonged data processing that compromises the workflow in the hospital. Therefore, a novel concept for water jet drilling was investigated: colliding water jets (CWJ). The pursued working principle is as follows: two separate jets are focused to collide just below the surface of the bone tissue (Figure 1). The energy density of the individual jets exceeds

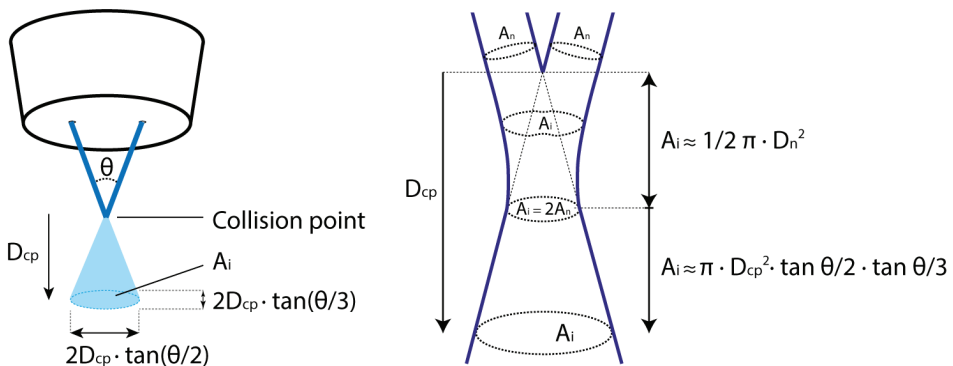


Figure 1. Left: working principle of colliding water jets. After water jet collision the coherency of the jet is compromised, resulting in spray with an elliptical surface area with a lower energy density than the individual jets. Right: an enlarged view of the colliding water jets. The impact area A_i is nearly constant up to a specific D_{cp} where A_i is equal to $2A_n$. Further increasing D_{cp} will result in quadratic rise in A_i . The dashed areas represent the various shapes and sizes of the impact area (A_i) and the cross sectional area of the water jet (A_n).

the threshold for machining bone, and will therefore penetrate the bone tissue. At the focal point where the two jets collide just below the surface, the coherency of both jets is compromised causing energy dissipation. As a result, the energy density of the water jets drops below the threshold required to penetrate bone tissue. At this point, no further drilling will occur and depth control is achieved regardless of local bone density.

In this manuscript, this concept of drilling depth control by CWJ is studied and compared to a standard single water jet drilling (SWJ). By determining significant differences between CWJ and SWJ in drilling depth, drilling depth variance and the influence of the drilling jet time (t_{wj} , s) on the drilling depth, the potential of CWJ as inherently safe depth control concept is verified.

Materials and methods

Theoretical overview

A theoretical overview is given that forms the basis for the concept that CWJ improves drilling depth control compared to SWJ. Before actual water jet drilling of a material takes place, a specific threshold needs to be exceeded. This threshold can be expressed in many units, such as the material's compressive strength, yield strength [16] and shear stress [17] in combination with the water jet's pressure [8, 15], nozzle diameter [9], jet time or transverse speed [18]. For this study, the threshold is expressed using a power density P_d ($[W/m^2]$ or $[kg/s^3]$) model, which can be applied universally for assessing whether a material is being machined. P_d models include the natural disintegration of the water jet to express the diminishing machining capacity of a water jet [19, 20]. The decrease in machining capacity can be expressed by an increasing distance from the center axis of the water jet or the distance between water jet initiation and the impact site [21-23]. When the minimum power density for machining is met, the total energy of the water jet E_{wj} (J or W s) that interacts with the material determines the volume of bone that is removed. P_d is calculated by dividing the power of a jet p_{wj} (W or $kg\ m^2/s^3$) by the impact area of the water jet A_i (m^2), as provided in Equation (1):

$$P_d = \frac{P_{wj}}{A_i} \quad (1)$$

The power and energy of a water jet can be expressed with Equation (2) and (3) respectively,

$$P_{wj} = p_{wj} \cdot \dot{q}_{wj} \quad (2)$$

$$E_{wj} = p_{wj} \cdot \dot{q}_{wj} \cdot t_{wj} \quad (3)$$

where p_{wj} is the pressure (Pa or N/m²), \dot{q}_{wj} is the volume flow rate (m³/s) and t_{wj} is the water jet time (s). Using the simplified Bernoulli equation, the volume flow rate can be expressed as

$$\dot{q}_{wj} = c_d \cdot A_n \cdot v_{wj} = c_d \cdot \frac{\pi}{4} \cdot d_n^2 \cdot \sqrt{\frac{2 \cdot p_{wj}}{\rho_w}} \quad (4)$$

where A_n is the surface area of the nozzle (m²), v_{wj} is the velocity of the water jet (m/s), d_n is the nozzle diameter (m) and ρ_w is the density of the fluid (kg/m³). c_d is the coefficient of discharge of the nozzle, which compensates for losses in flow due to the shape of the nozzle, compressibility of the water and physical phenomena such as vena contracta. The value of c_d is usually between 0.6 and 0.9 [24-26]. Substitutions of Equations (3) and (4) in Equations (1) and (2) result in:

$$P_{wj} = p_{wj} \cdot c_d \cdot A_n \cdot v_{wj} = c_d \cdot \frac{\pi}{4} \cdot \sqrt{\frac{2}{\rho_w}} \cdot p_{wj}^{1.5} \cdot d_n^2 \quad (5)$$

$$P_d = \frac{p_{wj} \cdot c_d \cdot A_n \cdot v_{wj}}{A_i} = \frac{c_d \cdot \frac{\pi}{4} \cdot \sqrt{\frac{2}{\rho_w}} \cdot p_{wj}^{1.5} \cdot d_n^2}{A_i} \quad (6)$$

$$E_{wj} = p_{wj} \cdot c_d \cdot A_n \cdot v_{wj} \cdot t_{wj} = c_d \cdot \frac{\pi}{4} \cdot \sqrt{\frac{2}{\rho_w}} \cdot p_{wj}^{1.5} \cdot d_n^2 \cdot t_{wj} \quad (7)$$

P_d can be used to determine whether a material is being machined or not. For a full coherent water jet, A_i is equal to A_n directly after the initiation of the jet. This makes P_d solely dependent on the machine setting p_{wj} , since v_{wj} is also a product of p_{wj} (Equations 4 and 5). This indicates that the size of the nozzle diameter does not influence the capability of machining, which was also concluded in a previous study [27]. In that experiment, the volume of material removed did increase with an increase in nozzle diameter since the total energy of the water jet was larger (Equation 3 and 7). However, per added volume of water (which can be considered equal to the energy), no significant differences were found in the volume of removed material.

The impact angle can have an effect on the drilling depth, variance in drilling depth and shape of the hole. After the collision of two water jets, the individual

coherent jets will break up in many small droplets which are spread over a greater area than the combined cross sectional area of the water jets (Figure 1, right). Comparable to a particle hitting a surface, a water droplet will reflect and proceed its path in the opposite direction with a similar or shallower angle after a collision. Some particles are pushed outwards in perpendicular direction. The resulting spray forms into a cone shape with an elliptical cross section (Figure 1), with minimal spray outside this cone. Pilot experiments showed that the angle of the cone in the plane of the water jets is equal to the impact angle of the two jets, with a fictitious origin at the first location where the two water jets collide (Figure 1, right). The angle of the spray cone perpendicular to the plane of the water jets is approximately 2/3 of the impact angle (Figure 1, left). Therefore, it is expected that the shape of the hole is not fully circular (Figure 1). The area (A_i) over which the power of the water jet (p_{wj}) is spread can be determined by Equation 8 for impact surfaces that are larger than the combined cross sectional areas A_n of the individual water jets. A smaller A_i than twice the cross sectional areas of the water jets would imply compression of water during the collision, which is not the case for pressures that are used for bone surgery. Instead, the colliding water pushes the outer sides of the water jet that is still coherent further outwards, resulting in a cross sectional area that is at least equal to the combined cross sectional areas of the water jets. In practise, this means that up to a specific distance from the collision point D_{cp} (m), which is defined by the nozzle diameter D_n and the impact angle θ , A_i is considered to be nearly constant (Equation 9). For larger values of D_{cp} , A_i increases quadratically over distance from the collision point (D_{cp}) and linearly to the impact angle (θ) of the water jets (Equation 8), thereby rapidly lowering the energy density P_d (Equation 6).

$$\text{for } A_i > \frac{1}{2} \pi \cdot D_n^2 \text{ or } D_{cp} > \frac{D_n}{\sqrt{2} \sqrt{\tan \frac{\theta}{2} \cdot \tan \frac{\theta}{3}}} : A_i \approx \pi \cdot D_{cp}^2 \cdot \tan \frac{\theta}{2} \cdot \tan \frac{\theta}{3} \quad (8)$$

$$\text{for } A_i \leq \frac{1}{2} \pi \cdot D_n^2 \text{ or } D_{cp} \leq \frac{D_n}{\sqrt{2} \sqrt{\tan \frac{\theta}{2} \cdot \tan \frac{\theta}{3}}} : A_i \approx \frac{1}{2} \pi \cdot D_n^2 \quad (9)$$

Since a minimal threshold in P_d is required before machining is feasible, it is expected that below the point of collision the combined water jet will not be powerful enough to erode the bone tissue any further. At this point, depth control is achieved.

In Figure 2 (top), the distance after the collision point D_{cp} is plotted against the theoretical power density P_d for several impact angles by rewriting Equation 6 and 8. In previous studies, the most conservative pressure setting to water jet drill in bone

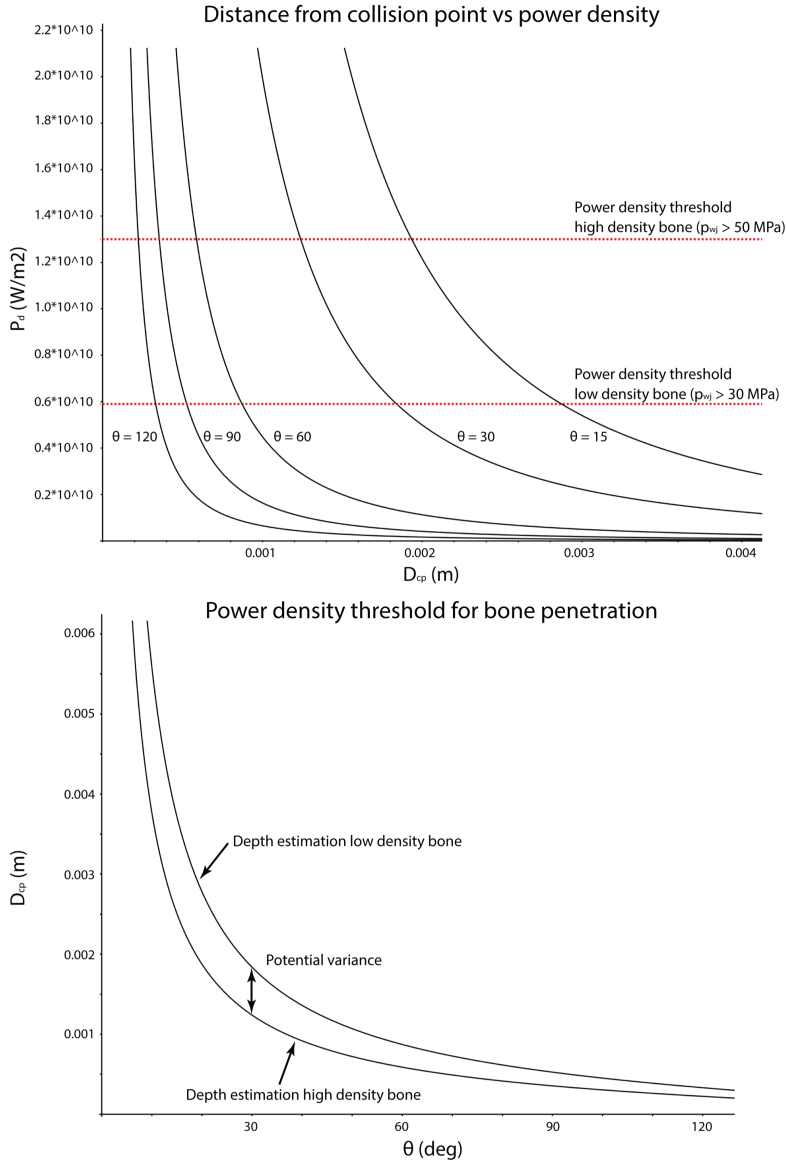


Figure 2. Top: the power density P_d plotted against the distance after the collision point D_{cp} for several impact angles θ . The P_d of a colliding jet is maximized to the P_d of an individual jet according to Eq. 8. The two horizontal lines represent the minimum and maximum power density thresholds required to machine bone tissue with a water jet. The threshold is not constant for bone due to the natural inhomogeneity of the tissue. Bottom: the two power density thresholds plotted in a D_{cp}/θ graph. In this graph, D_{cp} is equivalent to the predicted drilling depth. The difference between the lines represent the potential variance in drilling depth that can occur due to natural inhomogeneity of the tissue. Both graphs were plotted for a pressure of 70 MPa, a nozzle diameter of 0.3 mm and a C_d of 0.8.

tissue ranged between 30 and 50 MPa, depending on the bone density [8, 15, 28]. Assuming full jet coherence at the impact site and a C_d of 0.8, the power density P_d to start machining bone tissue lies between 5.9×10^9 (low density bone) and 1.3×10^{10} W/m² (high density bone) (Equation 6, horizontal lines in Figure 2 (top)). In Figure 2 (bottom), D_{cp} is plotted against θ using the power density thresholds for reference. When the collision point of the two jets (Figure 1) is set at the surface area of the material, D_{cp} values in Figure 2 (bottom) are equal to the expected drilling depths. The potential variance that can occur due to natural inhomogeneity in bone is the difference between the two threshold lines. The expected drilling depth and variance is affected by θ . To make the influence of θ more concrete: when two individual water jets collide under an angle of 30 degrees with an initial pressure of 70 MPa, the low density bone threshold is being exceeded up to 1.8 mm after the water jet collision, whereas high density bone threshold is exceeded up to 1.2 mm after the water jet collision. The difference, 0.6 mm, is the potential variance that can occur due to differences in bone density. For a collision angle of 90 degrees, the power density thresholds are exceeded up to 0.50 mm (low density bone) and 0.34 mm (high density bone), with a potential variance of only 0.16 mm. Hence, the drilling depth and variance will drop for an increase of θ .

To summarize, a water jet requires a minimum power density to machine a material (Equation 6). Once this threshold is met, the total energy of the water jet that is directed towards the material determines the volume of the material that is machined (Equation 7). When using colliding water jets, the minimum energy density to machine materials is met before the collision (Equation 6), but drops below the threshold promptly after the collision (Equation 6 and 8, Figure 2). From this point, the total energy directed towards the material does not play a significant role in the machining of the material since the minimum requirement for machining is not met. A_n increase in impact angle will result in shallower holes with a smaller variance, but a larger hole diameter.

Experiment conditions and considerations

Nozzle diameters and pressure

The nozzle diameter and pressure were chosen to meet two requirements. First, before collision, the individual water jets should be able to machine bone tissue to allow comparison between the colliding and single jet nozzle conditions. Secondly, considering the future application in orthopaedic surgery, a minimal volume flow is strived for to minimize the quantity of xenobiotic substances for the patient and to allow commercially available irrigation systems to remove the superfluous water at the surgical site [27]. The nozzle diameter has a larger influence on the volume flow than the pressure (power of 2 versus power of 1.5, Equation 4). Therefore, to achieve

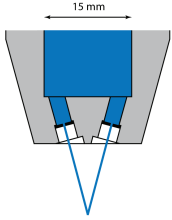
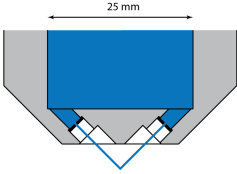
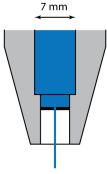
a minimum flow, the smallest nozzle diameter in combination with a fixed pressure was pursued. In previous studies, the smallest volume flow (Equation 4) to machine bone tissue was determined, which was achieved by the following machine settings: a nozzle diameter of 0.3 mm, a pressure of 70 MPa and a jet time of 5 s. These settings resulted in drilling depths between 4 and 8 mm [9, 15, 27], which are sufficient for bone debridement treatments where holes between 2 and 4 mm are required [29]. Therefore, two 0.3 mm diameter nozzles were used to create the colliding water jet condition. To allow direct comparison with a SWJ, the total energy E_{wj} (Equation 3) of the CWJ directed towards the bone should be equal to that of the SWJ [27]. For identical jet times, this means the power p_{wj} of the water jet should be in the same order of magnitude (Equation 5). With an assumed c_d of 0.8, p_{wj} for each individual jet of the CWJ is approximately 1480 W (Equation 4), thus multiplied by two gives the required power for the single jet. The commercially available nozzle diameter that comes closest to this magnitude is 0.4 mm in diameter (expected power of 2640 W), which was therefore used for the SWJ.

Specimens

Fourteen bone specimens were obtained freshly from one batch of 7 pigs (weight approximately 82 kg, similar age, nutrition and race) after termination of an animal experiment of different purpose. Talar bones (2 per animal) were frozen directly after harvesting. Talar bone was used since it is a part of an articular joint, which is similar to bone that is treated in clinical bone debridement treatments. The cartilage on the tibial dome of the talus was removed using a scalpel to allow the water jets to drill directly in to the bone. Three hours prior to the experiment, the bone specimens were thawed to room temperature whilst frequently adding a 0.9% saline solution.

Impact angle and collision point

Besides the potential effect on the drilling depth, drilling depth variance and hole diameter, the impact angle of the colliding water jets also affects the minimum size of the design of the nozzle. To create coherent water jets, the individual water jet requires a minimum inlet distance in front of the orifice. This causes the total size of the nozzle to increase when using larger angles (Table 1). For arthroscopic surgery, the size of the nozzle is to be kept minimal. Therefore, a small impact angle is strived for. To determine whether a small impact angle performs worse, two different impact angles were tested: 30 (CWJ 30) and 90 (CWJ 90) degrees (Table 1). To determine whether CWJ can machine bone tissue regardless its density, the collision point of the water jets was set at the bone surface, allowing both hard subchondral tissue (bone surface) and the underlying trabecular bone of lower density to be exposed to the colliding water jets.

Table 1. Specification of the three nozzle conditions that were tested in this study.			
			
Collision angle	30	90	-
Nozzle diameter	2 x 0.3 mm	2 x 0.3 mm	1 x 0.4 mm
Pressure	70 MPa	70 MPa	70 MPa
Jet times (n)	1 (10), 3 (10), 5 (10), 8 (10) s	1 (10), 3 (10), 5 (10), 8 (10) s	1 (6), 3 (6), 5 (6) s
Estimated power ($C_d = 0.8$)	2960 W	2960 W	2640 W
Abbreviation	CWJ 30	CWJ 90	SWJ

Jet times

The jet time t_{wj} linearly affects the total energy of the water jet E_{wj} (Equation 7), which is a measure for determining how much bone is being machined. Therefore, t_{wj} has a direct effect on the drilling depth and on the variance in drilling depth due to the inhomogeneity of the bone tissue. The extent of the influence of t_{wj} for SWJ has been determined in previous research [15, 30]. The working principle of CWJ eliminates the influence of t_{wj} on the drilling depth since the threshold for machining bone is not dependent on the jet time (Equation 6 and 8). To determine a difference in influence of the jet time on the drilling depth of condition CWJ with respect to condition SWJ, four jet times were tested for the CWJ: 1, 3, 5 and 8 s. Condition SWJ was tested six times for jet times of 1,3 and 5 s (Table 1).

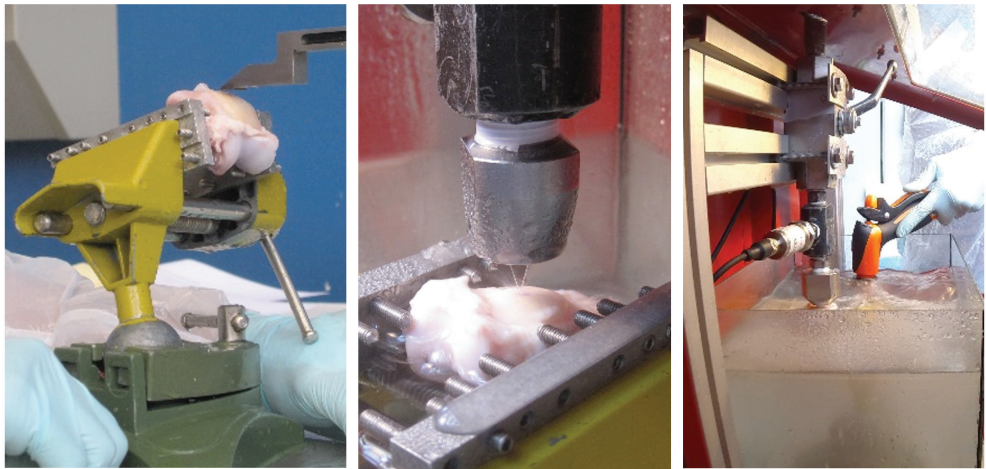


Figure 3. (left) Height and perpendicular alignment. (center) Alignment drilling location to the water jet. (right) Specimen and nozzle are submerged in water in an aquarium.

Experiment set-up and procedures

A custom made water jet set-up was used to create a water jets within 0.3 s with an accuracy of ± 0.2 MPa [9, 15]. Pressures were monitored at the nozzle using a KLPT-WH pressure transmitter (Koppen & Lethem, Newark, United Kingdom). For the CWJ, nozzle holders were made that allowed precise positioning of industrial sapphire nozzles to achieve a collision of the water jets. Two alignment steps were taken to ensure a precise, constant and perpendicular alignment of the (colliding) water jet on the superior surface of the talar bones. First, the bone specimen was locked in an omni-directional clamp (Figure 3_{left}). A height calliper was used to adjust the specimen to the proper height and perpendicular alignment (Figure 3a). Subsequently, the fully fixated clamp with the specimen was placed into an aquarium and aligned with the water jet (Figure 3_{center}). A continuous low pressure water jet (<0.2 MPa) was used to verify proper alignment. A misalignment would result in either two distinct backsplashes (surface too high) or a large incoherent backsplash (surface too low). To mimic arthroscopic surgery, the specimen and nozzle were submerged with water to a depth of 40 mm measured from the top of the articular surface to the water level (Figure 3_{right}). 98 holes were drilled in porcine tali using the machine settings as given in Table 1. Unsuccessful drillings due to potential misalignment or pressure under/overshoot were not repeated due to the limited available space on the articular surface of the bone tissue.

Measurements

Micro Computer Tomography (μ CT) scans were made of each specimen to measure the hole depth and diameter using a Scanco microCT 80 scanner with a spatial resolution of 37 μ m. ImageJ version 1.46 m [31, 32] with the Stack Alignment plugin [33] were used to process the mCT scans. The maximum value of the drilling depth as measured in the coronal (L_1) and sagittal (L_2) plane was used to set the hole depth (Figure 4). As for several orthopaedic treatments, such as drilling pilot holes for screw fixation and bone debridement treatments, the proper diameter of a hole determines correct fixation or affects the patients' healing, the hole diameters were measured and compared. The hole diameter was measured in two directions (D_{long} and D_{short}) perpendicular to each other (Figure 4) to allow differences in hole shape to be determined for the different nozzle conditions. Three individuals performed each measurement. A difference in measurement greater than 0.3 mm resulted in a full re-measurement of the specific hole.

Statistical analysis

To determine an increased control of the drilling depth when using CWJ compared to SWJ, at least one of the following three requirements have to be met.

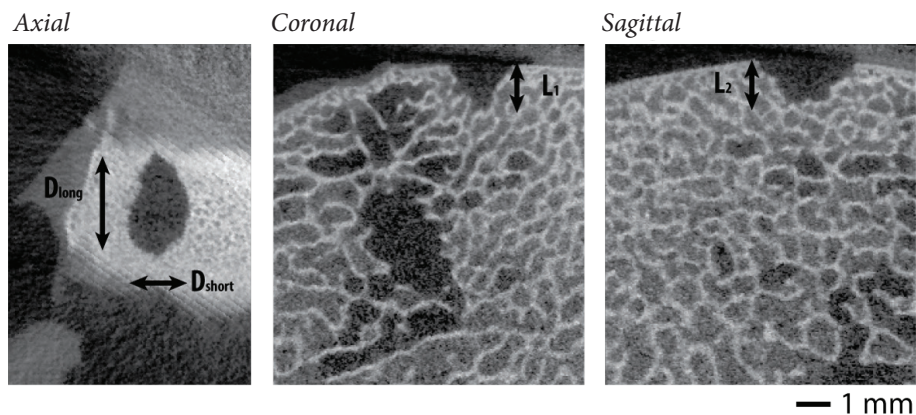


Figure 4. mCT scans of a hole drilled in a talus bone by two colliding water jets. The diameter of the hole is measured in two directions. First, the greatest distance is measured as D_{long} . Then, the greatest distance of the hole perpendicular to D_{long} is measured as D_{short} . The drilling depth is determined by the maximum depth (either L_1 or L_2) in the coronal or sagittal plane. Inhomogeneity in the bone tissue is visible in the coronal and sagittal plane: the outer layer of the bone is more dense. At greater depth the density drops and occasionally cavities arise.

First, the variance in drilling depth should be significantly lower for CWJ than for SWJ. This is expected based on the theoretical consideration that within a few tenths of a mm after collision the P_d drops from the upper power density threshold to the lower power density threshold to machine bone tissue (Figure 2, bottom). For condition SWJ, the same drop in P_d requires several mm [8, 30]. To verify a significant difference in the variance between the nozzles for each jet time (homogeneity of variance), a non-parametric Levene's test was used ($p < 0.05$) [34, 35]. The non-parametric Levene's test was used because it is considered to be more robust for non-normal distributions and unequal groups compared to the standard Levene's in combination with Brown-Forsythe test [34, 35].

Second, the influence of the jet time on the drilling depth should be significantly smaller for the CWJ than for the SWJ. The expectation that CWJ is less influenced by the jet time is derived from Equations 6 and 7. The total energy of a water jet, which greatly depends on the jet time, determines the volume of the material that is machined (Equation 7). However, before any machining takes place the minimum power density threshold needs to be exceeded (Equation 6). Promptly after the collision of the CWJ this threshold is not met (Figure 2). Consequently, the jet time nor the total energy of the water jet (Equation 7) is expected to influence the drilling procedure for CWJ, whereas these parameters do affect the drilling procedure for SWJ (Equation 7). To test the influence of the jet time on the drilling depth, regression analyses were performed using a power function as a curve estimation ($p < 0.05$). The power function was chosen, because this proved to be the optimal representation for

the drilling or cutting depth over time [16, 30, 36]. R values of the power functions are compared to determine differences in strength and direction of the models. Coefficient of determination (R^2) values of the models are compared to indicate what percentage of the drilling depth can be explained due to an increase in water jet time.

Third, the drilling depth for CWJ should be significantly lower than for SWJ. Within a few tenths of a mm after collision of the CWJ, the power density can drop below the minimum threshold for machining low density bone tissue causing the drilling process to stop (Figure 2, bottom). For SWJ, the power density is almost maintained causing continuation of the drilling process. Consequently, the holes of SWJ are expected to be deeper than the CWJ for identical machine settings. A Welch test with post hoc Games-Howell was used to determine differences in drilling depth between the CWJ 30, CWJ 90 and SWJ for each jet time. The Welch test was used due to its robust performance for unequal sample sizes and unequal variances in the data.

Differences in hole diameter between the CWJ 30, CWJ 90 and SWJ were analysed per jet time and per diameter measurement (D_{short} and D_{long}) with a One Way Anova test ($p < 0.05$) and a Bonferroni post hoc test to highlight individual differences. For a clear overview, Tukey boxplots are depicted to show the results for the homogeneity of variance, mean drilling depth and hole diameters.

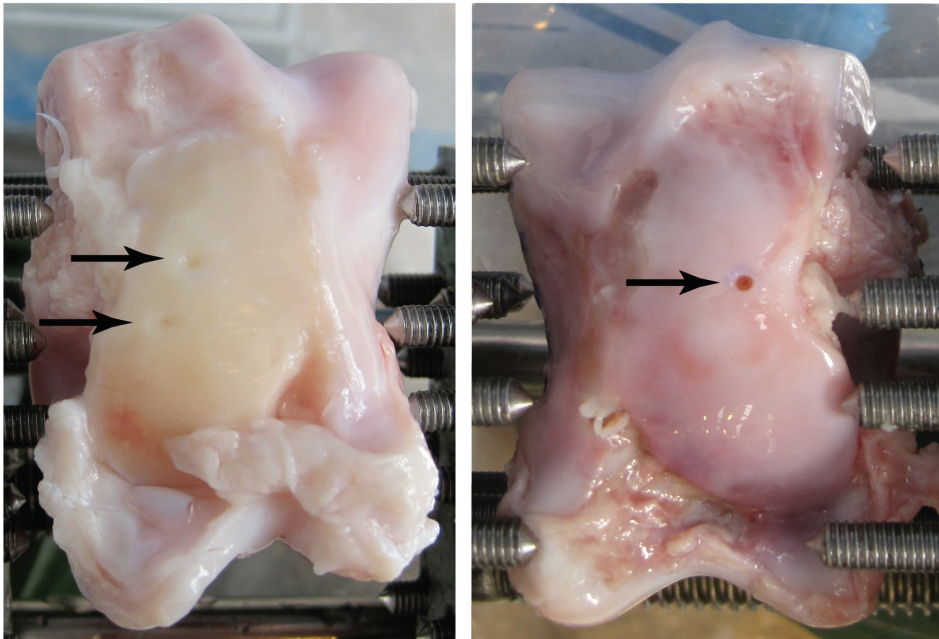


Figure 5. Holes are indicated by arrows. Left: two holes drilled by colliding water jets. Right: hole drilled by a single water jet.

Table 2. The mean drilling depth, standard deviation (SD), lower and upper bounds of the 95% confidence interval (CI) and the range of the 95% confidence interval (95% CI - 5% CI) for all nozzle conditions and jet times.

Condition\ t_{jet} (s)	Mean drilling depth								Lower bound 95% CI								Upper bound 95% CI								CI range (95% CI - 5% CI)							
	1	3	5	8	average	comb. av.	SD	1	3	5	8	1	3	5	8	1	3	5	8	1	3	5	8									
SWJ	3.0	5.9	5.5		4.8		2.0	2.3	3.2	4.9		3.8	8.6	6.1		1.5	5.4	1.2														
CWJ 30	0.6	0.8	1.1	0.9	0.9	0.9	0.3	0.5	0.6	0.8	0.8	0.8	0.9	1.4	1.0	0.3	0.3	0.6	0.2													
CWJ 90	0.7	1.1	1.1	1.2	1.0		0.3	0.6	0.9	0.8	1.0	0.8	1.3	1.3	1.5	0.2	0.4	0.5	0.5													

Results

All conditions resulted in holes being drilled in bone tissue (Figures 4 and 5). 3 holes were excluded due to incomplete drilling cycle as the maximum-pressure safety system was activated (1 hole) or due to an alignment error of the bone relative to the nozzle (2 holes).

The variance in drilling depth for the CWJ conditions is significantly lower than for the SWJ condition (Figure 6). The range of the 95% confidence intervals in drilling depth where 2-18 times smaller for CWJ than for SWJ (Table 2, column CI range). The maximum range of the 95% confidence interval found for the CWJ condition was 0.6 mm (Table 2, column CI range, row CWJ30, $t_{wj} = 5s$), whereas for the SWJ condition the maximum range of the confidence interval was 5.4 mm (Table 2, column CI range, row SWJ, $t_{wj} = 3s$). No differences in variance in drilling depth were found between the conditions CWJ 30 and CWJ 90, except for a jet time of 8 s ($p = 0.022$).

The regression analyses yielded three significant power functions (Table 3). The strength (R) and direction (R and the power function's coefficients) of the power function of condition SWJ is higher than for the CWJ 30 or CWJ 90. The coefficient of determination (R^2) indicates that approximately 30% of the variance can be explained by the jet time for condition CWJ, and 46% for the SWJ.

Significant lower means of the drilling depth were found for CWJ compared to SWJ (Figure 6). The difference in mean drilling depth is approximately a factor 5 for each jet time (Table 2, column mean drilling depth). For jet times of 3 and 8 s, CWJ 30 and CWJ 90 significantly differed by 0.3 mm with deeper holes for condition CWJ90.

Significant differences were found in D_{long} for the individual jet times (Figure 7). Condition CWJ 90 resulted in larger hole diameters than condition CWJ 30 or SWJ. No differences were found between CWJ 30 and SWJ.

The D_{short} showed significant smaller holes for SWJ compared to both CWJ conditions for a jet time of 3 s (Figure 6). When using a 5 s jet time, CWJ 30 and 90 differed significantly.

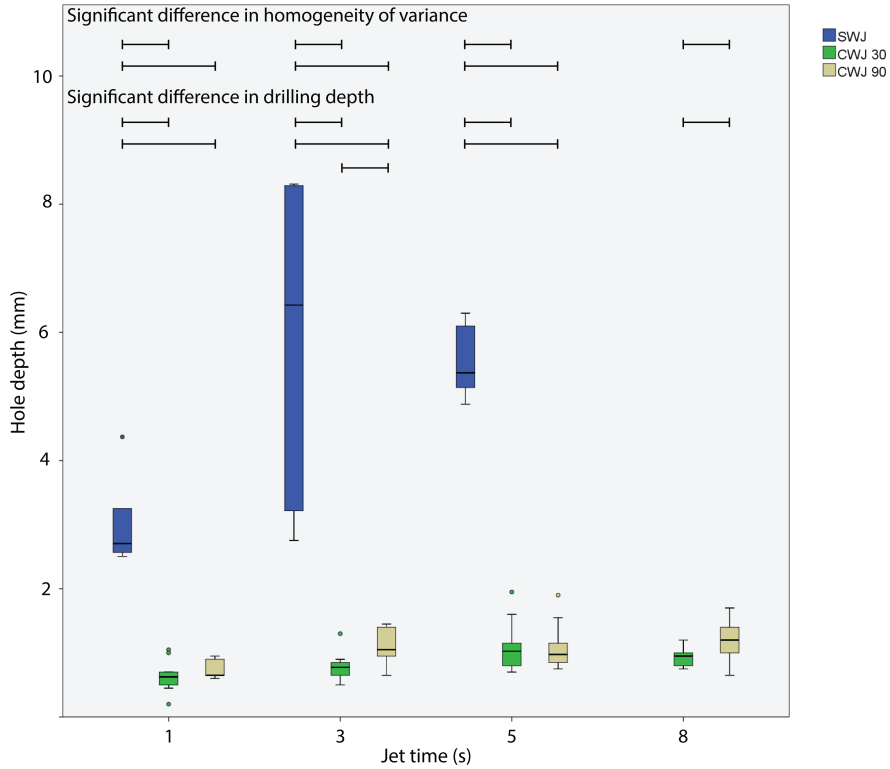


Figure 6. Tukey boxplot of the holes depths for each nozzle condition per jet time. Horizontal whiskered lines in the graph indicate significant difference in homogeneity of variance (top) or mean drilling depth (bottom). Dots indicate outliers.

Table 3. Power functions that describe drilling depth for a given jet time.

Nozzle	Power function	<i>p</i>	<i>R</i>	<i>R</i> ²
SWJ	$L_{hole} = 3.0 \cdot t_{wj}^{0.41}$	< 0.01	0.68	0.46
CWJ 30	$L_{hole} = 0.60 \cdot t_{wj}^{0.25}$	< 0.01	0.52	0.27
CWJ 90	$L_{hole} = 0.75 \cdot t_{wj}^{0.23}$	< 0.01	0.56	0.32

L_{hole} in mm, t_{wj} in s

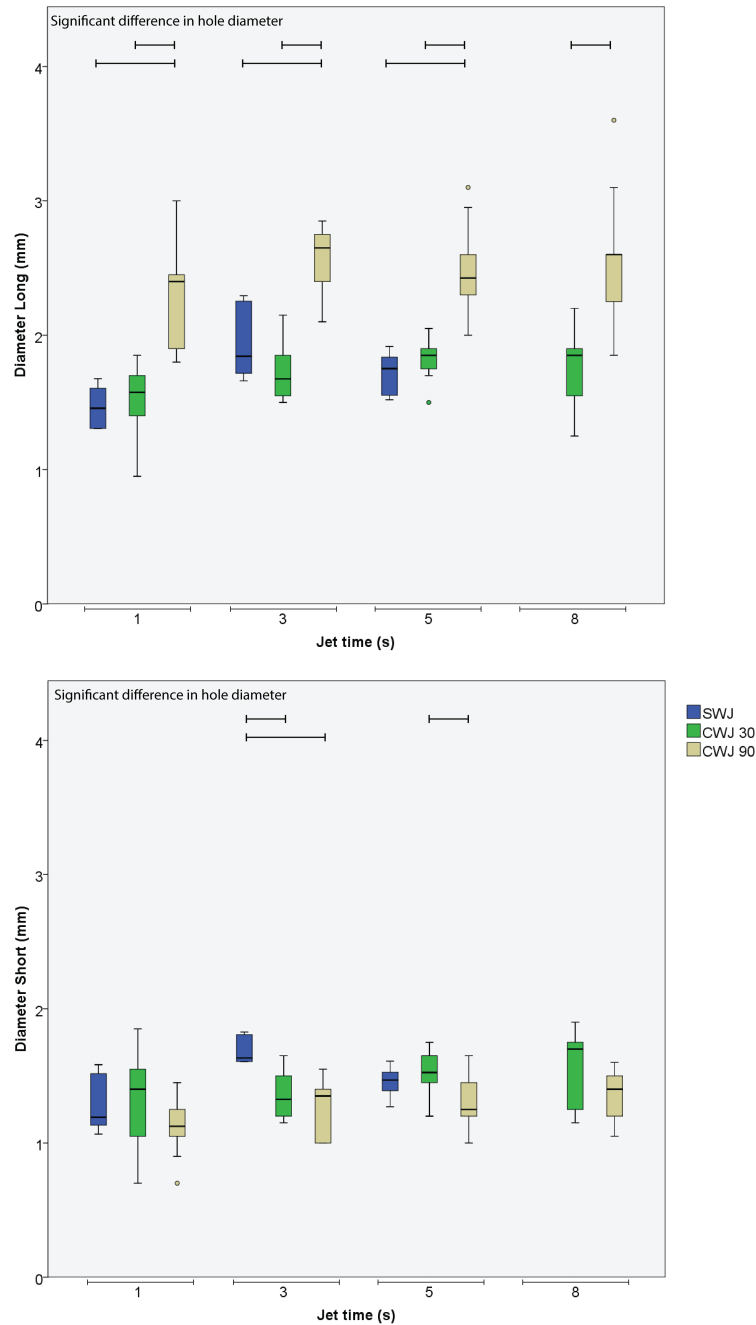


Figure 7. Tukey boxplots of the diameter long (top) and diameter short (bottom) measurements for a given jet time. Horizontal whiskered lines in the graph indicate significant difference in hole diameter. Dots indicate outliers.

Discussion

This study confirms the potential inherent drilling depth control by applying two colliding water jets compared to a single water jet. This is based on three observations: a smaller variance in drilling depth, a lower influence of the jet time on the drilling depth and lower means in drilling depth when using colliding water jets.

First, the variation in drilling depth is significantly lower for the CWJ than for the SWJ (Figure 6). Expressed using the range of the 95% confidence interval, the maximum variance is 0.6 mm and 5.4 mm for condition CWJ and SWJ respectively. This value of 0.6 mm is more than three times smaller than the allowed 2 mm variation to perform bone debridement treatment [29]. Hence, when colliding water jet drilling is performed in bone tissue, the influence of inhomogeneity in bone tissue will cause no safety issues with respect to depth control.

The variance in drilling depth of condition SWJ was smaller than expected for a jet time of 5 s, and vice versa larger for a jet time of 3 s (Figure 6, Table 2). Previous research showed that the influence of the jet time on the drilling depth should be larger [15, 30]. A reason for the more consistent variance in this study can be related to the smaller sample size of condition SWJ. Derived from the theoretical concepts, the variance for condition CWJ 30 was well within the range of the expected maximum 0.6-0.9 mm (Equation 6 and 8, Figure 6, Table 2). The variance for condition CWJ 90 was expected to be 0.4 mm smaller than for condition CWJ 30. However, no significant differences were found (Figure 6). The cause for this can be the natural architecture of bone, which consists of struts (trabecula) and cavities (trabecular spacing, Figure 4). As a result, removing one trabecula can result in an increase in depth with 0.15 to 0.45 mm [27] due to the underlying cavity. This can increase the drilling depth, variance in drilling depth and make differences diminish, thereby deviating from theoretical predictions.

The second evidence of the increased depth control of condition CWJ is that condition SWJ shows a stronger correlation between the jet time and the drilling depth for condition SWJ (Table 3: correlation coefficient R). Additionally, the coefficient of determination (R^2) indicates that a higher percentage of the drilling depth can be explained by the jet time for condition SWJ. Thus, condition CWJ is less affected by the jet time than condition SWJ, which improves depth control as an overshoot in drilling depth due to an accidentally induced increased drilling time is smaller.

The third evidence of improved depth control is the significant lower means in drilling depth of the holes for condition CWJ compared to condition SWJ (Figure 6). Regardless a similar quantity of energy being directed towards the bone tissue (Equation 7), there is a difference in mean drilling depth of factor 5 for each individual jet time when comparing condition CWJ to condition SWJ (Table 2, column mean drilling depth). Hence, the rapid drop in P_d below the minimum threshold for

machining bone for condition CWJ has a greater influence on the drilling depth than increasing E_{wj} . This makes CWJ an inherent stable method for controlling the drilling depth since the water jet machine settings play a negligible role on the drilling depth after the collision.

Mean drilling depths were expected to be in the range of 1.2-1.8 mm for condition CWJ 30 and 0.34-0.5 for condition CWJ 90 (Equation 6 and 8, Figure 2, bottom). The measured mean drilling depths were 0.9 and 1.0 mm for condition CWJ 30 and CWJ 90 respectively. As explained, the cause for the lack of difference may lie in the natural architecture of the bone, which diminishes differences in drilling depth and variance.

The D_{long} measurements for condition CWJ 90 were approximately 2/3 larger than the measurements of conditions CWJ 30 and SWJ (Figure 7). This is equivalent to the estimation of the length-width ratio of the shape of the water jet cone after collision (Figure 1), which was the basis for Equation 8. Condition CWJ 30 showed no significant larger D_{long} compared to condition SWJ. The nozzle diameter directly affects the size of the hole diameter [9, 37]. Therefore, a reason for the lack of difference in D_{long} between condition SWJ and condition CJW 30 can be that the absolute difference is too small due to the narrow impact angle (Equation 8, Figure 1) when comparing with a SWJ with a 0.1 mm larger nozzle diameter (Table 1). D_{short} measurements showed an occasional significant difference in diameter between the three nozzle conditions (Figure 7). Reasons for the sporadic contingency can be that condition SWJ used a 0.1 mm larger nozzle diameter than the CWJ conditions, or the smaller sample size of the SWJ condition. For all conditions, the diameter of water jet drilled holes are suitable for bone debridement treatments [29, 38]. For drilling pilot holes for screw fixations, SWJ or CWJ 30 is advised for consistent hole diameters.

Limitations of the study design might have affected the results. The study might have benefitted from an increase sample size for condition SWJ. Considering prior knowledge on the influence of the jet time on the drilling depth for condition SWJ [15, 30], the limited quantity of bone specimens that were available from a single batch (similar age, weight, nutrition), and the limitation that each bone specimen only allows a maximum number of holes to be drilled in, the SWJ condition was tested six times for jet times of 1,3 and 5 s (Table 1) instead of 10 times for CWJ. A previous study performed with a SWJ at three different jet times showed normally distributed drilling depths and homogeneous outcomes [15, 30]. For this study, this was not the case, which makes statistical analyses more difficult to interpret and outcomes occasionally contingent. The conclusions are not affected by the smaller sample size, since the mean and variance values for the drilling depth in previous studies was larger than in the current study. Therefore, it is likely an increase in sample size would have resulted in stronger significant differences.

Though the power of the three nozzle condition were strived for to be equal, the SWJ was slightly less powerful. Since deeper holes were drilled with the less

energetic SWJ than with the CWJ, the significance would only have increased if the power would have been equal. Therefore, it is unlikely that the conclusions of this study are affected by this.

Creating two colliding water jets was a constructive challenge, because the alignment of the water jets (and thus orientation of the nozzles in the holder) required precise manufacturing of the nozzle holder. For a minimal invasive instrument that can be used for arthroscopic surgery, achieving this accuracy can be even more challenging. Additionally, the collision point should be altered to collide approximately 2 mm deep in the bone, as hole depths between 2 and 4 mm are required for bone debridement treatments. This can be achieved by lowering the two nozzles in to the bone whilst drilling, or by placing the nozzle closer together and decreasing the angle collision angle. The latter option minimizes the (large) hole diameter, which is beneficial for treatments that require more precise dimensioning of the hole shape such as drilling pilot holes. Finally, to achieve coherent water jets, the guidance of the water towards the nozzle should be further researched (e.g. using one or two tubes).

The results of this study show that control over the drilling depth, regardless of inhomogeneity in bone tissue, can be achieved by using colliding water jets, thereby contributing to the safe application of water jet surgery in orthopaedic surgery. The small variance in drilling depth makes this method of water jet drilling safely applicable for bone debridement treatments and drilling pilot holes for screw fixation. For bone debridement treatments, hole depths between 2 and 4 mm are required [29]. The maximum range of the 95% confidence interval found in this study for condition CWJ was 0.6 mm, which is more than accurate enough for the 2.0 mm variance allowed for the treatment. For arthroscopic bone debridement treatments, an instrument is strived for with minimal dimensions. Since the impact angle of a CWJ has negligible effect on the drilling depth (Figure 6), but greatly influences the width of the hole in the direction of the water jets (Figure 1 and 7) and the minimum size of the nozzle (Table 1), a narrow impact angle is advised.

Conclusion

Using colliding water jets instead of a single water jet when water jet drilling in bone tissue results in a shallower drilling depth, smaller variance in drilling depth and a smaller influence of the jet time on the drilling depth. A_n increase of the impact angle of the colliding water jets has no effect on the drilling depth, but the angle does increase the diameter in the direction of the individual jets and the size of the design of the nozzle. Therefore, a small impact angle is advised for arthroscopic water jet instruments.

Acknowledgements

This research is supported by the Marti-Keuning Eckhart Stichting and the Dutch Technology Foundation STW (Grant number 10851), which is part of the Netherlands Organisation for Scientific Research (NWO), and which is partly funded by Ministry of Economic Affairs. The sponsor had no involvement in the study design, analysis or interpretation of the data. We are grateful to Mark Koster, Michiel van Breugel and Elio Sjak-Shie for their help in performing the experiment and measurements. We would like to thank Mark Scheper for the assistance in the statistical analyses and John Dukker and Andries van Oort for the fabrication of the nozzle holders.

References

1. Rau, H.G., A.P. Duessel, and S. Wurzbacher, The use of water-jet dissection in open and laparoscopic liver resection. *HPB*, 2008. 10(4): p. 275-280.
2. Hreha, P., et al., Water Jet Technology Used in Medicine. *Tehnicki Vjesnik-Technical Gazette*, 2010. 17(2): p. 237-240.
3. Yu, S., et al., Waterjet Dissection for Partial Nephrectomy Without Hilar Clamping in a Porcine Model. *International surgery*, 2014. 99(5): p. 677-680.
4. Oertel, J., et al., Waterjet dissection in the brain: review of the experimental and clinical data with special reference to meningioma surgery. *Neurosurgical Review*, 2003. 26(3): p. 168-174.
5. Basting, R., N. Djakovic, and P. Widmann, Use of water jet resection in organ-sparing kidney surgery. *Journal of Endourology*, 2000. 14(6): p. 501-505.
6. Schmolke, S., et al., Temperature measurements during abrasive water jet osteotomy. *Biomedizinische Technik*, 2004. 49(1-2): p. 18-21.
7. Schurr, M., et al., Histologic effects of different technologies for dissection in endoscopic surgery: Nd: YAG laser, high frequency and water-jet. *Endoscopic surgery and allied technologies*, 1993. 2(3-4): p. 195-201.
8. den Dunnen, S., et al., Pure waterjet drilling of articular bone: an in vitro feasibility study. *Journal of Mechanical Engineering - Strojnicki vestnik*, 2013. 59(7-8): p. 425-432.
9. den Dunnen, S., et al., Waterjet drilling in porcine bone: The effect of the nozzle diameter and bone architecture on the hole dimensions. *Journal of the Mechanical Behavior of Biomedical Materials*, 2013(0).
10. Honl, M., et al., Water jet cutting of bone and bone cement. A study of the possibilities and limitations of a new technique. *Biomedizinische Technik*, 2000. 45(9): p. 222-227.
11. Kuhlmann, C., et al., Evaluation of potential risks of abrasive water jet osteotomy in-vivo. *Biomedizinische Technik. Biomedical Engineering*, 2005. 50(10): p. 337.
12. Steadman, J.R., et al., Outcomes of microfracture for traumatic chondral defects of the knee: average 11-year follow-up. *Arthroscopy*, 2003. 19(5): p. 477-84.
13. Steadman, J.R., W.G. Rodkey, and J.J. Rodrigo, Microfracture: surgical technique and rehabilitation to treat chondral defects. *Clinical Orthopaedics and Related Research*, 2001. 391: p. s362.
14. Bronzino, J.D., The biomedical engineering handbook. 2nd ed. The electrical engineering handbook series. 2000, Boca Raton, FL: CRC Press.
15. den Dunnen, S., et al., How do jet time, pressure and bone volume fraction influence the drilling depth when waterjet drilling in porcine bone? *Journal of the Mechanical Behavior of Biomedical Materials*, 2016.
16. Mohamed, M.A.K., Waterjet cutting up to 900 MPa. 2004, Universitat Hannover. p. 122.
17. Hoogstrate, A., Towards high-definition abrasive waterjet cutting. TU Delft, 2000.
18. Chillman, A., et al. High pressure waterjets—an innovative means of alpha case removal for superplastically formed titanium alloys. in *Key Engineering Materials*. 2010. Trans Tech Publ.
19. Yanaida, K. and A. Ohashi. Flow characteristics of water jets in air. in *Fourth International Symposium on Jet Cutting Technology*, BHRA Fluid Engineering, Paper A. 1978.
20. Yanaida, K. and S.A. Ohashi. Flow Characteristics of Water Jets. in *Proceedings of the 5th International Conference on Jet Cutting Technology*. 1980. Hannover.
21. Chillman, A., M. Hashish, and M. Ramulu, Energy Based Modeling of Ultra High-Pressure Waterjet Surface Preparation Processes. *Journal of Pressure Vessel Technology-Transactions of the Asme*, 2011. 133(6).
22. Leach, S. and G. Walker. The application of high speed liquid jets to cutting. in *Proc. R. Soc. London, Ser. A*. 1966.
23. Abramovich, G., The Theory of Turbulent Jets. MIT Press. Cambridge, Massachusetts, 1963.
24. Annoni, M., et al. Orifice coefficients evaluation for water jet applications. in *16th IMEKA TC4 Symposium*. 2008.
25. Tafreshi, H.V. and B. Pourdeyhimi, The effects of nozzle geometry on waterjet breakup at high Reynolds numbers. *Experiments in fluids*, 2003. 35(4): p. 364-371.
26. Anantharamaiah, N., H.V. Tafreshi, and B. Pourdeyhimi, A study on flow through hydroentangling nozzles and their degradation. *Chemical engineering science*, 2006. 61(14): p. 4582-4594.
27. den Dunnen, S. and G.J.M. Tuijthof The influence of water jet diameter and bone structural properties on the efficiency of pure water jet drilling in porcine bone. article, 2014.
28. Honl, M., et al., The water jet as a new tool for endoprosthesis revision surgery - An in vitro study on human bone and bone cement. *Bio-Medical Materials and Engineering*, 2003. 13(4): p. 317-325.

29. Kok, A.C., et al., Is Technique Performance a Prognostic Factor in Bone Marrow Stimulation of the Talus? *Journal of Foot & Ankle Surgery*, 2012. 51(6): p. 777-782.
30. den Dunnen, S. and G.J.M. Tuijthof, Water jetting in bones: the influence of jet time on drilling depth variation, in 22nd International Conference on Water Jetting 2014. 2014: Haarlem, The Netherlands.
31. Abràmoff, M.D., P.J. Magalhães, and S.J. Ram, Image processing with ImageJ. *Biophotonics international*, 2004. 11(7): p. 36-42.
32. Schneider, C.A., W.S. Rasband, and K.W. Eliceiri, NIH Image to ImageJ: 25 years of image analysis. *Nature Methods*, 2012. 9(7): p. 671-675.
33. Parker, J.A. Stack Alignment Align3 TP Plugin. [Software] 2010 2012/12/12; 2012/12/12:[Available from: <http://www.med.harvard.edu/jpnm/ij/plugins/Align3TP.html>].
34. Nordstokke, D.W. and B.D. Zumbo, A new nonparametric Levene test for equal variances. *Psicológica: Revista de metodología y psicología experimental*, 2010. 31(2): p. 401-430.
35. Nordstokke, D.W., et al., The operating characteristics of the nonparametric Levene test for equal variances with assessment and evaluation data. *Practical Assessment, Research & Evaluation*, 2011. 16(5): p. 1-8.
36. Bach, F.-W., et al. Investigation of the AWIJ-Drilling Process in Cortical Bone. in *Proceedings of the 2007 American WJTA Conference and Expo*. 2007. Houston, USA.
37. den Dunnen, S., et al. Waterjet Drilling in Porcine Femur Bone: the Effect of Nozzle Diameter on Hole Geometry. in *BioMed*. 2013. Innsbruck.
38. Kok, A.C., et al., No Effect of Hole Geometry in Microfracture for Talar Osteochondral Defects. *Clinical Orthopaedics and Related Research*, 2013. 471(11): p. 3653-3662.

Chapter 6

Discussion

Introduction

The aim of this thesis is to develop a compliant arthroscopic surgical instrument for bone debridement treatments that is based on water jet technology and ensures safety by gaining control over the drilling depth.

The development of a surgical instrument entails an interactive cycle of research and design. This was dealt with by subdivision of the development steps into five research questions. The research questions are discussed in the order as presented in the introduction and include the answer to the questions, general recommendations and the potential applicability of the gathered knowledge outside its intended field. Research questions 4 and 5 include summaries of unpublished research focused on the development of working prototypes of a minimal invasive compliant water jet instrument. Finally, future research required for the further development of the water jet instrument is discussed, followed by a conclusion.

1. Is it possible to drill holes in articular bone tissue using pure water jets?

Yes, it is possible using pure water jets drill holes in bone tissue (Chapter 2). The minimum machine settings for drilling in any type of bone tissue are 37 MPa pressure and a water jet diameter of 0.6 mm.

Current surgical application of pure water jets primarily involves cutting of soft tissue. This research has proved that its application can be extended to the surgery of hard tissue, without requiring potentially harmful abrasives.

The minimum water pressure required to machine bone tissue is not constant. The density and structure of the bone affect the mechanical properties of the bone tissue. Since the density and structure varies within bone tissue, the bone's resistance against the destructive power of a water jet also varies. In a broader context, this allows selectivity in material removal when water jet cutting or drilling because different materials (or tissue types) have different material properties. For example, a water jet can remove the (softer) infected area of a tooth that is affected by caries, whilst keeping intact the (stronger) healthy surrounding tissue. Since only the affected area is removed, more healthy tissue is spared compared to a conventional dental drill. In orthopedic surgery, the less dense trabecular bone can be removed for the insertion of an implant without affecting the denser cortical bone. Furthermore, periprosthetic

interface tissue, which is a common symptom for hip and knee implant loosening, can be removed without damaging the implant, trabecular or cortical bone [1].

Additional research on the application of water jet technology for the selective machining of hard tissues is advised. Potential applications can be found in dentistry (drilling cavities, drilling pilot holes for implants, plaque removal) and orthopedic surgery (implant revisions, cartilage removal, tendon surgery).

2. What hole dimensions in the bone debridement treatments result in optimal healing for the patient?

Published studies do not provide enough details to determine the ‘optimal surgical technique’. A systematic review indicated that a hole depth variation between 2 and 4 mm until bleeding or fat droplets show is considered the standard method to perform bone debridement treatments (Chapter 3). Combining these hole depths with other key elements of the treatments (removal unstable cartilage and calcified layer, creating perpendicular rim at cartilage, distance between holes 3-4 mm in a spiral pattern) result in a success rate of 81% [2, 3]. An animal study on tali of goats indicated that deeper holes, or more holes with a smaller diameter do not influence cartilage healing [4]. Yet, different studies performed on other animals and bones did indicate an influence on cartilage healing when changing the hole dimensions [5] or puncturing technique [6, 7], leaving the matter indecisive.

Published studies do not provide enough details to determine the ‘optimal surgical technique’. Two methods are proposed that can facilitate the exploration for an optimal surgical technique. First, describing the executed surgical technique in detail (surgical instruments, approach, rinse settings, exerted forces etc.) instead of only referring to the inventor of the surgical technique. A detailed description increases the power of systematic review studies since more manuscripts are included. Additionally, the described subtle differences in surgical technique can inspire other surgeons to further improve the technique. Second, surgical treatment can be improved by objective measurement of relevant parameters during the treatment. Currently, details such as exertion forces on the instruments, pressure at the surgical spot, ringing settings and size of cuts are not measured, and thus not documented in literature. In cases where dimensions are described in literature [5, 6], estimates are given instead of quantitative measurements. Properly performed measurements, researched over a longer period, combined with patient outcomes and statistical analyses can identify subtle variations in treatment technique that improve healing.

3. What water jet machine settings are required to drill holes in bone of a set depth?

The key machine settings are the water jet pressure P_{MPa} (MPa), nozzle diameter D_n (mm) and the jet time t_{jet} (s). An increase in any of these settings will result in deeper and wider holes. The key structural property of the bone tissue that allows the best prediction of the drilling depth is the volume of mineralized bone per unit volume (BV/TV, range 0-1).

Three studies were performed to individually correlate the water jet machine settings (pressure P_{MPa} (MPa), nozzle diameter D_n (mm) and the jet time t_{jet} (s)) and bone structural properties to the drilling depth. This resulted in significant ($p < 0.001$) predictive equations with coefficients of determination $R^2 \geq 0.90$ for determining the hole depth for given machine settings and BV/TV (Chapter 4). For all three studies, identical secondary settings (stand-off distance, angle of attack, attack time, suspension, underwater jetting), equipment and measurements protocols were used. This allowed the formulation of a novel comprehensive predictive equation by using a standard multiple regression analysis, that indicates the influence of each individual setting on the drilling depth:

$$L_{\text{hole}} = 1.37 \cdot t_{\text{jet}}^{0.020} \cdot \left(1.12 - \frac{BV}{TV}\right) \cdot (P_{\text{MPa}} - 21.7) \cdot (D_n^2) \quad p < 0.001, R^2 = 0.89) \quad (1)$$

with the drilling depth L_{hole} in mm.

The predictive models presented in Chapter 4, as well as the comprehensive predictive model (Equation 1) show that to achieve a specific drilling depth, multiple combinations of machine settings can be used. Surgeons can benefit from this, as it allows precise adjustment of the machine settings to a specific need. For example, the slow increase of the drilling depth over longer jet times can be advantageous to carefully drill to a specific depth, thereby avoiding any overshoot in drilling depth.

The total volume of water that is directed towards the bone combined with a bone structural property is a leading measure for the volume of bone tissue that is being removed. This provides freedom in the development of water jet instruments as the nozzle diameter, pressure and jet time can be chosen in accordance to the maximum operating time requirements or dimensional limitations of a design. For example, in open spinal surgery, waterjet could be used to remove larger portions of bone in a laminectomy (removal of the posterior lamina which provides space for compressed nerves) without damaging the underlying dura and nerve structures using a larger nozzle with a limited pressure. By contrast, removal of cement surrounding an implant in arthroplasty revision surgery [8] would need a smaller nozzle diameter

to improve maneuvering, but use a higher pressure and jet time to access the entire implant surface. For minimally invasive surgery such as bone debridement treatments [9], a water jet instrument can be equipped with a small nozzle diameter, which allows thinner tubing, improving the instrument's handling and the ability to maneuver. In situations where surrounding tissue is easily damaged by over-pressure, such as the removal of periprosthetic interface tissue for treating loosened hip prostheses [1], the nozzle diameter and pressure can be lowered to minimize the volume flow. This allows an irrigation system to remove the superfluous water at the surgical site [10].

The nature of the thesis aim set us to apply an experimental approach to investigate the relationship between all dominant settings. Although we aimed to include as many samples as possible for each experiment, the sample size is limited due to finite testing times and range in bone structural properties. This has influenced the predictive equations, which are a product of statistics. Consequently, it is difficult to predict the strength of the predictive model outside of the tested setting ranges. Since our results are in line with previous research, extrapolation of the predictive equations outside the tested range (50-70 MPa, 1-8 s, 0.3-0.6 mm water jet diameter) is likely to return values that are close to empirical tests. More specific, previous studies indicated as well a linear correlation between drilling depth and pressure, a minimum threshold pressure value, a quadratic correlation of the nozzle diameter and the drilling depth, and a power function correlation between the jet time and the drilling depth [11-15]. For the lower range of untested machine settings (e.g. 30 MPa, 0.2 s, 0.2 mm water jet diameter), extrapolation serves no purpose since the water jet is not powerful enough to machine bone tissue. For the machine settings above the tested range, the predictive equations provide an indication of the drilling depths, but one should be aware that the variation will increase and thus the range of variation depth.

For predictive models that involve medical applications, the accuracy or strength within the tested sample range can be essential for the safe application of a novel device. Instead of solely providing the predictive equation, also providing the potential variation in absolute values should be considered for future studies involving medical equipment. Comparing the maximum variation with the maximum variation allowed for the intended treatment should be considered more valuable to judge the performance of a novel medical instrument than the significance (p) or coefficient of determination (R^2).

A method to indicate the absolute values of the potential variation is by specifying the 95% confidence intervals, either as a predictive equation, or with example values (Table 1). Additionally, the 95% confidence intervals can indicate the strength of the predictive model within the tested range. This allows to identify a range of (machine) settings where the medical instrument can provide a higher accuracy, which can be beneficial for medical treatments such as spinal surgery [16], or for further research to extend the overall accuracy of the predictive model. For

Table 1. Example values for the machine settings with the corresponding outcomes of the predictive model from Equation 1.						
T_{jet} (s)	BV/TV	P_{MPa}	D_n (mm)	5% CI	Model (mm)	95% CI
1	0.3	70	0.3	3.6	4.9	5.3
2	0.5	70	0.3	2.5	3.7	4.4
3	0.7	70	0.3	1.5	2.5	3.3

T_{jet} : jet time; BV/TV: bone volume fraction; D_n : nozzle diameter; 5% CI: 5% Confidence interval; Model: predicted outcome; 95% CI: 95% Confidence interval.

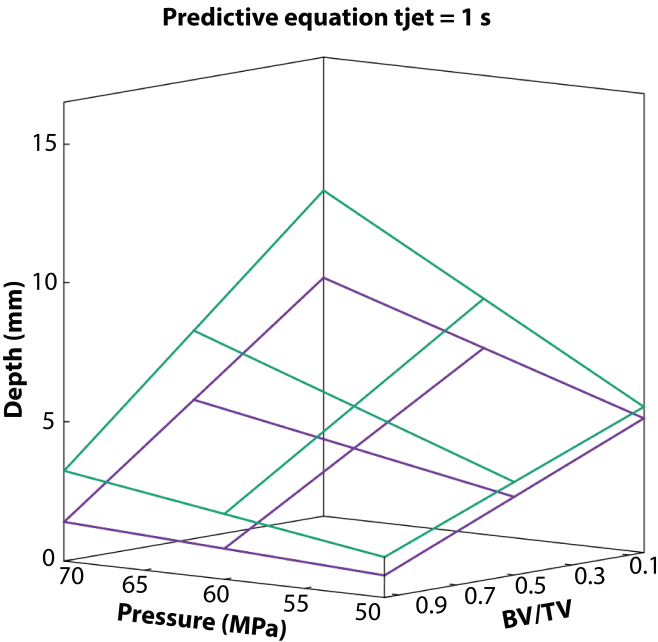


Figure 1. The 5% (purple) and 95% (green) confidence interval of a predictive model presented in Chapter 3. As the pressure increases, the potential variation increases.

example, in Figure 1 the potential variation of the effect of jet time and pressure on the drilling depth is presented. The proximity of the two surfaces representing the confidence intervals shows that for low pressures and short jet times (surfaces close together) the accuracy of the predictive equation is higher. Therefore, for operations where the drilling depth is critical, such as surgical dissection in close proximity to neural or vascular structures, oncological dissection or in bone that has a close relationship with undamaged cartilage., applying these specific machine settings are advised.

Last decades, research has been published involving the influence of water jet machine settings on the machinability of an industrial material [17]. In some, material properties of the industrial material were taken in to account [18]. Yet, the structural properties of the material are often ignored, whilst this can affect its machinability. Open structures in a material can guide the destructive flow of a (pure) water jet towards cavities, where the stream is split up and energy is dissipated. As a result, shallower cutting or drilling depths are achieved than when machining in solid materials. Therefore, the structure of the material should be considered when researching the influence of machine settings on the water jet cutting capacity of an open structured material.

4. How can drilling depth be controlled considering the heterogeneity of the bone tissue?

The natural heterogeneity of bone tissue affects the drilling efficiency of a water jet, causing variations in drilling depth. Four approaches were researched in gaining control over the drilling depth (Figure 2). These are discussed in an order of preference based on safety (avoiding an overshoot in drilling depth) and minimizing the dimensions (to allow arthroscopic surgery):

1. Feed forward system where the bone structure acts as input for a controller to determine the machine settings.
2. Inherently safe water jet configuration.
3. Feedback system (closed loop) where visual feedback acts as the input for the surgeon (controller) to determine the machine settings.
4. Feedback system where the drilling depth acts as input for the water jet instrument (controller) to determine the machine settings.

Each approach will be discussed.

1. Feed forward system with pre-operative knowledge of BV/TV

In Chapter 4, the influence of the primary machine settings and the bone structural properties on the water jet drilling depth were researched. This lead to a set of equations that allow prediction of the drilling depth when the local BV/TV is known. Within the lower range of machine settings that were tested (50 MPa pressure, 1 s jet time, 0.4 mm nozzle diameter), the accuracy and potential variation of the drilling depth is well within the 2 mm allowed variance in drilling depth for bone debridement treatments [19]. Thus, depth control is assured.

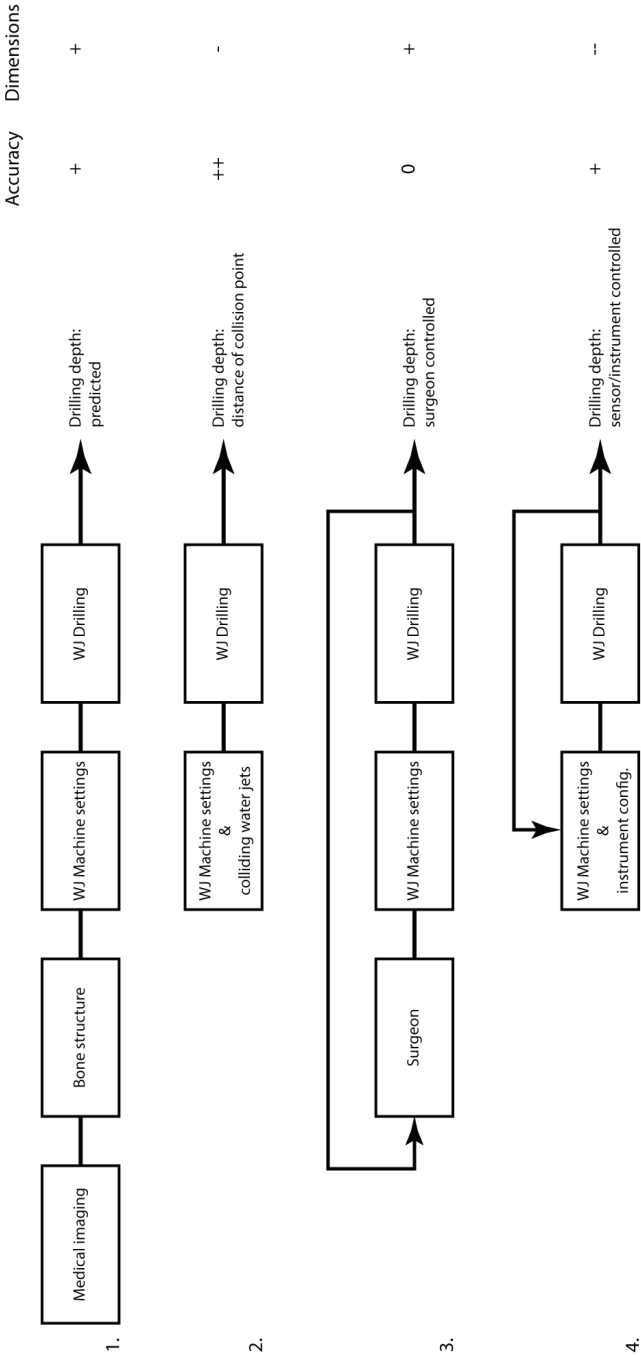


Figure 2. Four approaches for gaining control over the drilling depth whilst water jetting in heterogeneous bone tissue. From top to bottom: feed forward system, colliding water jets, visual feedback system, sensor feedback system.

For the application of the feed forward approach the bone's local BV/TV is required preoperatively. Methods to measure the local BV/TV in vivo are not widely available in hospitals. However, advancements of conventional CT scanners indicate that the spatial resolution increases every generation [20], making its BV/TV measurements more accurate and usable to water jet drilling. Additionally, micro-CT scanners for scanning human extremities are getting more common in hospitals for research purposes. Adopting these micro-CT scanners in diagnostic protocols allows the local BV/TV to be determined for bones in the ankle and knee.

The big advantage of the feed forward approach is that the nozzle tip does not require an additional control mechanism. Hence, the outer dimensions can be kept to a minimum, the design can be kept as simple as possible with a minimum of parts and this increases the robustness and valorization possibilities. To summarize, the evolving medical imaging techniques and the limited dimensions of the water jet instrument make the feed forward system a safe and feasible control method for the near future.

2. Inherently safe water jet configuration by colliding water jets

A system that inherently cannot drill holes deeper than a pre-set value is preferred since it takes away safety concerns of surgeons, induced by errors in machine settings or by incorrect interpretation of pre-operative scans. Colliding water jets provide inherent depth control[21]. Contrary to traditional water jet machining of bone, bone architecture and water jet time barely affect the drilling depth when using colliding water jets. The variation in drilling depth indicated by the 5-95% confidence interval was found to be maximally 0.6 mm [21]. This is well below the maximum allowed potential variation of 2 mm that is required for bone debridement treatments. Therefore, colliding water jet drilling is considered a safe and viable option for bone debridement treatments.

Challenges in implementing colliding water jets in arthroscopy are the size of the nozzle and the increased complexity of the design. The size of a nozzle head is larger compared to a single water jet since the water from the tubing is first to be separated and then guided towards two orifices that are placed a few mm apart from each other. The increased dimensions can impair the maneuverability in the tight space of a joint. Additionally, implementing extra tubing and orifices make the instrument more complex, which can increase the manufacturing costs. Finally, adjusting the drilling depth during an operation requires an instrument change since the collision point cannot be adjusted.

Colliding jets can be useful for applications that require precise cutting or drilling to a specific depth. For clinical applications, making incisions in soft tissue such as skin can be considered [22, 23]. For industrial applications, the mining industry can benefit from precise drilling that colliding water jets can offer by not

allowing fragile layers of earth to be penetrated. In the food industry, (shallow) cuts in food can be made to allow filling or seasoning, without affecting the integrity of the food itself. Finally, colliding water jets can prove to be valuable in situations where debris has to be removed during rescue missions. For example, salvaging victims from earthquake sites currently requires removing debris by hand. Heavy machinery (e.g. pneumatic hammer, excavating equipment) either produces too much vibrations (risking collapse), or can physically hurt the victims under the debris by the induced forces. Colliding water jets do not cause vibrations, and can machine debris up to a specific depth, avoiding collateral damage to the victim.

3. Feedback system controlled by the surgeon

For this control system the surgeon (controller) can adjust their actions by evaluating the visual feedback of the drilling depth provided by the arthroscope (controller input). This control option is similar to the current bone debridement treatments with awls. In fact this is in many arthroscopic treatments the manner of judging the progress and quality of the surgical procedure. If the surgeon determines that a hole is not deep enough, he/she can evoke an additional water jet burst until the desired depth is reached. Consequently, the surgeon is in full control and is not bound to a predetermined drilling depth. However, visual feedback from arthroscopes can only provide rough estimates of the drilling depth, impairing the accuracy. This feedback approach distinguishes itself in simplicity by eliminating medical imaging based on radiology and by allowing the use of the most basic form of a water jet instrument: a pump, tubing and a nozzle. As a consequence, the dimensions of the water jet instrument can be kept to a minimum, allowing decent maneuverability in the tight joint spaces.

Two requirements have to be met to avoid an overshoot in drilling depth. First, the surgeon has to have proper sight on the location where the holes are being drilled. Proper sight is crucial as the visual feedback on the drilling depth (or the occurrence of blood droplets) provides the information to the surgeon (controller) whether further action is required. The second requirement is that the water jet bursts are to increase the drilling depth, without causing an overshoot. It is likely that the surgeon requires multiple tries, starting at “the safe side”, before the adequate (powerful) machine settings can be set. Both requirements for avoiding an overshoot are considered achievable, making this proposed feedback loop approach feasible, yet with a lower accuracy than approach 1 or 2.

4. Feedback system controlled by the water jet instrument

Instead of the surgeon, the process of evaluating and deciding whether drilling is to be continued to achieve a specific drilling depth can also be performed by

adding a sensor to the medical instrument. A feedback loop can be introduced that automatically shuts down the water jet for a given depth (Figure 2). The input of the feedback can either originate internally near the nozzle in the joint, or by an external instrument such as a medical imaging device. Three concepts were developed where the sensor (depth gauge) and controller (water jet termination system) were combined in the nozzle (Figure 3). Additionally, a probe-based depth control system was prototyped and tested. For this concept, the sensory input originates at the nozzle and is fed back to a controller that is able to shut down the pump.

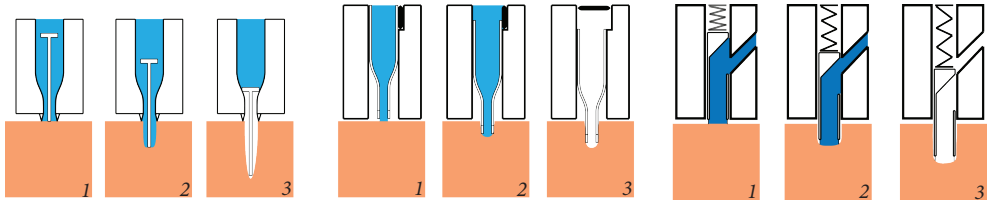


Figure 3. Three concepts where the part for measuring the drilling depth doubles as a shut-off mechanism for the stream of water. As the drilling progresses and the hole increases in depth (1 -> 2), a gauging rod or nozzle tube is lowered in the hole. When a specific depth is achieved (3), the gauging rod cuts off the water supply, by either a stopper mechanism or a valve.

Probe-based depth control system

A 3D printed nozzle with a build-in water jet orifice and 0.4 mm Nickel Titanium depth probe was designed and developed (Figure 4, left) [24]. The depth probe allows measurements on the hole depth to be performed, which can be used by a controller to either shut down the water jet (real-time closed loop control whilst water jet drilling) or to adapt the machine settings for the next water jet burst (iterative closed loop control for consecutive drilling). A linear actuator with a displacement sensor that is fastened to a load sensor is used to lower the probe in to the hole (Figure 4, right). As a result, a specific force/displacement profile is generated at the controller

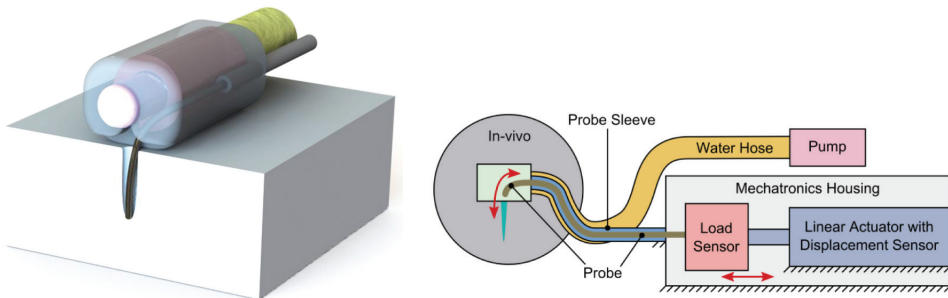


Figure 4. Probe-based depth control system. An integrated probe connected to a load sensor allows depth measurements, allowing a controller to execute a water jet drilling strategy to achieve a specific drilling depth.

using the data from the load and displacement sensor. Depth measurements of holes with a diameter larger than 1.0 mm resulted in a standard deviation of 0.61 mm. Therefore, the probe-based depth control system is considered a viable solution with concern to drilling depth accuracy for bone debridement treatments.

In general, closed loop systems where the instrument evaluates and controls the drilling depth offer a potential in the development of a water jet drilling instrument, but comes at the cost of an increased overall complexity, larger nozzle size and higher manufacturing costs.

5. What remaining challenges need to be addressed for arthroscopic water jet drilling?

This thesis presents a novel method to machine holes in bone tissue for bone debridement treatments by using water jets. Though the main challenge, depth control, has been thoroughly covered in the previous chapters, further investigations are required for the actual development of an arthroscopic surgical instrument. Four key challenges are briefly discussed in the next paragraphs.

Nozzle stability

A water jet at an orifice results in a thrust force in the opposite direction. As a result, a nozzle in the articular joint can start moving after the jet initiation, which can lead to inaccurate drilling as well as unwanted damage to surrounding tissue. A pilot experiment showed that exerting a force of 10 N at the opposite side of the nozzle will prevent any movement larger than 0.15 mm, which is acceptable for accurate drilling [25]. Exerting a force of 10N can be achieved by compressing the joint after positioning the nozzle. Though these preliminary experiments are promising for ensuring the stability of the nozzle whilst water jet drilling, further investigations are required since these tests were performed with a maximum pressure of 20 MPa, which is approximately half the pressure required for drilling in bone tissue.

Tubing and connections

Arthroscopic articular surgery involves dimensional restrictions of the surgical instruments. Existing industrial water jet equipment relies on the application of massive, strong and rigid materials that are over dimensioned to sustain water pressures up to 70 MPa. This is the opposite of the small, compliant minimally invasive instrument that is strived for. On-scale prototypes were build and tested for

compliance, burst pressure and leakage. Kevlar braided tubing is considered optimal for an arthroscopic water jet instrument due to its ability to sustain pressures up to 110 MPa, the maximum outer diameter of the tubing (< 5 mm), minimum inner diameter (> 1.5 mm) to accommodate the volume flow, and its ability to maintain a level of flexibility for the placement in joints. Moreover, specific types of Kevlar braided tubing have been approved for medical use, which makes the process of acquiring medical approval for a novel instrument shorter.

Connecting a nozzle to tubing requires an insert and a shell (Figure 5) that are tightened respectively to the inside and outside of the tubing. For industrial applications, the length of this rigid connection is usually between 50 and 100 mm. For the arthroscopic water jet instrument, flexibility is required. Experiments were performed to minimize the length of the rigid connection between the nozzle and the tubing by varying the connection shape, length and tightness of the fit. A prototype equipped with a 7 mm long connection assembled with a sealant was able to sustain 72 MPa of pressure. Hence, medical grade flexible high-pressure tubing is available and minimizing the length of the rigid connection is feasible. However, cadaver testing is required to test the strength of the connection in a clinical setting, and to determine whether the length of rigid nozzle impairs the maneuvering in a joint.

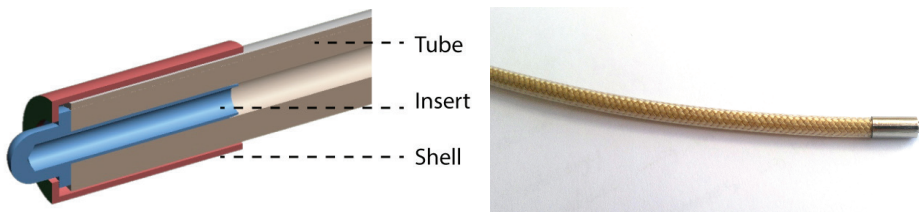


Figure 5. Left: cross section of the prototypes of the minimally invasive water jet instrument. Right: prototype.

Incoherency water jet caused by scaling down the water jet instrument

The custom build water jet instrument used for the research in this thesis produced coherent water jets. The relative large dimensions of the water jet instrument and lack of curvature of the tubing were the primary contributors for the coherency. Scaling down the dimensions to the intended water jet instrument and introducing curvatures in the tubing induces turbulence in the water flow, which can lead to an incoherent water jet. An incoherent water jet will dissipate its energy over a larger surface area of the workpiece compared to a coherent water jet. As a consequence, the drilling performance of the water jet can be impaired.

Preliminary experiments with prototypes that were built to meet the dimensional restrictions of arthroscopy indicate that the coherency of the water jet is negatively affected by introducing curvature in tubing and reduction of the

dimensions. However, the drilling performance was only marginally affected as bone tissue could still be drilled with similar pressures that were used in the industrial size set-up [26]. Cadaver experiments are to be performed to determine the potential increase in pressure required to machine bone tissue whilst using arthroscopically sized prototypes.

Ergonomics, shape, level of compliance

The shape and level of compliance of the tubing and the nozzle affect among other things the minimum required dimensions of the incision, the minimum dimensions of a joint that can be treated, the ability to position the instrument and the stability of the nozzle whilst water jetting. Additional research is required with respect to the ergonomics of the instrument. For this, testing various prototypes on cadavers by orthopedic surgeons should be considered. Three categories of prototypes that have been developed can act as a starting point (Figure 6).

Though the key challenges have to be investigated further for the development of an arthroscopic water jet instrument, so far none of the challenges has been found insurmountable. Since the feasibility of water jet drilling in combination with depth control has been established, the next step in the development of the arthroscopic water jet instrument should be in vivo testing on animals. This allows to determine whether water jets can provide similar healing as existing treatments and identify potential risks. Furthermore, cadaver testing should be performed to further develop the on-scale prototypes with respect to nozzle stability, ergonomics and loss of water jet coherency.

Conclusion

It is possible to drill in bone tissue by using pure water jets. Inhomogeneities in bone structure cause variations in hole depth when water jet drilling in bone. Four methods have been developed to demonstrate drilling depth control is feasible. The methods differ in complexity, accuracy and dimensional requirements. Outside the field of orthopedic surgery, the depth control methods can be used in dentistry, mining and food industry. Preliminary tests with prototypes indicated that key secondary challenges (stability of nozzle whilst water jetting, connecting nozzle to the tube, scaling down dimensions, ergonomics) can be solved. Cadaver and in vivo experiments with on-scale prototypes are to be performed as a first step in the continuation of the development of an arthroscopic water jet instrument.



Figure 6. Three categories of prototypes that have been developed. Top: compliant tubing equipped with a disc shaped nozzle to provide stability during water jet drilling and counteract potential damage to the opposite cartilage surface. Center: rigid tubing, allowing the instrument to be smaller than 2 mm in diameter. Bottom: compliant tubing equipped with a 9 mm long rigid nozzle.

References

1. Kraaij, G., et al., Waterjet cutting of periprosthetic interface tissue in loosened hip prostheses: An in vitro feasibility study. *Medical engineering & physics*, 2015. 37(2): p. 245-250.
2. Kok, A.C., et al., Is Technique Performance a Prognostic Factor in Bone Marrow Stimulation of the Talus? *Journal of Foot & Ankle Surgery*, 2012. 51(6): p. 777-782.
3. Steadman, J.R., et al., Outcomes of microfracture for traumatic chondral defects of the knee: average 11-year follow-up. *Arthroscopy*, 2003. 19(5): p. 477-84.
4. Kok, A.C., et al., No Effect of Hole Geometry in Microfracture for Talar Osteochondral Defects. *Clinical Orthopaedics and Related Research*, 2013. 471(11): p. 3653-3662.
5. Chen, H., et al., Depth of subchondral perforation influences the outcome of bone marrow stimulation cartilage repair. *Journal of Orthopaedic Research*, 2011. 29(8): p. 1178-1184.
6. Chen, H., et al., Drilling and microfracture lead to different bone structure and necrosis during bone-marrow stimulation for cartilage repair. *Journal of Orthopaedic Research*, 2009. 27(11): p. 1432-1438.
7. Orth, P., et al., Effect of subchondral drilling on the microarchitecture of subchondral bone: analysis in a large animal model at 6 months. *The American journal of sports medicine*, 2012. 40(4): p. 828-836.
8. Honl, M., et al., The water jet as a new tool for endoprosthesis revision surgery - An in vitro study on human bone and bone cement. *Bio-Medical Materials and Engineering*, 2003. 13(4): p. 317-325.
9. Steadman, J.R., W.G. Rodkey, and J.J. Rodrigo, Microfracture: surgical technique and rehabilitation to treat chondral defects. *Clin Orthop Relat Res*, 2001(391 Suppl): p. S362-9.
10. den Dunnen, S. and G.J.M. Tuijthof The influence of water jet diameter and bone structural properties on the efficiency of pure water jet drilling in porcine bone. article, 2014.
11. Mohamed, M.A.K., Waterjet cutting up to 900 MPa. 2004, Universitat Hannover. p. 122.
12. Pandey, N.P., Vijay; Katiyar, Jitendra Kr., Investigation of drilling time v/s material thickness using abrasive waterjet machining. *International Journal of Advances in Engineering & Technology*, 2012. 4(1): p. 672-678.
13. Bach, F.-W., et al. Investigation of the AWIJ-Drilling Process in Cortical Bone. in *Proceedings of the 2007 American WJTA Conference and Expo*. 2007. Houston, USA.
14. Orbanic, H. and M. Junkar, An experimental study of drilling small and deep blind holes with an abrasive water jet. *Proceedings of the Institution of Mechanical Engineers Part B-Journal of Engineering Manufacture*, 2004. 218(5): p. 503-508.
15. Honl, M., et al., Water jet cutting of bone and bone cement. A study of the possibilities and limitations of a new technique. *Biomedizinische Technik*, 2000. 45(9): p. 222-227.
16. Endo, T., et al., New Application of Actuator-Driven Pulsed Water Jet for Spinal Cord Dissection: An Experimental Study in Pigs. *Journal of Neurological Surgery Part A: Central European Neurosurgery*, 2017. 78(02): p. 137-143.
17. Yuvaraj, N. and M.P. Kumar, Investigation of process parameters influence in abrasive water jet cutting of D2 steel. *Materials and Manufacturing Processes*, 2017. 32(2): p. 151-161.
18. Tikhomirov, R.A., et al., High-pressure jetcutting. 1992, New York: ASME Press. 197.
19. den Dunnen, S., et al., How do jet time, pressure and bone volume fraction influence the drilling depth when waterjet drilling in porcine bone? *Journal of the Mechanical Behavior of Biomedical Materials*, 2016.
20. Hsieh, J., *Computed tomography: principles, design, artifacts, and recent advances*, third edition. 2015: SPIE Bellingham, WA. 666.
21. den Dunnen, S., et al., Colliding jets provide depth control for water jetting in bone tissue. *Journal of the mechanical behavior of biomedical materials*, 2017. 72: p. 219-228.
22. Rennekampff, H.-O., et al., Debridement of burn wounds with a water jet surgical tool. *Burns*, 2006. 32(1): p. 64-69.
23. Tenenhaus, M., D. Bhavsar, and H.-O. Rennekampff, Treatment of deep partial thickness and indeterminate depth facial burn wounds with water-jet debridement and a biosynthetic dressing. *Injury*, 2007. 38(5): p. S38-S44.
24. Sjak-Shie, E.E., Depth Control for Blind Water Jet Drilling in Bone. 2013.
25. Jansma, M.J.L., H.M.; Robertson, P.D.; Kool, F.W., Arthroscopic water-jet drilling in bone: Stabilizing the nozzle to ensure accurate drilling TU Delft Bachelor Thesis, 2013.
26. Wabeke, D.W., Miniaturization of a Water-JetDrill for Microfracture Surgery. 2017.

Acknowledgements

Gabrielle, de kennis en kunde die je op mij hebt over weten te brengen zijn onmisbaar geweest in het promotietraject. Deze vaardigheden zal ik de rest van mijn leven meedragen en kunnen toepassen. Snel, accuraat, gevat, gefocust, kritisch en met een duidelijke visie: af en toe lastig, maar bovenal behulpzaam. Je hebt niet alleen de kwaliteit van mijn werk positief beïnvloed, maar tevens mijn denken. Hartelijk dank voor je vrijwel onuitputtelijke steun.

Jenny, bedankt voor je input tijdens het promotietraject, en de steun voor het niet werk gerelateerde. Mede door jouw inzet ben ik altijd welkom gebleven op de TU Delft, waardoor ik deze thesis af heb kunnen ronden. Je deur staat letterlijk altijd open, en een vraag wordt altijd vriendelijk tegemoetgezien en beantwoord. Ik wens voor de gehele BME afdeling dat je deze laagdrempeligheid, vriendelijkheid, kennis en compassie nooit zal verliezen.

Gino, elk gesprek dat ik met je heb gevoerd heeft een positieve en vrolijke insteek gehad. Bedankt voor deze prettige manier van begeleiden en alle input op de manuscripten.

During the years of my promotion I have shared rooms with many fellow PhD students. Chunman, Bram, Ewout, Loubna, Awaz, Aimee, Annetje, Elise, Marjon, Tim, Paul, Costansa, Ingmar, Bob, Mona and many others: thank you for the good times. Helene, Gert and Arjo, though I have never shared a room with you, I really enjoyed working together and sharing excitement and occasional frustration with you. Thank you for making the job even more exciting. Lars, bedankt voor de introductie in de wereld van microCT scanners en botarchitectuur.

Een deel van het project is uitgevoerd op het AMC. Samengepropt zijn in te kleine kamertjes gaf een nieuwe dimensie aan het samenwerken. Inger, bedankt voor de hulp aan de statistiek en uiteraard de gezelligheid. Leendert, je kundige blik op de studies heb ik altijd zeer gewaardeerd. Aimee, wat heerlijk om met jou samen te werken. Je bent vlot en fijn in de omgang. Je lijkt de wereld altijd aan te kunnen. Bedankt voor de hulp in de afrondende fase van deze thesis. Geniet van de kleine (dingen in het leven).

John, Andries en Reinier. Vele nozzle-houders, nozzles, connectoren en slangetjes hebben jullie met kundigheid en accuratesse weten te vervaardigen, af en toe zelfs onder tijdsdruk. Het was mij een genoegen om samen te werken. Ton, bedankt voor de hulp met het voor mij werkbaar krijgen van de trekbank. Fijn dat ik

altijd even langs kon lopen wanneer iets niet zo liep als gepland.

De afgelopen jaren hebben veel studenten bijgedragen aan het onderzoek. Daan, Elio, Mark, Michiel, Hans, Folkert, Joost, Daniel, Myrth en Chris: hartelijk dank voor jullie verrichtingen die vaak gepaard gingen met hard werken, plezier en tegenslagen, maar altijd een mooi resultaat opleverden.

Anouk, bedankt dat je altijd een oogje in het zeil hield over de belangrijkste zaken in het leven, die niets met werkprestaties te maken hadden. Diones en Sabrina, bedankt voor de praktische ondersteuning.

Astrid, bedankt voor je hulp, begrip en rust die je wekelijks met je meebracht. Je bezoeken waren niet alleen waardevol voor ons, maar ook voor de kinderen.

Marjon, Nicolien, Ingrid, Linda, Yara en Masha, bedankt voor de begeleiding. De lessen die jullie mij hebben geleerd pas ik nog dagelijks toe.

Het leven is simpelweg leuker met vrienden. Freek en Sonja, bedankt voor de regelmatige belletjes en bezoeken. Mark, bedankt dat je me fysiek weer op de benen hebt gekregen. Het delen van de promotieperikelen was een genoegen. Moge jij ook spoedig je dissertatie afronden. Daan, Jelmer, Mark, Floor, Karin, Tim en Karlijn, bedankt voor de gezelligheid.

Heshmat, Sousan en Hamed. Bedankt voor alle praktische hulp en ondersteuning de afgelopen jaren. Van verstoppingen tot het verzorgen van de kinderen: wij konden altijd bij jullie terecht.

Jeroen en Marein, jullie frisse kijk op gebeurtenissen tijdens mijn promotietraject deed mij regelmatig met een andere bril naar deze gebeurtenissen kijken. Mijn dank hiervoor. Jeroen, van kinds af aan speel je de rol als grote broer met verve. Bedankt voor je hulp, voor zowel het wetenschappelijke als in het leven.

Pa en ma. Dit promotietraject met goed gevolg afleggen was zonder jullie ondersteuning niet mogelijk geweest. Bedankt voor het zorgdragen voor niet alleen mijzelf, maar ook voor mijn gezin. Van kinds af aan gaven jullie mij het vertrouwen dat ik altijd op jullie kon rekenen, mocht dit nodig zijn. De praktijk blijkt hiermee in overeenstemming. Ik hoop dat ik voor mijn kinderen ook dit gevoel een leven lang kan bieden. Jullie hulp en betrokkenheid is van onschatbare waarde.

Wytse, Elise en Louise. Tijd is relatief. Vanuit een bepaald perspectief lijkt het traag te verlopen. Echter, wanneer ik naar jullie kijk, vliegt de tijd. Het is prachtig

jullie op te zien groeien. Bedankt voor alle vrolijkheid die jullie dagelijks met jullie meebrengen.

Hoda, je bent de drijvende kracht achter ons gezin. Geen letter van dit proefschrift was zonder jou mogelijk geweest. Bedankt hiervoor, en je eeuwige geduld. De toekomst lijkt steeds rooskleuriger te worden. We gaan ervan genieten!

Steven

Curriculum Vitae

- 23-12-1981 Born in Papendrecht, the Netherlands
- 1994 – 2000 Gymnasium at Gymnasium Camphusianum in Gorinchem
- 2000 – 2001 Computer Science and Engineering, Delft University of Technology
- 2001 – 2005 Bachelor Industrial Design Engineering, Delft University of
2007 – 2007 Technology
- 2007 – 2009 Master Integrated Product Design, consisting of 50% Industrial
Design Engineering and 50% Bio Mechanical Engineering courses,
Delft University of Technology
- 2010 – present PhD candidate at the department of Biomechanical Engineering,
Delft University of Technology

List of publications

Journals

den Dunnen S., Dankelman J., Kerkhoffs G.M.M.J., Tuijthof G.J.M., Colliding jets provide depth control for water jetting in bone tissue, *Journal of the Mechanical Behavior of Biomedical Materials*, 72, 219-228, 2017

den Dunnen S., Dankelman J., Kerkhoffs G.M.M.J., Tuijthof G.J.M., How do jet time, pressure and bone volume fraction influence the drilling depth when waterjet drilling in porcine bone? *Journal of the Mechanical Behavior of Biomedical Materials*, 62, 495-503, 2016

den Dunnen S., Tuijthof G.J.M., The influence of water jet diameter and bone structural properties on the efficiency of pure water jet drilling in porcine bone, *Mechanical Sciences*, 5, p53–58, 2014

den Dunnen S., Mulder M., Kerkhoffs G.M.M.J., Dankelman J., Tuijthof G.J.M., Waterjet drilling in porcine bone: The effect of the nozzle diameter and bone architecture on the hole dimensions. *Journal of the Mechanical Behavior of Biomedical Materials*, p84-93, Nov 2013.

Kok A.C., Tuijthof G.J.M., **den Dunnen S.**, van Tiel J., Siebelt M., Everts V., van Dijk C.N., Kerkhoffs G.M., No effect of hole geometry in microfracture for talar osteochondral defects, *Clinical Orthopaedics and Related Research*, 471(11):3653-62, 2013.

den Dunnen S., Kraaij G., Biskup C., Kerkhoffs G.M.M.J., Tuijthof G.J.M., Pure waterjet drilling of articular bone: an in vitro feasibility study. *Strojniski Vestnik - Journal of Mechanical Engineering*, 59(7-8), 425-432, 2013.

Kok A.C., **den Dunnen S.**, Tuijthof G.J.M., van Dijk C.N., Kerkhoffs G.M., Is technique performance a prognostic factor in bone marrow stimulation of the talus? *Foot and Ankle Surgery*, 51(6), 777-82, Nov 2012.

Song, Y, Vergeest, JSM, Langerak, TR, **den Dunnen, S.**, Rooij, M de & Nyirenda, PJ

(2004). Freeform shape modifications in selective clay milling. In XY Shao & C Deng (Eds.), ICMA 2004 Proceedings of the international conference on Manufacturing Automation; Advanced design and manufacturing in global competition (pp. 747-754). Bury St Edmunds and London, UK: Professional Engineering Publishing.

Conferences and proceedings

den Dunnen S., Tuijthof G.J.M., Water jetting in bones: the influence of jet time on drilling depth variation, 22nd International Conference on Water Jetting 2014, Haarlem 3-5 sept, The Netherlands, Full paper

den Dunnen S., Tuijthof G.J.M., The Influence of Waterjet Diameter and Bone Structural Properties on the Efficiency of Pure Waterjet Drilling in Porcine Bone, Design of Medical Devices, Delft, The Netherlands, 7-9 Oct. 2013. Full paper

den Dunnen S., Mulder L., Kerkhoffs G.M.M.J., Dankelman J., Tuijthof G.J.M., Waterjet drilling in porcine femur bone: the effect of nozzle diameter on hole geometry. Oral presentation. 10th IASTED International Conference on Biomedical Engineering, Innsbruck, Austria, Feb 13-15 2013. Full paper

den Dunnen S., Mulder L., Kok, A.C., Kerkhoffs G.M.M.J., Dankelman J., Tuijthof G.J.M., Waterjet drilling in bone: correlation between bone architecture and hole depth. Oral presentation. Annual meeting of the Dutch Orthopaedic Society (NOV), Amsterdam, NL, Feb 7-8 2013.

den Dunnen S., Mulder L., Kerkhoffs G.M.M.J., Dankelman J., Tuijthof G.J.M., Waterjet drilling in bone: a model to predict drilling depth using bone architecture and nozzle diameter. Oral presentation. 4th Dutch Bio-Medical Engineering Conference, Egmond aan Zee, The Netherlands, 24-25 January 2013.

den Dunnen S., Mulder L., Kok A.C., Dankelman J., Kerkhoffs G.M.M.J., Tuijthof G.J.M., Waterjet drilling in bone: the effects of nozzle diameter and joint type on hole depth and diameter. Poster presentation. 20th Annual meeting of the European Orthopedic Research Society (EORS), Amsterdam, NL, September 26-28 2012.

Kraaij G., **den Dunnen S.**, Dankelman J., Nelissen R.G.H.H., Valstar E.R., Reducing the pressure for waterjet dissection in minimally invasive hip refixation. Poster presentation. 20th Annual meeting of the European Orthopedic Research Society

(EORS), Amsterdam, NL, September 26-28 2012.

den Dunnen S., Mulder L., Dankelman J., Kerkhoffs G.M.M.J., Tuijthof G.J.M., Waterjets in orthopedics: can we apply this safely. Poster presentation. 9th European Foot & Ankle Society (EFAS) Congress, Noordwijk Aan Zee, NL, September 6-8 2012.

den Dunnen S., Kraaij G., Biskup C., Kerkhoffs G.M.M.J., Tuijthof G.J.M., Effect of waterjets- drilling in bone, Oral presentation. Annual meeting of the Dutch Orthopaedic Society (NOV), Groningen, January 27-28 2011.

den Dunnen S., Kraaij G., Biskup C., Hassel T., Kerkhoffs G.M.M.J., Tuijthof G.J.M., Effect of waterjet drilling in bone, Poster presentation. Third Dutch Conference on Biomedical Engineering, Egmond aan Zee, January 20-21 2011.

Awards

22nd International Conference on Water Jetting 2014 – best paper award, 2014

NWO-STW nominatie Simon Stevin Leerling-prijs, 2013

International Society for Prosthetics and Orthotics Nederland afstudeerprijs, 2010

